

**International
Journal of
Engineering
Technologies
(IJET)**

**Printed ISSN: 2149-0104
e-ISSN: 2149-5262**

**Volume: 4
No: 2
June 2018**

© Istanbul Gelisim University Press, 2018
Certificate Number: 23696
All rights reserved.

International Journal of Engineering Technologies is an international peer-reviewed journal and published quarterly. The opinions, thoughts, postulations or proposals within the articles are but reflections of the authors and do not, in any way, represent those of the Istanbul Gelisim University.

CORRESPONDENCE and COMMUNICATION:

Istanbul Gelisim University Faculty of Engineering and Architecture
Cihangir Mah. Şehit P. Onb. Murat Şengöz Sk. No: 8
34315 Avcilar / Istanbul / TURKEY
Phone: +90 212 4227020 Ext. 221
Fax: +90 212 4227401
e-Mail: ijet@gelisim.edu.tr
Web site: <http://ijet.gelisim.edu.tr>
<http://dergipark.gov.tr/ijet>
Twitter: [@IJETJOURNAL](https://twitter.com/IJETJOURNAL)

Printing and binding:

Anka Matbaa
Certificate Number: 12328
Phone: +90 212 5659033 - 4800571
E-mail: ankamatbaa@gmail.com

International Journal of Engineering Technologies (IJET) is included in:



**International Journal of Engineering Technologies (IJET) is
harvested by the following service:**

Organization	URL	Starting Date
The OpenAIRE2020 Project	https://www.openaire.eu	2015
GOOGLE SCHOLAR	https://scholar.google.com.tr/	2015
WORLDCAT	https://www.worldcat.org/	2015
IDEALONLINE	http://www.idealonline.com.tr/	2018



INTERNATIONAL JOURNAL OF ENGINEERING TECHNOLOGIES (IJET)
International Peer-Reviewed Journal
Volume 4, No 2, June 2018 Printed ISSN: 2149-0104, e-ISSN: 2149-5262

Owner on Behalf of Istanbul Gelisim University
Rector Prof. Dr. Burhan AYKAC

Editor-in-Chief

Prof. Dr. Mustafa BAYRAM

Associate Editors

Assoc. Prof. Dr. Baris SEVİM

Asst. Prof. Dr. Ahmet AKTAS

Asst. Prof. Dr. Yalcin CEKIC

Asst. Prof. Dr. Ali ETEMADI

Publication Board

Prof. Dr. Mustafa BAYRAM

Prof. Dr. Nuri KURUOGLU

Asst. Prof. Dr. Ahmet AKTAS

Asst. Prof. Dr. Yalcin CEKIC

Asst. Prof. Dr. Mehmet Akif SENOL

Layout Editor

Asst. Prof. Dr. Ahmet AKTAS

Copyeditor

Res. Asst. Mehmet Ali BARISKAN

Proofreader

Asst. Prof. Dr. Ahmet AKTAS

Contributor

Ahmet Senol ARMAGAN

Cover Design

Mustafa FIDAN

Tarik Kaan YAGAN

Editorial Board

Professor Abdelghani AISSAOUI, University of Bechar, Algeria

Professor Gheorghe-Daniel ANDREESCU, Politehnica University of Timișoara, Romania

Associate Professor Juan Ignacio ARRIBAS, Universidad Valladolid, Spain

Professor Goce ARSOV, SS Cyril and Methodius University, Macedonia

Professor Mustafa BAYRAM, Istanbul Gelisim University, Turkey

Associate Professor K. Nur BEKIROGLU, Yildiz Technical University, Turkey

Professor Maria CARMEZIM, EST Setúbal/Polytechnic Institute of Setúbal, Portugal

Professor Luis COELHO, EST Setúbal/Polytechnic Institute of Setúbal, Portugal

Professor Filote CONSTANTIN, Stefan cel Mare University, Romania

Professor Mamadou Lamina DOUMBIA, University of Québec at Trois-Rivières, Canada

Professor Tsuyoshi HIGUCHI, Nagasaki University, Japan

Professor Dan IONEL, Regal Beloit Corp. and University of Wisconsin Milwaukee, United States

Professor Luis M. San JOSE-REVUELTA, Universidad de Valladolid, Spain

Professor Vladimir KATIC, University of Novi Sad, Serbia

Professor Fujio KUROKAWA, Nagasaki University, Japan

Professor Salman KURTULAN, Istanbul Technical University, Turkey

Professor João MARTINS, University/Institution: FCT/UNL, Portugal

Professor Ahmed MASMOUDI, University of Sfax, Tunisia

Professor Marija MIROSEVIC, University of Dubrovnik, Croatia

Professor Mato MISKOVIC, HEP Group, Croatia

Professor Isamu MORIGUCHI, Nagasaki University, Japan

Professor Adel NASIRI, University of Wisconsin-Milwaukee, United States

Professor Tamara NESTOROVIĆ, Ruhr-Universität Bochum, Germany

Professor Nilesh PATEL, Oakland University, United States

Professor Victor Fernão PIRES, ESTSetúbal/Polytechnic Institute of Setúbal, Portugal

Professor Miguel A. SANZ-BOBI, Comillas Pontifical University /Engineering School, Spain

Professor Dragan ŠEŠLIJA, University of Novi Sad, Serbia

Professor Branko SKORIC, University of Novi Sad, Serbia

Professor Tadashi SUETSUGU, Fukuoka University, Japan

Professor Takaharu TAKESHITA, Nagoya Institute of Technology, Japan

Professor Yoshito TANAKA, Nagasaki Institute of Applied Science, Japan

Professor Stanimir VALTCHEV, Universidade NOVA de Lisboa, (Portugal) + Burgas Free University, (Bulgaria)

Professor Birsen YAZICI, Rensselaer Polytechnic Institute, United States

Professor Mohammad ZAMI, King Fahd University of Petroleum and Minerals, Saudi Arabia

Associate Professor Lale T. ERGENE, Istanbul Technical University, Turkey

Associate Professor Leila PARSA, Rensselaer Polytechnic Institute, United States

Associate Professor Yuichiro SHIBATA, Nagasaki University, Japan

Associate Professor Kiruba SIVASUBRAMANIAM HARAN, University of Illinois, United States

Associate Professor Yilmaz SOZER, University of Akron, United States

Associate Professor Mohammad TAHA, Rafik Hariri University (RHU), Lebanon

Assistant Professor Kyungnam KO, Jeju National University, Republic of Korea

Assistant Professor Hidenori MARUTA, Nagasaki University, Japan

Assistant Professor Hulya OBDAN, Istanbul Yildiz Technical University, Turkey

Assistant Professor Mehmet Akif SENOL, Istanbul Gelisim University, Turkey

Dr. Jorge Guillermo CALDERÓN-GUIZAR, Instituto de Investigaciones Eléctricas, Mexico

Dr. Rafael CASTELLANOS-BUSTAMANTE, Instituto de Investigaciones Eléctricas, Mexico

Dr. Guray GUVEN, Conductive Technologies Inc., United States

Dr. Tuncay KAMAS, Eskişehir Osmangazi University, Turkey

Dr. Nobumasa MATSUI, Faculty of Engineering, Nagasaki Institute of Applied Science, Nagasaki, Japan

Dr. Cristea MIRON, Politehnica University in Bucharest, Romania

Dr. Hiroyuki OSUGA, Mitsubishi Electric Corporation, Japan

Dr. Youcef SOUFI, University of Tébessa, Algeria

Dr. Hector ZELAYA, ABB Corporate Research, Sweden

From the Editor

Dear Colleagues,

On behalf of the editorial board of International Journal of Engineering Technologies (IJET), I would like to share our happiness to publish the fourteenth issue of IJET. My special thanks are for members of Editorial Board, Publication Board, Editorial Team, Referees, Authors and other technical staff.

Please find the fourteenth issue of International Journal of Engineering Technologies at <http://ijet.gelisim.edu.tr> or <http://dergipark.gov.tr/ijet>. We invite you to review the Table of Contents by visiting our web site and review articles and items of interest. IJET will continue to publish high level scientific research papers in the field of Engineering Technologies as an international peer-reviewed scientific and academic journal of Istanbul Gelisim University.

Thanks for your continuing interest in our work,

Professor Mustafa BAYRAM
Istanbul Gelisim University
mbayram@gelisim.edu.tr

<http://ijet.gelisim.edu.tr>
<http://dergipark.gov.tr/ijet>

Printed ISSN: 2149-0104

e-ISSN: 2149-5262

International Journal of
Engineering Technologies
IJET

Table of Contents

	<u>Page</u>
<i>From the Editor</i>	<i>vii</i>
<i>Table of Contents</i>	<i>ix</i>
• Application of Genetic Algorithm to Solar Panel Efficiency; A Case Study of Port-Harcourt Metropolis /	60-69
Roland Uhumwangho, Berebon Victor Leesi, Ameze Big-Alabo	
• Comparative Experimental FWA & FOWA Aggregated VLCSPPs' LUR Estimation for GIS Based VEED /	70-80
Burak Omer Saracoglu	
• Information Systems for Repair Alternatives and Initial Cost Estimation of Damaged Building Structures /	81-89
Can Balkaya	
• Investigation of Natural Frequency for Continuous Steel Bridges with Variable Cross-sections by using Finite Element Method /	90-102
Hüseyin Sağlık, Bilge Doran, Can Balkaya	
• A General Approach to Accreditation of Environmental Laboratories in Turkey /	103-107
Perihan Akan, Ozlem Muge Testik	
• Investigation on Industry 4.0 and Virtual Commissioning /	108-114
Akın Aras, Murat Ayaz, Engin Özdemir, Nurettin Abut	
• A Novel Method for Increasing the Noise Immunity of Military Radio Systems via Self-Tuned Phased Array Antennas /	115-118
Yalcin İsayev, Mustafa Emre Aydemir, Ahed İsayev, L.H. Mammadova	
• Analysis of a Soft Switching High Voltage Gain DC/DC Boost Converter for PV Systems /	119-123
Sarah Al-Hajm, Mehmet Ucar	
• A Parallel Iterated Local Search Algorithm on GPUs for Quadratic Assignment Problem /	124-128
Erdener Özçetin, Gürkan Öztürk	

International Journal of Engineering Technologies, IJET

e-Mail: ijet@gelisim.edu.tr

Web site: <http://ijet.gelisim.edu.tr>
<http://dergipark.gov.tr/ijet>

Twitter: [@IJETJOURNAL](https://twitter.com/IJETJOURNAL)

Application of Genetic Algorithm to Solar Panel Efficiency; A Case Study of Port-Harcourt Metropolis

Roland Uhumwangho*, Berebon Victor Leesi *[‡] and Ameze Big-Alabo*

*Department of Electrical/Electronic Engineering, Faculty of Engineering University of Port-Harcourt
East-West Road, Choba, Port Harcourt, Rivers State, P.M.B. 5323
tripodeng@yahoo.com, adokorvictor@gmail.com, ameze.odia@uniport.edu.ng

[‡] Corresponding Author; Second Author, Tel: +234(0)8030975526,

Received: 09.12.2017 Accepted: 16.04.2018

Abstract

This study focuses on the evaluation of solar panel efficiency used within Port Harcourt environment. A major factor affecting the efficiency of solar panels is the difference in region or weather and the ability of the solar panel to convert incident radiation into electrical energy. Solar panels have varying efficiency levels under different weather conditions. Most times solar panels fall short of expected efficiencies. It is therefore important to have adequate knowledge of the performance characteristics of a panel under specific weather to ensure maximum output. For this research work, the panel whose efficiency was evaluated is China Solar 125W. The panel is a Polycrystalline solar panel made of Gallium Arsenide having a very high surface recombination ability. The panel has 72 cells and a cross sectional area of... To evaluate the efficiency of the panel two methods were adopted to establish the response of the panel specific to Port Harcourt weather. The first method involved taking hourly reading of the parameters of the panel by subjecting the panel to outdoor atmospheric condition and recording the values obtained and comparing the result with that on the manufacturers sheet. The second method involved the collection of weather data. The weather data for Port-Harcourt was collected from the center for data collation Rivers State University. The peak radiation value obtained from the weather data for the year under consideration is used to calculate the efficiency of the panel and the value obtained compared with the maximum efficiency stipulated by the manufacturer. This efficiency was found to be low. Genetic Algorithm was then used to determine the optimal parameters of the cells making up the panel to obtain an optimized cell to improve the efficiency of the panel. To do this the cell initial properties were extracted and tabulated genetic algorithm used to improve this properties achieving better efficiency in the process.

Keywords: Genetic Algorithm, Solar Panels, Weather, Optimization, Efficiency.

1. Introduction

The issue of power generation still remains remarkably an issue of concern especially in the developing countries. The current practice in the electrical industry according to Balzhiser and Richard (1977) favors a shift from the conventional power generation techniques to a much more modern one, (renewable energy). Chief among the various renewable energy sources is

the sun. In order to harness this energy effectively the use of specially designed solar panels is required. Solar panels are made of solar cells designed to trap incoming solar radiation and convert them into useful energy in the form of electricity. The efficiency of the solar cell is very important in defining the overall performance of the panels itself.

1.1 Aim and Objectives

The aim of this research work is to improve the efficiency solar panels using genetic algorithm.

The objectives are:

To evaluate the selected solar panel for cell efficiency.

To use genetic algorithm to determine the most appropriate parameters of the cell to give maximum efficiency.

1.2 Limitation

The cell efficiency is influenced by a number of factors including the weather of the immediate environment of installation. Panel performance in Port Harcourt is found to be usually poor and therefore an improvement in the efficiency of the panel is desired if proper use is to be made of the abundance of sunlight that characterizes this place.

2. Literature Review

In the design of photo voltaic systems, the major challenge has always been to optimize the panel for better efficiency. Therefore, several methods have been employed to attempt an improvement in one aspect or the other using different applications. Among these methods the most popular been HOMER PRO, PVPLANNER, and PV-F CHART.

HOMER PRO

This is most suitable for micro grid systems; it is not designed specifically for pv systems. Though it has the capacity to accommodate a large amount of data, it's major short coming is the fact that it presents results of pv system optimization in a less comprehensible manner.

PVPLANNER

This software provides accurate satellite data making solar radiation and and pv power estimation easy. It also automatically calculates shading. Long term annual and monthly data is included in the basic design. The software therefore has the constraint of preventing data from other sources.

PV-F CHART

The pv chart calculates power based on generic module and inverter. The data must be inputted manually making quick comparison of generation data difficult. Its major constraint

though is that it is not suitable for power calculation in real world situation.

Genetic algorithm is defined as a robust search parameter technique that is based on Darwins principle of natural selection and survival of the fittest (Anisha et al 2014). Genetic algorithm differs from the conventional algorithms in the sense that it can handle a larger set of data than the conventional algorithm. This makes Genetic algorithms to more robust in nature than the conventional method. Genetic algorithms are also very easy to use (as compared to the other methods). This is because genetic algorithms eliminate the burden of solving complex derivatives associated with differential algorithms.

Several methods have been used to optimize one aspect of solar photovoltaic systems or another with huge success for instance, Nanget2010 carried out a research with the aim of establishing the correct angle of tilt for a solar panel to attract maximum sunlight. In Nangets work differential algorithm was employed with success and it was established that inclining panels relative to the sun produced better result and hence aided in the improvement of efficiency. However, the difference in latitude means no angle is absolutely ideal. Therefore, panel installers still have to maximize output by locating and placing the panels at the correct angle within the installation site.

Rizala, Hasta and Feriyadi (2013) in their research applied genetic algorithm successfully to track sunlight. This method ensures maximum ray is incident on the panel at all times. It is important to point out here that exposing panels to excessive sunlight may increase the top and ultimately destroy the cell.

2.1 Applications

Genetic algorithms find useful applications in sciences, Engineering and even management. They have successfully been used for timetabling and scheduling operations such as job shop scheduling, scheduling in printed circuit board assembly among many other useful applications examples are climatology, bioinformatics as well as design of anti-terrorism systems. They are also key components of mobile communication infrastructure optimization.

Genetic algorithm has also been used to optimize the cost of solar panels. Bernal and Lopez (2009) used genetic algorithm in their research work to minimize the cost of solar pv arrays. The positioning of sun trackers to maximize the collection of the solar radiation on the panels is another area where genetic algorithm has been used extensively with high degree of success.

3. Materials and Methodology

The method used in this paper involved selection of the solar panel taking into consideration its efficiency in relation to the Port Harcourt weather. This is important for establishing varying latitudes on the panel performance. This is because a

panel offering high efficiency in one area may not necessarily do same in another area due to the latitudinal differences.

Port Harcourt is the capital and largest city of Rivers State, Nigeria, with coordinates latitude 4 46' 38" and longitude 7 00' 48". Port Harcourt has an elevation of about 52fts above sea level. The driest month is January and the month with the highest precipitation is September. It lies along the Bonny River and is located in the Niger Delta.

As of 2016, the Port Harcourt urban area has an estimated population of 1,865,000 inhabitants, up from 1,382,592 as of 2006. The dense population of Port Harcourt makes for very high demand in electrical energy

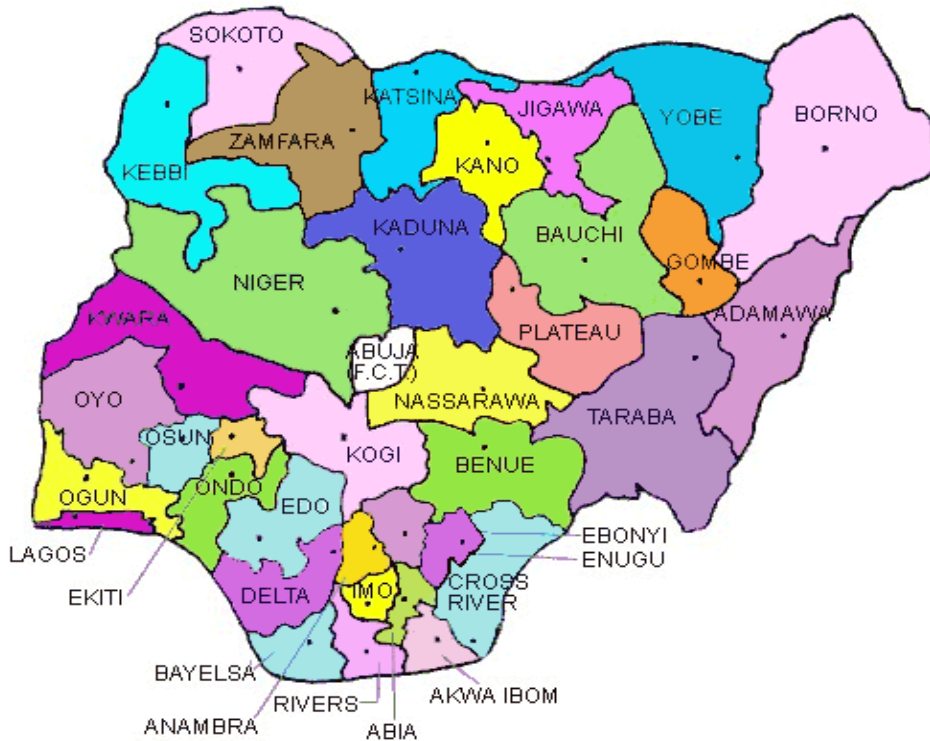


Fig. 1. Map of Nigeria highlighting the position of River State at the bottom.

The selected solar panel has a rating of 125 W and is made of gallium arsenide cells. The panel in consideration has a dimension of 67cm x 147cm and is made up of 36 cells. The panel data sheet was obtained and the data collected and recorded. The panel was then subjected to test by placing it on a roof top and taking hourly measurements using a

Multimeter. Consequent results showed a variation in parameter values indicative of the effect of the different intensity on the panel efficiency though these changes were only small.

Table 1. showing hourly variation in open circuit voltage against time from 6am to 6pm

Time	6	7	8	9	10	11	12	1	2	3	4	5	6
Voc	15.1	16	17.6	18.8	19.2	19.2	18.04	18.7	18.8	18.4	18.4	18.0	15.0

3.1 Efficiency Evaluation of a (125W) Gallium Arsenide Solar Panel

Next, the weather data comprising amount of rainfall, wind speed, relative humidity, and solar intensity spanning a year was collected from the Centre for Data Collation and Analysis Rivers State University Port Harcourt. The peak radiation value obtained from the collated data was used to evaluate the efficiency of the panel. A section of the table of weather data

showing the peak radiation value for the period in consideration is extracted and given in the table 1 below due to the volume of the data.

The peak value was chosen to maximize output. From table 2 this value is 606 W/m². The area of the panel in meter was calculated and recorded as 0.9849 m²

Table 2. showing an extract of Port Harcourt Weather Data

TOA5	PORT HARCOURT									
RECORD	Batt_Volt_Min	Rain_m m_Tot	SlrW_ Avg	AirTC _Avg	RH	T107_C _Avg	WS_ms _Avg	WindDir	Bar Press _Avg	VW
RN	Volts	Mm	W/m ²	Deg °C	%	Deg °C	Meters/ Second	Degrees	mV	
	Min	Tot	Avg	Avg	Smp	Avg	Avg	Smp	Avg	Smp
51818	13.98	0	606.6	33.49	49.15	29.11	1.903	41.87	1047	0.131
51819	13.96	0	594.8	33.65	48.5	29.12	0.957	26.87	1048	0.13
51820	13.95	0	596.5	34.17	46.22	29.18	1.206	62.7	1049	0.13
51821	13.95	0	599.9	34.41	45.99	29.18	0.913	190.7	1049	0.131
51822	13.93	0	592.5	34.9	45.48	29.21	0.757	32.84	1051	0.131
51823	13.78	0	491.2	34.45	48.23	29.26	1.6	354.8	1052	0.13
51824	13.84	0	548.2	34.58	46.09	29.25	1.995	345.3	1052	0.131
51825	13.81	0	395.2	34.31	47.21	29.25	2.122	8.99	1052	0.131
51826	13.82	0	270.6	33.87	48.53	29.25	2.221	21.51	1050	0.131

Source: Centre for Data Collation Rivers State University

In the design of photovoltaic panels, the efficiency is defined as the ability of the panel to convert incoming solar radiation into useful energy. Efficiency is therefore dependent on the cells ability to trap and convert the incident radiation. It is important to determine the efficiency of panels so that manufacturers and installers or solar panels would easily be

able to define what panel would be suitable for installation for a given power.

Manufacturers define the efficiency of a panel to be the ratio of the power to the product of the incident radiation and area. For the panel in consideration,

$$\text{Max Efficiency} = \frac{P_{max}}{S \times A_c} \quad (3.1)$$

$$eff = \frac{125}{\frac{(67 \times 147)}{10,000} \times 1000} = 12.7\% \quad (3.2)$$

Efficiency evaluation of the proposed optimized model of solar cell

The cell structure is basically an NP GaAs cell. Between the substrate and cell is sandwiched a doped P+ with the primary function of creating an electric field delayed rear face. This is to lower the recombination rate and improve the electrical characteristics of the cell.

The efficiency of the cell is dependent on the following factors:

- The short circuit current density
- Open circuit voltage
- The current density due to intensive concentration of GaAs.

3.2 Efficiency Optimization with Genetic Algorithm Technique

The optimized efficiency is calculated using the relation below:

$$\eta = J_{sc}(V_{oc} - \beta) / s_{ol} \quad (1.2)$$

$$\alpha = 1 + \ln(1 + V/V_T) \quad (1.3)$$

$$\beta = V_T \times \alpha \quad (1.4)$$

Where

s_{ol} = peak optical power density = solar irradiance at temperature of 301K.

This is achieved by the help of the genetic algorithm.

Optimization Technique

The objective function is defined as;

$$F_{obj} = \text{maximize } (eff)$$

By optimizing the constraint function:

$$F [x(1), x(2), x(3), x(4) x(5)]$$

Where

x(1) = Doping of base

x(2) = doping of p-layer

x(3) = doping of n-layer

x(4) = width of base

x(5) = cell voltage.

These are the parameters to be optimized in order to improve and optimize efficiency

Table 3. Range structure of Solar cell before optimization.

S/No	Parameters	Range of Values
1	Calculated Efficiency (%)	12.7
2	x(1), Doping of base (cm ⁻³)	[1e20 to 1e25]
3	x(2), Doping of P-layer (cm ⁻³)	[1e20 to 1e25]
4	x(3), Doping of n-layer (cm ⁻³)	[1e20 to 1e25]
5	x(4), Doping of width of base (cm)	[1e-7 to 1e-5]
6	x(5), Doping of cell Voltage (V)	[0.5 to 1]

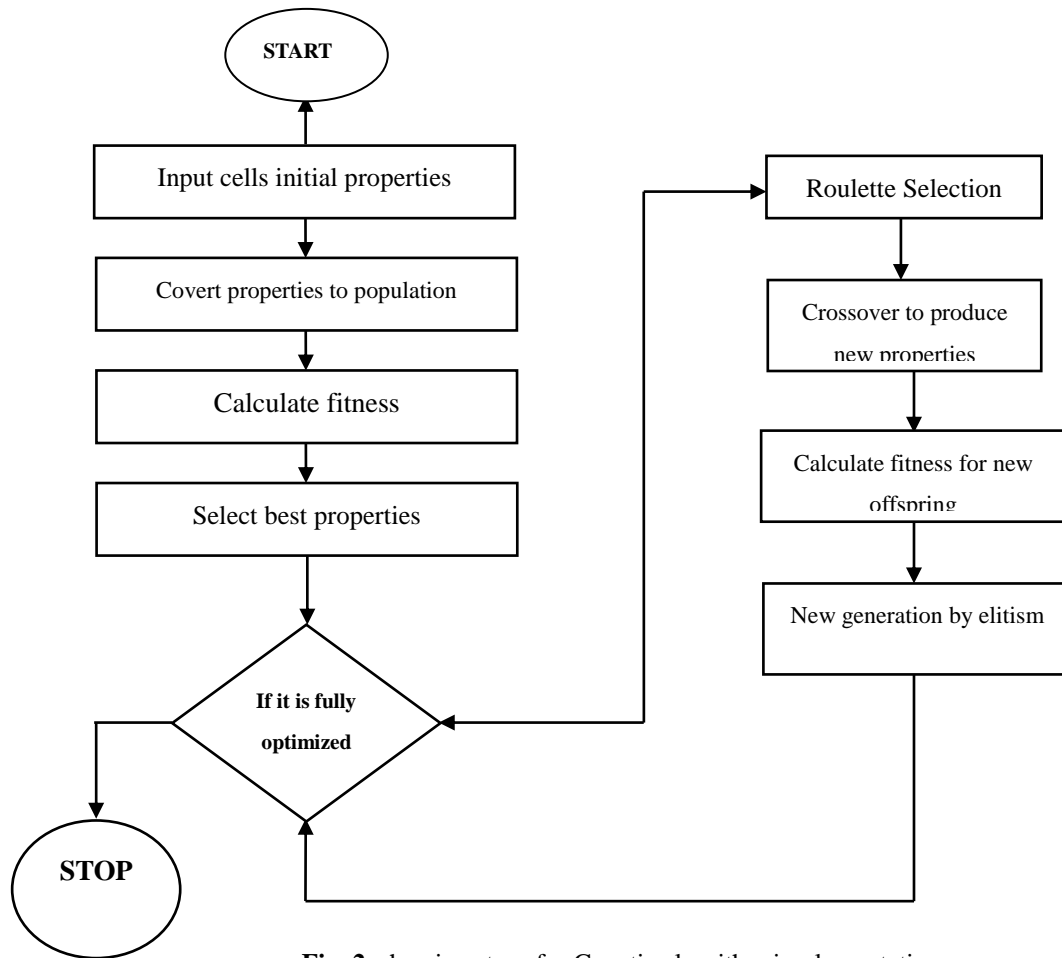


Fig. 2. showing steps for Genetic algorithm implementation

The cell properties given in table 1 above and the weather data in table 2 were fed into the program with the function set to maximize efficiency.

The initial properties of the cell were converted by the program into population

Fitness for each parameter was calculated with maximum radiation kept at 606w/m^2

The system was programmed to run for 2mins and to repeat until a value representing the maximum for each parameter corresponding to the peak radiation value obtained.

When this values are reached the program ends. The new values obtained represent the maximum and therefore the optimized values of the parameters.

Results and Discussions

Results

The results presented here show the efficiency of the panel at different solar cell parameter variations. The results are presented as below in figure 3 to figure 7.

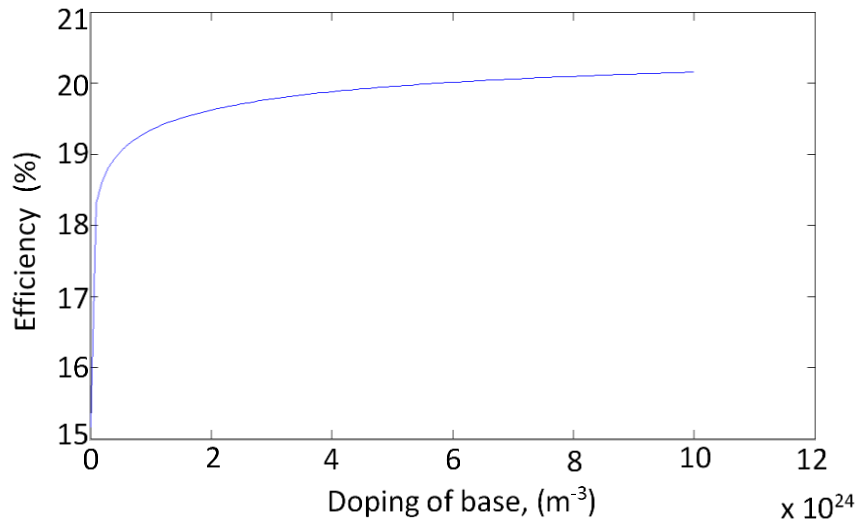


Fig. 3. Optimal Efficiency as function of doping of Base of solar cell

Fig. 3 shows the efficiency of the solar cell as function of optimizing the base layer of the solar cell. The value of the efficiency gotten by optimization of the solar cell is said to be maximum at the point with which the base of the solar cell is doped to optimal position. From the graph the value of the

efficiency is measured to be 20.1538% at an optimal base value of $1e^{-25}$ centimeters. The graph confirms that as more and more the base layer of the solar cell is doped, the efficiency becomes improved gradually until it reaches its optimal value

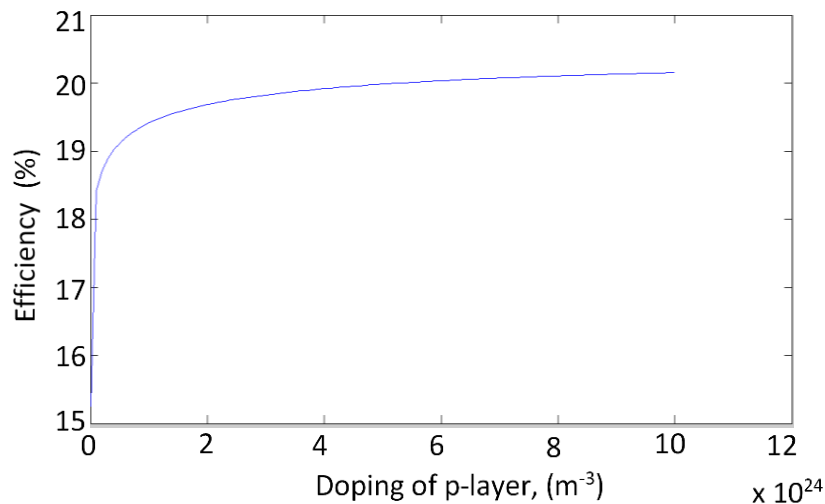


Fig. 4. Optimal Efficiency as function of doping of P-layer of solar cell

Similarly, Fig. 4 also records the efficiency of the solar cell at an optimal doping level of the p-layer of the solar cell. The doping optimizes the p-layer and as such produces the best efficiency at the optimum doped layer of the p-layer. The efficiency is measured to be 20.1538% at an optimal p-layer doped surface of $1e^{25}$ centimeters. The graph confirms that as

more and more the p-layer of the solar cell is doped, the efficiency becomes improved gradually until it reaches its optimal value. Although, the variation in p-layer doping level did not cause a large change in efficiency as the values of efficiency is almost constant at varying p-layer doping level of solar cell.

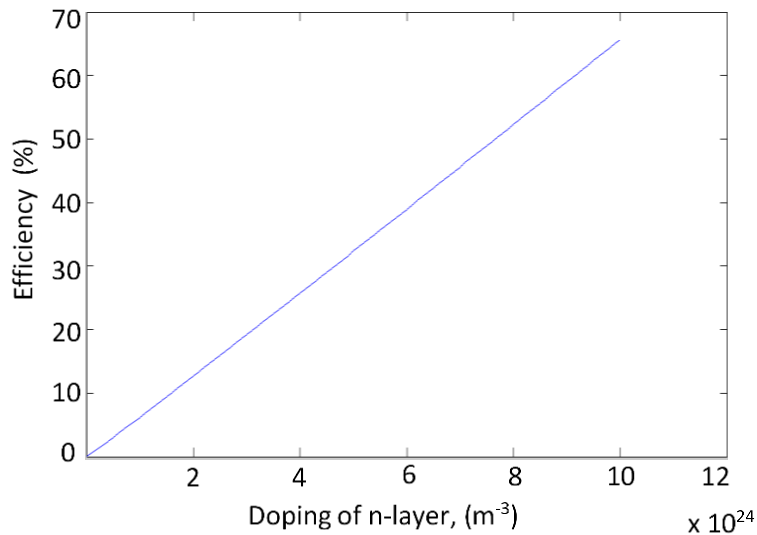


Fig. 5. Optimal Efficiency as function of doping of n-layer of solar cell

Also, fig. 5 shows the evaluated efficiency of the solar cell at an optimal doping level of the n-layer of the solar cell. The doping optimizes the n-layer and as such produces the best efficiency at the optimum doped layer of the n-layer. The efficiency is measured to be 20.1538% at an optimal n-layer doped surface of $4.345e24$ centimeters. The graph also shows

that as more and more the n-layer of the solar cell is doped, the efficiency becomes improved until it reaches its optimal value. Although, the effect of doping the n-layer on efficiency is minimal compared to the effect on efficiency when p-layer is doped, the efficiency greatly varies at varying n-layer doping level.

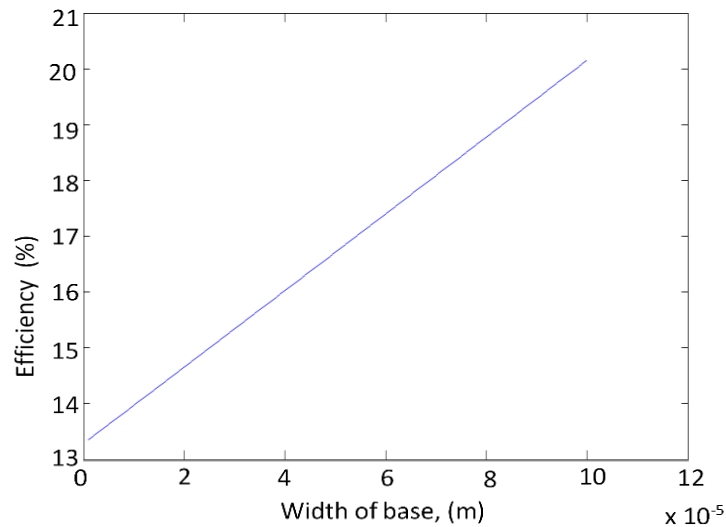


Fig. 6. Optimal Efficiency as function of varying width of base of the solar cell

Fig. 6 shows the variations of the width of the base at optimum efficiency. The efficiency is determined at the point where the value of the optimum solution for the width of the base of the solar cell is achieved. The efficiency is 20.1538% at

optimal doped width of the base gotten at $1e-0.5$ centimeters. The graph shows that as the width of the base of the solar cell is doped, the efficiency becomes improved rapidly until it reaches its optimal value. The variation effect of the width of

the base caused a significant variation in efficiency.

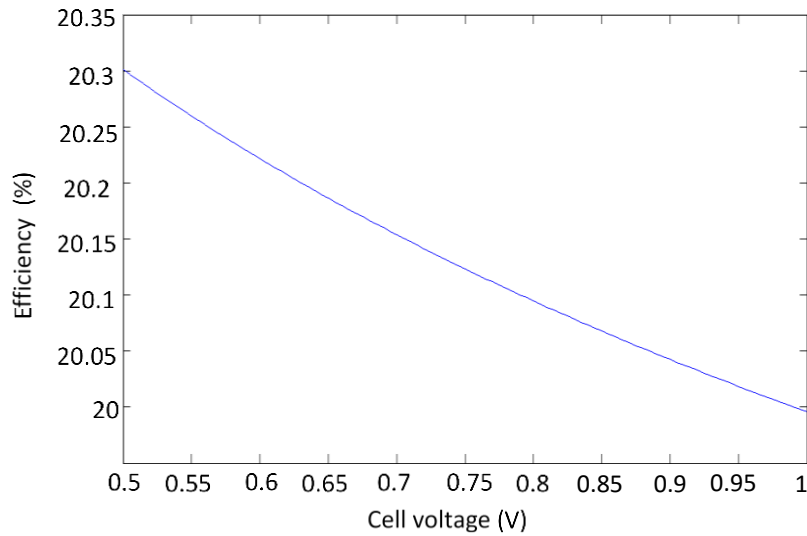


Fig. 7. Optimal Efficiency as function of varying cell voltage of the solar

Finally figure 7 plots the efficiency at varying cell voltage. At the point where the cell voltage is optimum, the maximum solar cell efficiency is determined. The value of efficiency at optimal cell voltage is read from the graph as 20.1538%. The optimal cell voltage is gotten as 0.7V. The graph also illustrates that as one increases the cell voltage above a certain initial threshold value, the efficiency of the cell will drop very insignificantly until it arrives at its optimal point where the value of the cell voltage at that point gives the best efficiency under any operating condition of the panel.

From Table 1 and 2, the value of the optimized efficiency is seen to have improved from 11.17% to 20.15% respectively.

This new efficiency value is as a result of optimizing the parameters $x(1)$, $x(2)$, $x(3)$, $x(4)$, and $x(5)$. The optimization of the parameters is referred to as doping of the layers of the solar cell so as to maximize efficiency of the solar cell at any time of the day and peak daily radiation (solar irradiance).

Similarly, the range of the solar parameters shown initially in table 1.1 was optimized and its best optimum point where computed with help of the genetic algorithm as shown in table 4.

Table 4. Results of simulation

S/No	Optimized Parameters	Optimal Values
1	Optimized Efficiency (%)	20.15
2	$x(1)$, Doping of base (cm^{-3})	$1.0\text{e}+25$
3	$x(2)$, Doping of P-layer (cm^{-3})	$1.0\text{e}+25$
4	$x(3)$, Doping of n-layer (cm^{-3})	$4.3\text{e}+24$
5	$x(4)$, Doping of width of base (cm)	$1.0\text{e}-05$
6	$x(5)$, Doping of cell Voltage (V)	0.7

4. Conclusion

The cell properties as given in table 1 and the solar radiation data as given in table 4 were fed into the program and the function set to maximize efficiency by maximizing component values of the solar cell subject to the maximum radiation. The program was designed to run for two minutes and stop when maximum values are reached.

The result of the research shows an improvement of 2.15% on the initial efficiency of the panel. This improvement is as a result of optimizing the parameters $x(1)$, $x(2)$, $x(3)$, $x(4)$, and $x(5)$. This is achieved using genetic algorithm and hence proves genetic algorithm adequate to optimize solar panel efficiency

5. Recommendation

It is my recommendation that before installation, selected panels should first be evaluated for efficiency as weather varies. Although silicon is widely accepted as the best material for pv panels because of its availability, other materials can give similar results on optimization. Finally, genetic algorithm should be used for parameter selection in the design stage of the panel to give optimal result.

Acknowledgement

I want to briefly acknowledge the efforts of the following persons and institutions for their contributions to the success of this work. My father Mr Adokor MkinéBari, the director and staff of the centre for data collation Rivers State University, Staff of the Rivers State Sustainable Development Agency and Professor Christopher Ahiakwo for their unending supports through the course of this research work

References

- [1] Balzhiser and Richard E. (1977) R &D Status report “fossil fuel and advance system division” EPRI Journal vol. 2 (No.5) pp 49 – 53.
- [2] Bernal-Augustine, J. L.; Dofó Lopez, R (2009) Multi-objective design and control of hybrid systems minimizing cost and unmet loads. *Electrical power research* Vol. 79, pp 170 – 181.
- [3] Durand, H. L (1979) “Present status and prospects of photovoltaic energy conversion; proceeding of the photovoltaic solar energy conversion conference pp 93-105
- [4] Enrique, J. M., Duran, E. Sidrach-de-cardona, M. Andjuor, J. M. (2007) Theoretical assessment of the maximum power point tracking efficiency of photo voltaic facilities with different converter topologies. *Solar energy*, vol. 81, issue 1 pp 31-38
- [5] Furkan, D., Mehmet, E. M. (2010) “Critical factors that affect solar cells, smart grid and renewable energy, Vol. 1, pp 47-50
- [6] Haupt, R. L., Haupt, S. E., (1998). *Practical Genetic algorithms* (New York: Wiley)
- [7] Holland, J. H. (1992) *Adaption in Natural and Artificial System* MIT Press, Cambridge, MA
- [8] Omubo-Pepple, V. B., Israel-Cookey, C. I. Alamino, K (2009) “Effect of Temperature, flux and relative humidity on the efficient conversion of solar energy to electricity” Department of Physics, Rivers State University of Science and Technology *European Journal of Scientific Research* Vol. 35, No.2, pp 173-180.
- [9] Peippo K., Lund P.D. (1994). Optimal size of solar array and inverter in grid connected photovoltaic cell interconnection circuits.
- [10] Rizala, Y. Hasta, S., and Feriyadi, W. (2013) “Application of solar position Algorithm for sun tracking, system energy procedure. Vol. 32, pp 160-165
- [11] Storn, R and Price, K. V (1997) Differential evolution a simple and efficient heuristic for global optimization over continuous spaces *Journal of Global Optimization* pp 341-35.

Comparative Experimental FWA & FOWA Aggregated VLCSPPs' LUR Estimation for GIS Based VEED

Burak Omer Saracoglu*

*Orhantepe Mahallesi, Tekel Caddesi, Istanbul, Turkey

‡Burak Omer Saracoglu, Orhantepe Mahallesi, Tekel Caddesi, Istanbul, Turkey, burakomersaracoglu@hotmail.com

Received: 16.12.2017 Accepted:16.05.2018

Abstract- Solar power conversion technologies are photovoltaics (PV), concentrated solar power (CSP), and concentrated photovoltaics (CPV). These technologies need sufficient amount of appropriate land. In super grids and Global Grid, large sized power plants play the key role, so that this study only focuses on very large solar power plants (VLSPP). VLSPPs are defined as the power plants that have the installed power of 1.000 MW (peak in PV) or more in this study. Solar land use requirements (LUR) should be studied, analyzed and estimated for each solar power technology. This study investigates only the LUR of very large concentrated solar power plants (VLCSPPs). Under unsharp conditions, a fuzzy weighted average/weight averaging (fuzzy WA: FWA) aggregated and an ordered fuzzy weighted average/weight averaging (fuzzy OWA: FOWA) aggregated solar LUR models on a worldwide basis are built for LUR prediction on the geospatial information systems (GIS) at the very early engineering design (VEED) phase. These two models are presented in a comparative way. Five experimental criteria (direct normal irradiance: DNI, engineering design year, net installed power, cooling method, storage capacity) are only included in these models. The mean absolute percentage error (MAPE) of land area (hectares) and solar field aperture area (m²) are respectively %331,35 (FWA), %505,14 (FOWA) and %914,86 (FWA), % 1374,45 (FOWA).

Keywords Concentrated solar power, FuzzME, Fuzzy Ordered Weighted Average, Fuzzy Weighted Average, land use requirement.

1. Introduction

Solar power can supply the largest electricity amount to humans by 89.000 TW_p theoretical, 58.000 TW_e extractable, and 7.500 TW_c technical world potential estimations (TW_p: terawatt equivalent photonic fuel power, TW_c: terawatt equivalent chemical fuel power) [1]. It is presented that only 0,00015 TW_c was supplied in 2001 [1].

The research, development, demonstration, and deployment (RD³) engineers try to increase the usage of this resource. In today's capabilities, there are three solar power technologies: photovoltaics (PV) [2], concentrated solar power (concentrating solar power, concentrated solar thermal) (CSP) [3], concentrated photovoltaics (CPV) [4].

Today, the CSP technology is usually classified under parabolic trough, linear Fresnel, power tower, and parabolic dish technologies [5,6] as shown in Fig.1. This study investigates all of these CSP technologies at once.

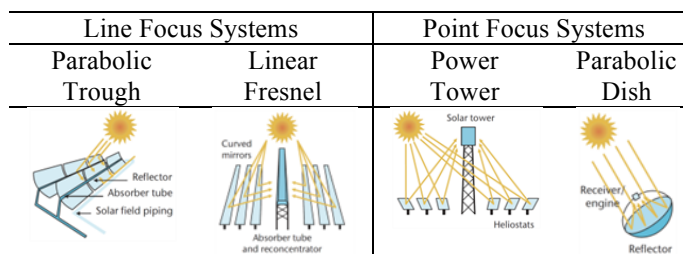


Fig. 1. CSP technology families (Source: [5,6]).

The most efficient investment approach in solar power plants is by economies of scale approach (see [7] for economies of scale). As a result, large size solar power plants shall first be investigated in detail.

Very large concentrated solar power plant (VLCSP) concept is researched in this manner. The definition isn't

clear yet, but it is discriminated as the CSP plants that have the installed power of 1.000 MW or more [8].

The most effective way of generating and consuming of electricity is also by considering economies of scale. Therefore, super grids and Global Grid are researched and tried to be modelled and designed (e.g. European Supergrid [9], Supergrid for America [10], DESERTEC [11], Gobitec [12,13], Asian Super Grid [12,13], Global Grid [14]).

A detailed literature review on Google Scholar [15] and Directory of Open Access Journals [16] was performed by some key terms in this study. It had been observed in previous studies that Google Scholar had been the most dominant academic publication online database (highest number of documents for each search term: author's experience). Moreover, both of these online websites had "open access" publications, so that all RD³ engineers would be able to find these publications.

The search term of this study was "land use" and "concentrated solar". Only English documents were searched on Google Scholar (1930 results) and Directory of Open Access Journals (0 results) until 21/12/2015. The titles and abstracts were first reviewed and the related documents (papers, reports, presentations, etc.) with this study were saved in their specific folder (only 19 studies). After this observation, previously known documents on some websites (e.g. [17-21]) were also once more checked. Only a few documents could be added, but one of them was the most important one (Ong et.al.'s study at the National Renewable Energy Laboratory (NREL): author's point of view).

Ong et.al. studied the direct land use ("disturbed land due to physical infrastructure development") and the total land use ("all land enclosed by the site boundary") requirements of the utility scale ground mounted small and large photovoltaic (PV) and concentrating solar power (CSP) plants in the United States [22]. There were 25 projects with a capacity (MW_{AC}) of 3747 in the total land use requirements for CSP plants (parabolic trough, tower, dish Stirling, linear Fresnel) analysis. The capacity weighted average land use ($acres/MW_{AC}$) was presented as 10 and the generation weighted average land use ($acres/GWh/yr$) was given as 3,5. There were 18 projects with a capacity of 2218 in the direct land use requirements analysis. The capacity weighted average land use was presented as 7,7 and the generation weighted average land use was presented as 2,7. In their dataset, the least installed power (MW_{AC}) was 1,5 (Maricopa Solar Project with Stirling Engine) followed by 5 (Sierra SunTower with tower). The most installed power was 370 (Ivanpah all with tower) followed by 354 (SEGS all with parabolic trough) and 280 (Solana all with parabolic trough) [22]. Purohit et.al. investigated the possibility of generating electricity from CSP technologies (parabolic trough collector, linear Fresnel reflector, central receiver system: tower with heliostats, parabolic dish) in the Northwestern India [23]. They presented that the area (collector/heliostat) (m^2) was 34–550 (parabolic trough), 40–120 (central receiver), 92 (dish). They also added that the land requirement (m^2/MW) was 40000 (parabolic trough), 83600 (central receiver), 18000 for linear Fresnel and 16000 for

dish [23]. Other studies also gave some similar information (see [24-29]).

It was understood that fuzzy WA and OWA aggregated based models hadn't been applied in any CSP LUR analysis study until 21/12/2015. Hence, this study is also one of the first studies that step up VLCSP designs on the World, however, it had to be underlined that there were already some announced intentions (Morocco's Noor-Ouarzazate Solar Complex aimed 2000 MW, designed as only for 510 MW by I, II, III at a cost of US\$ 2677 million [30,31,32], Oman's Miraah aimed 1021 MW thermal only for steam at a cost of US\$ 600 million [33,34], China's Ordos aimed 2000 MW at a cost of US\$ 5 billion [35,36], Tunisia's TuNur CSP farm aimed 2250 MW at a cost of US\$ 13.8 billion, with a note of the DESERTEC's cancellation/withdrawal at a cost of US\$ 530 billion [37,38,39,40]). Thus, VLCSP designs are only remained as intentions today.

Shortly; it is deducted that by looking at figures E-1 to E-4 on [22], LUR and capacity of CSP plants in the U.S.A. don't show any linear characteristics. It is stated that this study is most probably a unique (the only one and first) in this field in this respect. There are five aims of this study as to start helping to model Global Grid, to start helping design process of VLCSPs in Global Grid and other grids, to start helping to find possible alternative VLCSPs locations in Global Grid by geographic information system (GIS) tools (e.g. ArcGIS, Google Earth, Netcad) in very early engineering design (VEED) stages, to start studying LUR estimations of VLCSPs and CSPs, to start modelling LUR estimations by fuzzy weighted average/weight averaging (fuzzy WA) aggregated models and ordered fuzzy weighted average/weight averaging (fuzzy OWA) aggregated models, to start a GIS tool RD³ for VLCSP design process.

2. Preliminaries & Experimental Fuzzy WA & OWA Models for VLCSP Design GIS Tool

These experimental proposed fuzzy WA and OWA aggregated models have 5 factors/inputs and 2 outputs/findings (Factor 1: F_1 : Direct Normal Irradiance, F_2 : engineering design year, F_3 : net installed power, F_4 : cooling method, F_5 : storage capacity factors, Finding 1: O_1 : solar field aperture area, O_2 : land area). The author believes that simple models obeying strictly main principles and approaches will show the RD³ progress direction (factor reduction or increment, defining membership functions). One of the important modelling principles in this subject is the magical number 7 (George Armitage Miller (1920–2012) (magical number 7) [41], Richard M. Shiffrin (1968–alive) and Robert M. Nosofsky (alive) (magical number 7, 7 ± 2 rule) [42]). Accordingly, only 5 factors are used in this study as:

- F_1 : Direct Normal Irradiance (DNI) ($kWh/m^2/year$):

"direct irradiance received on a plane normal to the sun over the total solar spectrum" [43]. DNI is used for CSP and concentrating photovoltaic (CPV) systems [8,43,44]. Solar spectrum discrimination isn't taken into account in this study.

CSP minimum DNI rule of thumb or application (kWh/m²/year): 2000 [6], 1800 (technical), 2000 (economical), 1600 (future technical) [23], 902 (demonstration solar tower), 2012 (commercial example) [26], 2000 (commercial) [28], 1800 (5 kWh/(m² day) [29], 800–900 W/m² (normal incident radiation), 1600–2800 kWh/m² (annual normal incident radiation) [45], 2,2 MWh/m²/year or 6,0 kWh/m²/day (annual average) [46], limited suitability below 1800, suitable 1800–2000, highly suitable 2000–2500, excellent 2500–3000 [47], 800 W/m² (normal incident radiation) and range 1600–2800 [48].

Location & design constraint: DNI ≥ 1600 kWh/m²/year (decision in this study).

It can be seen on Fig.2, that the possible VLCSPPs' regions are dispersed on the World very smoothly just like created for only super grids and Global Grid. The Creator wants us to think on a worldwide basis (only one piece, spacious enough). Hence, super grids and Global Grid is seemed very possible.

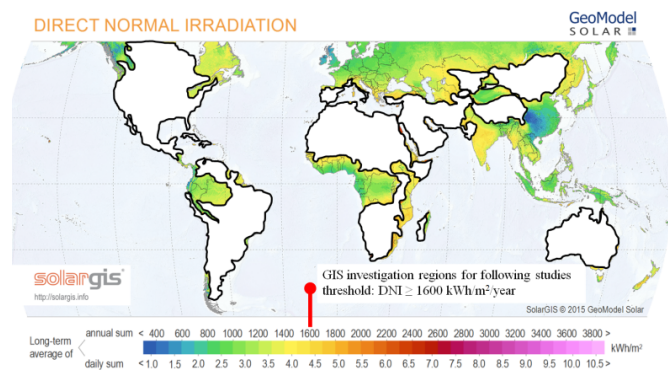


Fig. 2. Rule of thumb representation on DNI World Map for following GIS investigation studies (white regions) (Basemap: GeoModel Solar [49]) (generated by Microsoft Office Excel 2007 <https://products.office.com/en-us/home> or Apache OpenOffice 4.1.5 <http://www.openoffice.org/> & Paint.NET <http://www.getpaint.net/index.html>).

➤ F₂: Engineering Design Year:

The RD³ engineer (author) thinks that technical and technological breakthroughs are important in CSP technology, so that it should be taken into account during modelling.

The author (also by his own conceptual design studies) very well knows and experiences that design date and grid connection date has more than some decades duration gap. Technical and technological capabilities are related to design. Hence, engineering design years are tried to be estimated in this study (10 years earlier than generation start date).

➤ F₃: Net Installed Power (Net Turbine Capacity in MW):

This factor is the most important factor in this study. When the installed power of a CSP plant increases the LUR increases. The net installed power and the net turbine capacity are used in the same manner in this study. The unit is taken as megawatt (MW). The current model covers up to 5.000 MW according to design of 1.000 MW at first.

➤ F₄: Cooling Method:

There are three systems (wet: once-through or recirculating, dry: direct or indirect, hybrid: water conservation or plume abatement) [50,51]. The design preferences are made according to water availability. The current model has two distinguishable systems as wet and dry cooling methods.

➤ F₅: Storage Capacity (hours):

There are three main thermal energy storage concepts as active (two-tank systems, thermocline, steam accumulators), passive (enhanced heat structures, packed bed systems) and combined according to Kuravi et.al.'s approach [52]. The Energy Initiative Massachusetts Institute of Technology has two groups (short term and long term thermal energy storage) [53]. The author thinks that this factor is important in this study, because the LUR varies with these criteria.

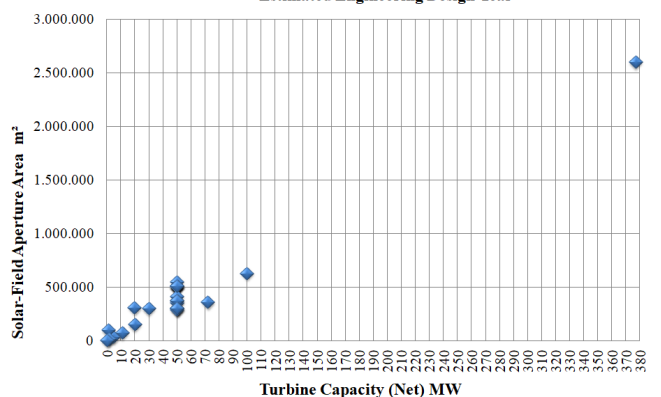
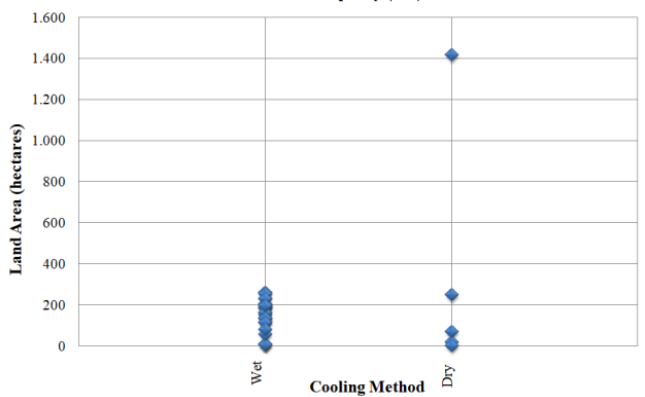
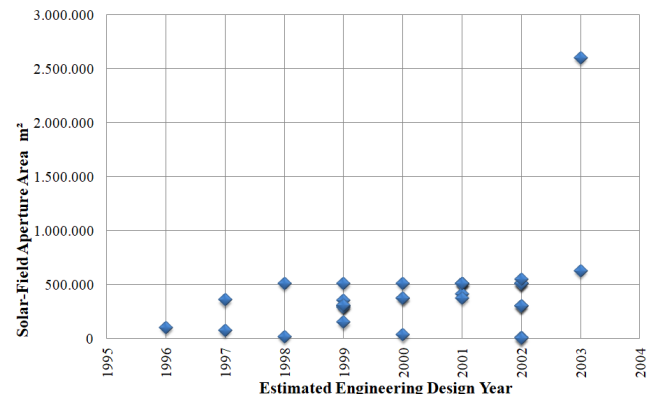
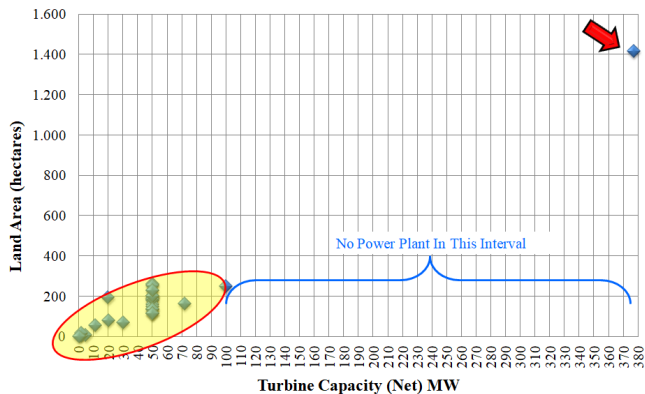
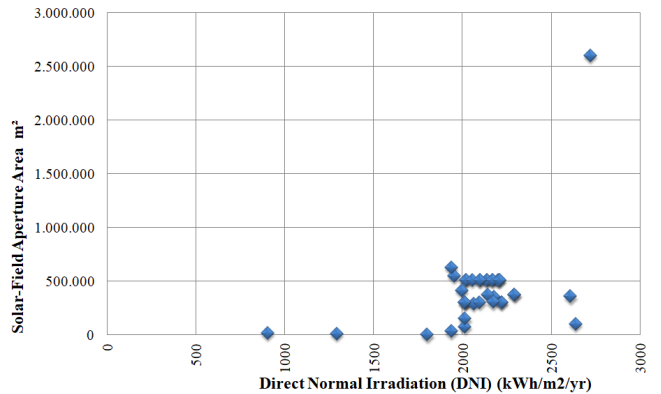
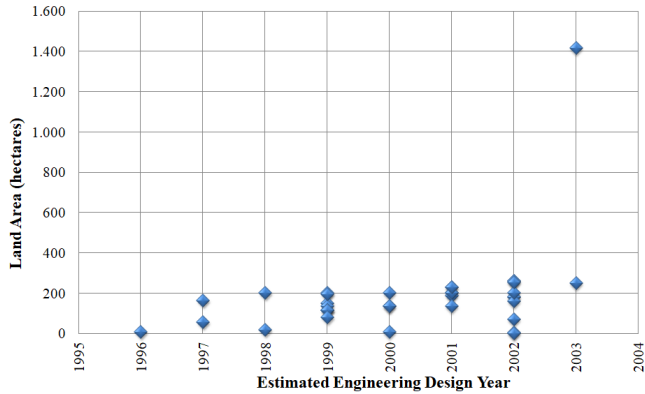
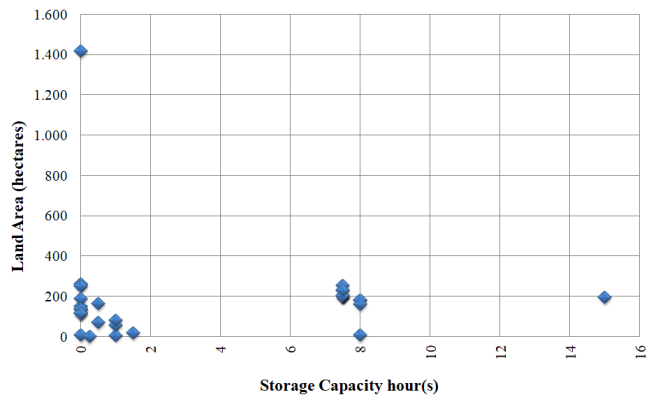
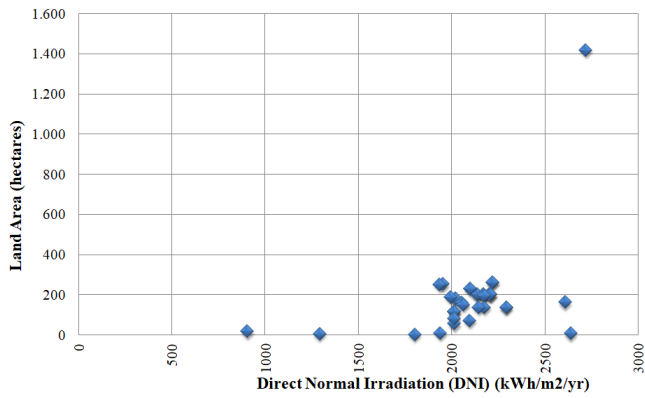
➤ O₁: Solar Field Aperture Area (m²):

It is defined as "the area in which the solar radiation enters the collector" [54].

➤ O₂: Land Area (hectares):

It is defined as "land area required for the entire system including the solar field land area" [55].

There are only 36 previous projects' data (from the U.S. Department of Energy, Office of Energy Efficiency and Renewable Energy, NREL official webpage [56]) in the current dataset (electronic supplementary material files: ESM, please visit author's researcher's profiles such as ResearchGate). All data and information are used directly without any verification and validation. There are 28 parabolic trough, 6 power tower and 2 linear Fresnel reflector applications in this dataset. The inputs and output in this dataset are presented in Fig.3. The minimum values are 902 (F₁), 1996 (F₂), 0,3 (F₃), 400 (O₁), 1 (O₂). The maximum values are 2717 (F₁), 2003 (F₂), 377 (F₃), 2600000 (O₁), 1417 (O₂).



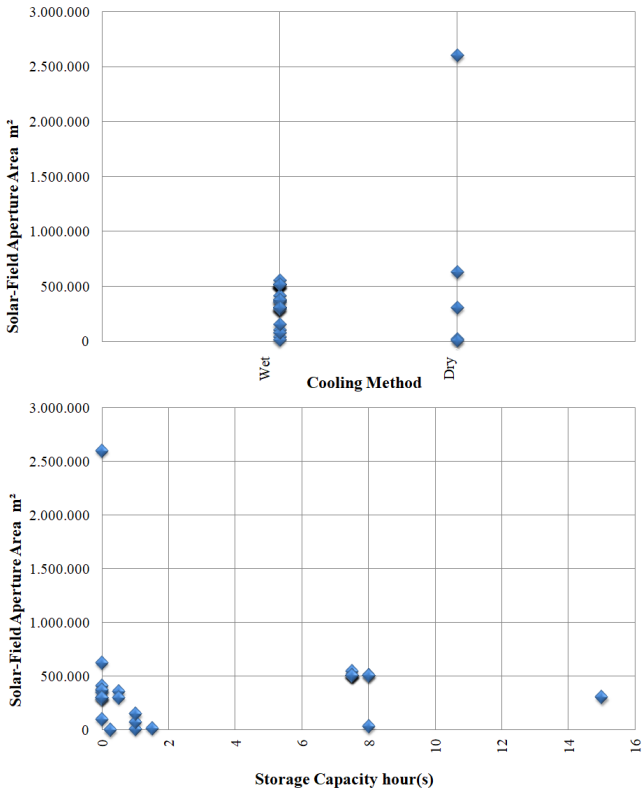


Fig. 3. Inputs and outputs (top to bottom): DNI, engineering design year, net installed power, cooling method, storage capacity versus land area and then solar field aperture area (see ESM) (generated by Microsoft Office Excel 2007 or Apache OpenOffice 4.1.5 & Paint.NET), Data: [56].

Before current modelling, two important rules of thumb are also investigated as:

➤ CSP rule of thumb for slope:

terrain slope angle (%) < 4, 1, 7, 1, 1 (in that study and others) [6], solar field slope (%) < 1–2 (parabolic trough), 2–4 (central receiver), 4 (linear Fresnel), 10 or more (dish) [26], slope (%) < 3 (1 most economical) [29], slope < 2,1 [47].

➤ CSP rule of thumb for cost:

capital (Dollars/kW) 3972 (parabolic trough), 4000+ (solar tower), 12578 (dish) [28], cost installed (\$/W) 3,49–2,34 (parabolic trough), 3,83–2,16 (central receiver), 11,00–1,14 (dish) [48], capital cost (\$/kW) 2900 (parabolic trough), 2400–2900 (power tower), 2900 (dish) [29]. Accordingly, the cost of a VLCSP will be in almost five to ten of billions dollars.

In this study, the models are directly built on the FuzzME Software (developed by Holecek, Talasova, Pavlacka and Bebcakova [57,58]). There are many modelling options on it (fuzzy weighted average, OWA, WOWA, Choquet integral, expert system). Fuzzy WA & OWA are only applied in this experimental study due to the inspiration of some studies by fuzzy WA and OWA in other fields (e.g. [59,60]).

A few preliminaries of fuzzy WA and OWA:

Fuzzy weighted average (see original [61] to avoid any misinterpretation or shift):

normalized fuzzy weights \forall fuzzy numbers

$$V_i \in [0,1], i = 1,2, \dots, m \text{ if}$$

$\forall \alpha \in (0,1) \wedge \forall i \in \{1,2, \dots, m\}$ following holds

$\forall v_i \in V_{i\alpha}$ there exists

$$v_j \in V_{j\alpha}, j = 1,2, \dots, m, j \neq i \text{ s.t. } v_i + \sum_{j=1, j \neq i}^m v_j = 1$$

fuzzy weighted average \forall fuzzy numbers

$$U_i \in [0,1], i = 1,2, \dots, m \wedge W_j \in [0,1], j = 1,2, \dots, m$$

membership function

$$U(u) \forall u \in \mathfrak{K} \text{ is}$$

$$U(u)$$

$$= \max \{ \min \{ U_1(u_1), U_2(u_2), \dots, U_m(u_m), W_1(w_1), W_2(w_2), \dots, W_m(w_m) \} \}$$

$$u = \frac{w_1 u_1 + w_2 u_2 + \dots + w_m u_m}{w_1 + w_2 + \dots + w_m}, \sum_{i=1}^m w_i \neq 0$$

For the computing algorithm of its calculation see [61,62].

Fuzzy ordered weighted average (see original [62,63]):

$$u = \frac{w_1 u_{\emptyset(1)} + w_2 u_{\emptyset(2)} + \dots + w_m u_{\emptyset(m)}}{w_1 + w_2 + \dots + w_m}, \sum_{i=1}^m w_i \neq 0$$

where \emptyset a permutation of the set of indices

$$u_{\emptyset(1)} \geq u_{\emptyset(2)} \geq \dots \geq u_{\emptyset(m)}$$

For the computing algorithm of its calculation see [62,63].

These preliminaries are all founded on the ordered weight averaging (OWA) operator by Ronald Robert Yager (alive) [64] and the fuzzy set and logic by Lotfali Askar Zadeh (1921–alive) [65]. The fuzzy logic operators are clearly presented by Henrik Legind Larsen [66] (Fig.4).

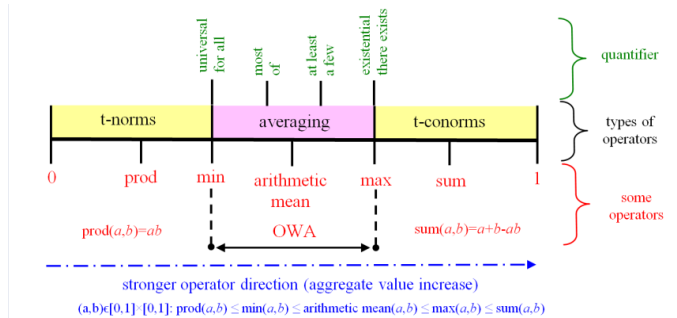


Fig. 4. Representation of fuzzy logic operators (drawn, redrawn and generated based on [66]).

The membership functions of these experimental models are modelled directly on FuzzME (Fig.5) (in ESM). In these experimental models, the uniform weights are assigned first, and then the fuzzy weights are defined by the guidance of FuzzME (Fig.6) (in ESM).

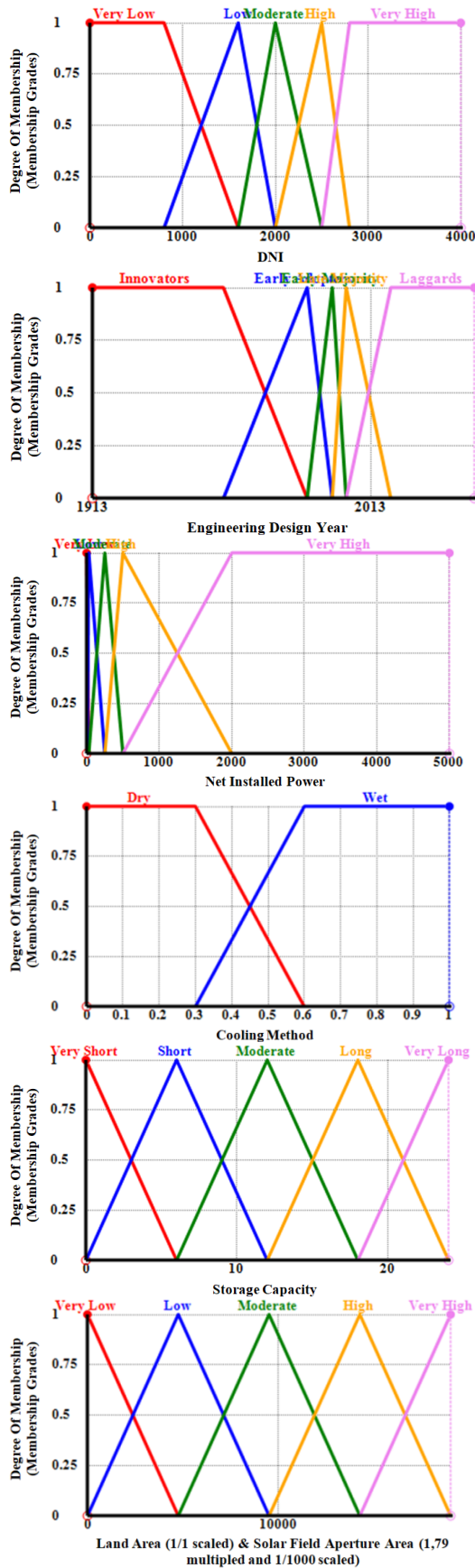


Fig. 5. Membership functions on FuzzME (open FuzzME models) * Note: from top to bottom: DNI (Increasing Scale: higher values are better), engineering design year (Increasing), net installed power (Increasing), cooling

method, storage capacity (Increasing), Land Area (1/1 scaled) & Solar Field Aperture Area (1,79 multiplied and 1/1000 scaled) on the FuzzME.

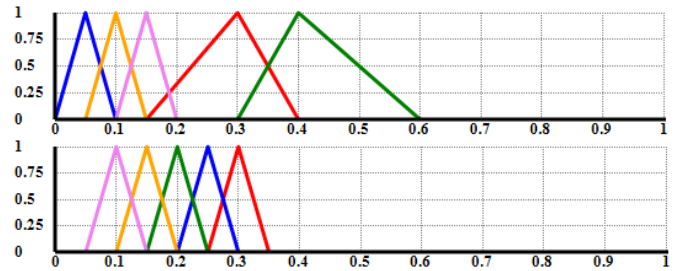


Fig. 6. Weights of fuzzy WA & OWA on FuzzME (open FuzzME models) * Note: Fuzzy WA weights (top), Fuzzy OWA weights (bottom)

These experimental models are tested on the historical projects data and information (see ESM) by using FuzzME and Microsoft Office Excel or Apache OpenOffice 4.1.5 (Fig.7). The errors are calculated according to the absolute percentage errors (APE), the maximum absolute percentage error (MAP), and the mean absolute percentage error (MAPE) like demand forecasting studies (see [67-72]). The MAPE of land area (hectares) (O_2) is %331,35 (FWA) and %505,14 (FOWA). The main errors occur for very small land area projects or small installed power projects (land area: 8; 6,5; 5,3; 1). When these projects are removed from the data set the model performance for MAPE increases approximately 6 times better. When the installed capacities increase in this model, the performance increases very well (For 377 MW error rate is %4). As a result, this model works well in bigger CSP plants rather than in small CSP plants in its current form (Fig.7). The MAPE of solar field aperture area (m^2) (O_1) is %914,86 (FWA) and % 1374,45 (FOWA). The same problem is observed in these models too. The main errors occur for very solar field aperture area projects or small installed power projects (solar field aperture area: 31860; 100000; 10000; 17650; 75000; 150000; 400). When these projects are removed from the data set the model performance for MAPE increases approximately 18 times better. When the installed capacities increase in this model, the performance increases very well (For 377 MW error rate is %4). As a result, this model works well in bigger CSP plants rather than in smaller CSP plants in its current form (Fig.5). When these fuzzy WA and fuzzy OWA models are compared, it is observed that the current fuzzy WA model is performed better. However, it is very clear, that these models need very serious improvement efforts, but it is also thought that this study is a good start for this research aim. Finally, some very large concentrated solar power plants (VLCSPPs) designs' land use requirement predictions are also made by the experimental FWA model (better performed model) on the Middle East and North Africa Region (F_1 : between 2500 and 2600, F_2 : between 2018 and 2020 (estimated early design calculations), F_3 : 500, 1000, 1500, 2000, 3000, 4000, 5000 (six alternative designs), F_4 : Dry, F_5 : between 10 to 18) (Fig.7).

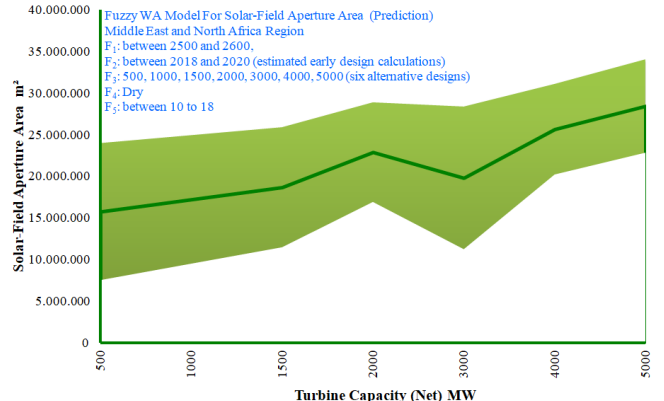
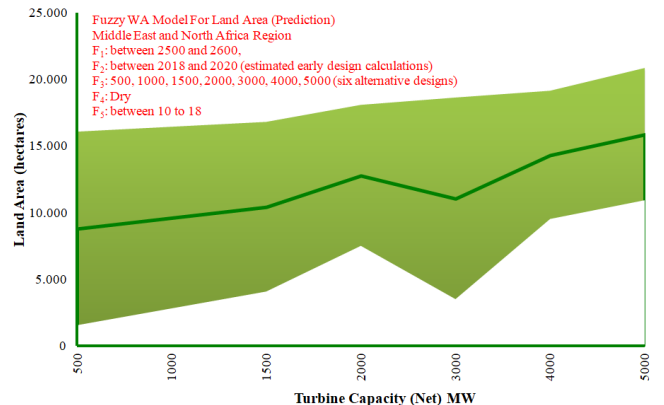
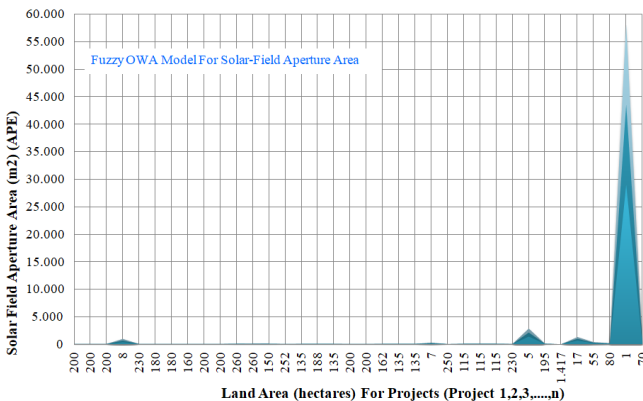
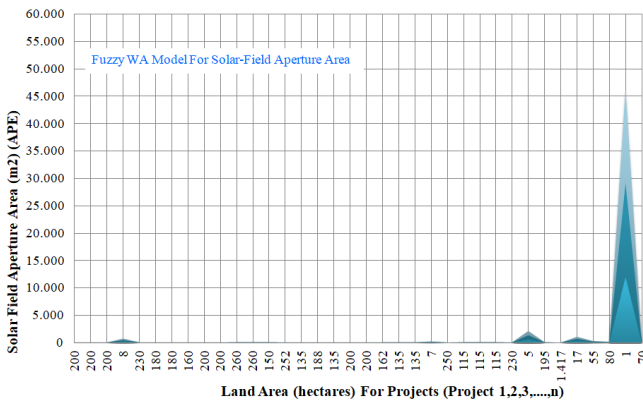
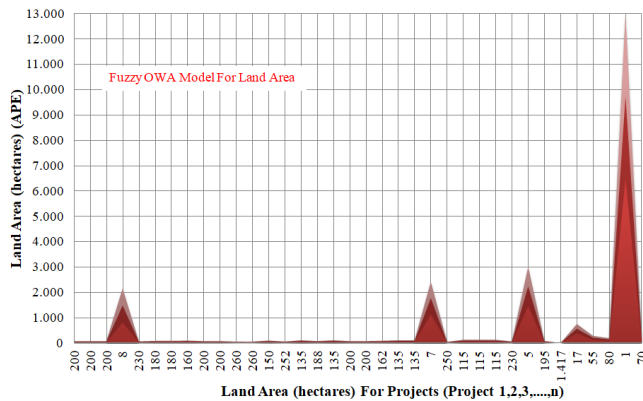
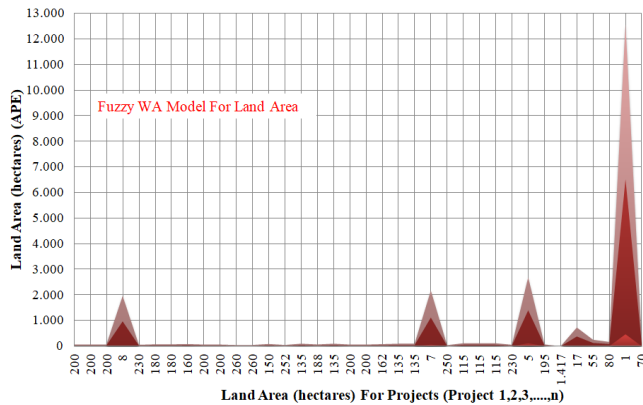


Fig. 7. FWA land area APE per project, FOWA land area APE per project, FWA solar field aperture area APE per project, FOWA solar field aperture area APE per project, FWA land area predictions, FWA solar field aperture area predictions (open ESM and FuzzME model files) *Note: from top to bottom.

One of the main outputs of these R&D efforts shall be some GIS applications (online and offline) for personal, laptop and tablet computers and also mobile phones. The design studies will be performed according to GIS software, coding and cognitive ergonomics principles and constraints in some specially organized R&D studies in near to medium term (Fig.8).

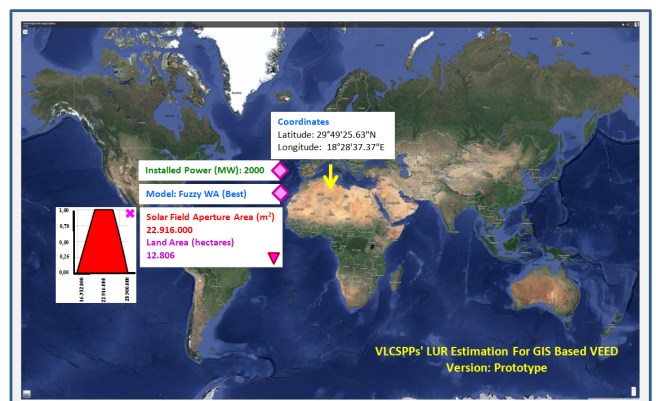


Fig. 8. GIS application interface screen view 1st prototype draft idea (see for base [73,74]) (e.g. Google Earth, ESRI, Autodesk Applications) (only current graphical interface study).

3. Conclusions and future work

This study presents a new idea of developing some plugins and applications on the geographic information systems software for the concentrated solar power plants land use requirements and estimations.

A comparative experimental fuzzy weighted average (fuzzy WA) and ordered fuzzy weighted average (fuzzy OWA) aggregated VLCSPPs land-use requirement estimation model is presented for very early engineering design studies (only on FuzzME, no integration of any GIS yet).

It is believed that these kinds of plugins, applications, and tools will increase the efficiency and effectiveness in the early engineering stages.

The models should be studied in detail with different approaches and views. Afterwards, GIS plugins and tools can be developed and presented for real world applications of international organizations, multinational foundations, governments, and investors.

These tools will hopefully very helpful for developing Supergrids and Global Grid, that will urgently be a must in mid to long term, when some critical issues are taken into account (see critical issues [75,76]).

Acknowledgements

The author would sincerely like to express his deepest thankfulness to The Guardian, The Controller, The Shelter, The Protector, The Bestower of Security and also to Dr. Jose Maria Merigo Lindahl, Dr. Pavel Holeček (FuzzME) (whole study improvement and review), Dr. Gregory Piatetsky-Shapiro (machine learning, data mining, and knowledge discovery lecture notes) and Dr. Henrik Legind Larsen (course in fuzzy logic notes) for consideration, guidance, and help.

References

- [1] J. Tsao, N. Lewis, and G. Crabtree, Solar FAQs Working Draft Version 2006 Apr 20, www.sandia.gov/~jytsao/Solar%20FAQs.pdf accessed on 14/10/2015.
- [2] Wikipedia, Wikimedia Foundation Inc., Photovoltaics, <http://en.wikipedia.org/wiki/Photovoltaics> accessed on 14/10/2015.
- [3] Wikipedia, Wikimedia Foundation Inc., Concentrated solar power, http://en.wikipedia.org/wiki/Concentrated_solar_power accessed on 14/10/2015.
- [4] Wikipedia, Wikimedia Foundation Inc., Concentrated photovoltaics, http://en.wikipedia.org/wiki/Concentrated_photovoltaics accessed on 14/10/2015.
- [5] The International Energy Agency (IEA), Technology Roadmap Solar Thermal Electricity, 2014.
- [6] J. Clifton, B.J. Boruff, "Assessing the potential for concentrated solar power development in rural Australia", *Energy Policy*, Vol. 38, pp. 5272–5280, 2010.
- [7] Investopedia: Economies of scale, <http://www.investopedia.com/terms/e/economiesofscale.p> accessed on 17/10/2015.
- [8] B.O. Saracoglu, "An Experimental Fuzzy Expert System Based Application For The Go/No-Go Decisions To The Geospatial Investigation Studies Of The Regions Of The Very Large Concentrated Solar Power Plants In The European Supergrid Concept", In *Advances In Intelligent and Soft Computing*, The 18th Online World Conference on Soft-Computing in Industrial Applications (WSC18), 6 December 2014.
- [9] Friends of the Supergrid: Roadmap to the Supergrid Technologies Final Report, http://www.cesi.it/news_ideas/ideas/Documents/FOSG%20%20WG2%20Final-report.pdf accessed on 14/10/2015.
- [10] T.J. Overbye, C. Starr, P.M. Grant, and T.R. Schneider, National Energy Supergrid Workshop Report. Crowne Plaza Cabana Palo Alto Hotel, Palo Alto, California, www.supergrid.illinois.edu/sg1/SuperGridReportFinal.pdf accessed on 14/10/2015.
- [11] DESERTEC Foundation: <http://www.desertec.org/> accessed on 11/06/2015.
- [12] S. Mano, B. Ovgor, Z. Samadov, M. Pudlik, V. Julch, D. Sokolov, and J.Y. Yoon, Gobitec and Asian Super Grid for renewable energies in Northeast Asia. Spotinov print Ltd., 2014.
- [13] B. Seliger, G.E. Kim, Tackling climate change, increasing energy security, engaging North Korea and moving forward Northeast Asian integration – “Green Growth” in Korea and the Gobitec project. Gobitec Outline Paper 1-03 10112009, 2009.
- [14] S. Chatzivasileiadis, D. Ernst, G. Andersson, "The Global Grid", *Renewable Energy*, Vol. 57, pp. 372–383. doi:10.1016/j.renene.2013.01.032, 2013.
- [15] Directory of Open Access Journals, <http://doaj.org> accessed until 21/12/2015.
- [16] Google Scholar, <http://scholar.google.com.tr/> accessed until 21/12/2015.
- [17] Global Energy Network Institute (GENI), <http://www.geni.org/> accessed until 21/12/2015.
- [18] Defense Technical Information Center, <http://www.dtic.mil/dtic/> accessed until 21/12/2015.
- [19] California Energy Commission, <http://www.energy.ca.gov/> accessed until 21/12/2015.
- [20] International Finance Corporation (IFC), <http://www.ifc.org/> accessed until 21/12/2015.
- [21] National Renewable Energy Laboratory (NREL), www.nrel.gov accessed until 21/12/2015.

- [22] S. Ong, C. Campbell, P. Denholm, R. Margolis, and G. Heath, Land-use requirements for solar power plants in the United States. Technical Report NREL/TP-6A20-56290 June 2013, Contract No. DE-AC36-08GO28308, Golden, CO: National Renewable Energy Laboratory, 2013, <http://www.nrel.gov/docs/fy13osti/56290.pdf> accessed on 14/10/2015.
- [23] I. Purohit, P. Purohit, S. Shekhar, "Evaluating the potential of concentrating solar power generation in Northwestern India", *Energy Policy*, Vol. 62, pp. 157-175, 2013.
- [24] R.R. Hernandez, S.B. Easter, M.L. Murphy-Mariscal, F.T. Maestre, M. Tavassoli, E.B. Allen, C.W. Barrows, J. Belnap, R. Ochoa-Hueso, S. Ravi, and M.F. Allen, "Environmental impacts of utility-scale solar energy". *Renewable and Sustainable Energy Reviews*, Vol. 29, pp. 766-779, 2014.
- [25] T. Wanderer, S. Herle, "Using a web-based SDSS for siting solar power plants", *Environmental Informatics and Renewable Energies*. pp. 100-108, 2013 <http://enviroinfo.eu/sites/default/files/pdfs/vol7995/0100.pdf> accessed on 14/10/2015.
- [26] O. Behar, A. Khellaf, K. Mohammedi, "A review of studies on central receiver solar thermal power plants", *Renewable and Sustainable Energy Reviews*, Vol. 23, pp. 12-39, 2013.
- [27] R.M. Horner, C.E. Clark, "Characterizing variability and reducing uncertainty in estimates of solar land use energy intensity", *Renewable and Sustainable Energy Reviews*, Vol. 23, pp. 129-137, 2013.
- [28] A. Ummadisingu, M.S. Soni, "Concentrating solar power-technology, potential and policy in India", *Renewable and Sustainable Energy Reviews*, Vol. 15, No: 9, pp. 5169-5175, 2011.
- [29] K. Kaygusuz, "Prospect of concentrating solar power in Turkey: the sustainable future", *Renewable and Sustainable Energy Reviews*, Vol. 15, No: 1, pp. 808-814, 2011.
- [30] The World Bank Group, Morocco's Noor-Ouarzazate Solar Complex: A Global Public Good (video file), <http://www.worldbank.org/en/news/video/2014/10/01/morocco-noor-ouarzazate-solar-complex>, <https://youtu.be/pitmsgaAlJM> accessed on 14/10/2015.
- [31] Sameh I. Mobarek (The World Bank Group Noor Ouarzazate Concentrated Solar Power Project Team Leader) e-mail correspondence on 21/12/2015.
- [32] The World Bank Group, MA- Noor Ouarzazate Concentrated Solar Power Project, <http://www.worldbank.org/projects/P131256?lang=en> accessed on 14/10/2015.
- [33] GlassPoint Solar, Petroleum Development Oman Miraah <http://www.glasspoint.com/miraah/> accessed on 14/10/2015.
- [34] C. Helman, "Ironic Or Economic? Oil Giant To Build World's Largest Solar Project", *Forbes/Energy*, 2015. <http://www.forbes.com/sites/christopherhelman/2015/07/08/oil-giant-to-build-worlds-largest-solar-project/> accessed on 14/10/2015.
- [35] Wikipedia®, List of solar thermal power stations https://en.wikipedia.org/wiki/List_of_solar_thermal_power_stations accessed on 22/12/2015.
- [36] T. Woody, "Solar and Biomass Plants to Work in Tandem in China", *The New York Times Company*, 2010, <http://green.blogs.nytimes.com/2010/01/11/solar-and-biomass-plants-to-work-in-tandem-in-china/> accessed on 14/10/2015.
- [37] Nur Energie: Tunisia, TuNur, <http://www.nurenergie.com/index.php/english/projects/tunisia> accessed on 22/12/2015.
- [38] A. Ebbage, "Low carbon brings Nur Energie closer to CSP export". *CSP Today*, <http://social.csptoday.com/markets/low-carbon-brings-nur-energie-closer-csp-export> on 22/12/2015.
- [39] E. Stenger, "Desertec abandons Sahara solar energy export dream", <http://www.edouardstenger.com/2013/07/24/desertec-abandons-sahara-solar-energy-export-dream/> on 22/12/2015.
- [40] J. Deign, "Desertec and Dii: the end of the affair", *CSP Today*, <http://social.csptoday.com/markets/desertec-and-dii-end-affair> on 22/12/2015.
- [41] G.A. Miller, "The magical number seven, plus or minus two: some limits on our capacity for processing information", *The Psychological Review*, Vol. 63, pp. 81-97, 1956.
- [42] R.M. Shiffrin, R.M. Nosofsky, "Seven plus or minus two: a commentary on capacity limitations", *Psychological Review*, Vol. 101, Issue. 2, pp. 357-361, 1994.
- [43] P. Blanc, B. Espinar, N. Geuder, C. Gueymard, R. Meyer, R. Pitz-Paal, B. Reinhardt, D. Renne, M. Sengupta, L. Wald, and S. Wilbert, "Direct normal irradiance related definitions and applications, the circumsolar issue", *Solar Energy*, Vol. 110, pp. 561-577, 2014.
- [44] B.O. Saracoglu, "An Experimental FOWA Aggregated Location Selection Model For The VLCPVPPs In The MENA Region In The Very Early Engineering Design", In *Advances In Intelligent and Soft Computing*, The 18th Online World Conference on Soft-Computing in Industrial Applications (WSC18), 6 December 2014.
- [45] M. Romero-Alvarez, E. Zarza, Concentrating Solar Thermal Power. D.Y. Goswami, F. Kreith, (Eds.). *Handbook Of Energy Efficiency And Renewable Energy*, CRC Press, 2007.

- [46] A. Miller, B. Lumby, Utility Scale Solar Power Plants, A Guide For Developers and Investors. The International Finance Corporation (IFC), 2012.
- [47] S. Hermann, A. Miketa, N. Fichaux, Estimating the Renewable Energy Potential in Africa A GIS-based approach. The International Finance Corporation (IFC), 2014.
- [48] M. Romero, A. Steinfeld, "Concentrating solar thermal power and thermochemical fuels", Energy & Environmental Science, Vol: 5, Issue: 11, pp. 9234-9245, 2012.
- [49] GeoModel Solar, <http://solargis.info/doc/free-solar-radiation-maps-DNI> on 22/12/2015.
- [50] U.S. Department of Energy (DOE U.S.): Concentrating solar power commercial application study: reducing water consumption of concentrating solar power electricity generation. In Report to Congress. Washington, DC, 2009.
- [51] Electric Power Research Institute (EPRI), Comparison of Alternate Cooling Technologies for U.S. Power Plants: Economic, Environmental, and Other Tradeoffs, Palo Alto, CA, 2004.
- [52] S. Kuravi, J. Trahan, D.Y. Goswami, M.M. Rahman, and E.K. Stefanakos, "Thermal energy storage technologies and systems for concentrating solar power plants", Progress in Energy and Combustion Science, Vol. 39, Issue. 4, pp. 285-319, 2013.
- [53] Energy Initiative Massachusetts Institute of Technology, The Future of Solar Energy An Interdisciplinary MIT Study <https://mitei.mit.edu/futureofsolar>, 2015.
- [54] European Solar Thermal Industry Federation (ESTIF), Recommendation: Converting solar thermal collector area into installed capacity (m^2 to kW_{th}), http://www.estif.org/fileadmin/estif/content/press/downloads/Technical_note_solar_thermal_capacity-4.doc accessed on 14/10/2015.
- [55] F. Kreith, S. Krumdieck, Principles of sustainable energy systems, CRC Press, 2013.
- [56] The National Renewable Energy Laboratory (NREL), Office of Energy Efficiency and Renewable Energy, the U.S. Department of Energy, http://www.nrel.gov/csp/solarpaces/by_project.cfm accessed latest accessed on 14/10/2015.
- [57] J. Talasova, P. Holecek, Multiple-Criteria Fuzzy Evaluation: The FuzzME Software Package, IFSA/EUSFLAT Conference 2009, pp. 681–686, 2009.
- [58] The website of FuzzME, <http://www.fuzzme.net>, <http://fuzzme.wz.cz/> accessed until 14/10/2015.
- [59] S. Linares-Mustaros, J.M. Merigo, J.C. Ferrer-Comalat, "Processing Extreme Values in Sales Forecasting", Cybernetics and Systems, Vol. 46, Issue: 3-4, pp. 207-229, 2015.
- [60] H. Song, R. Zhang, Y. Zhang, F. Xia, and Q. Miao, "Energy consumption combination forecast of Hebei province based on the IOWA operator", Energy Procedia, Vol. 5, pp. 2224-2229, 2011.
- [61] O. Pavlacka, J. Talasova, The fuzzy weighted average operation in decision making models, The 24th International Conference Mathematical Methods in Economics, 13th-15th September 2006, Plzen (Ed. L. Lukas), pp. 419–426, 2006.
- [62] J. Talasova, O. Pavlacka, I. Bebcakova, and P. Holecek, A framework for fuzzy models of multiple-criteria evaluation, International Conference On Fuzzy Set Theory And Applications Conference (FSTA), 2012.
- [63] P. Holecek, J. Talasova, T. Talasek, "Fuzzified weighted OWA (FWOWA) operator", International Journal Of Mathematics And Computers In Simulation, Vol. 9, pp. 213–221, 2015.
- [64] R.R. Yager, "On Ordered Weighted Averaging Aggregation Operators in Multicriteria Decision Making", IEEE Trans. On Systems, Man and Cyberneics Vol: 3, No: 1, pp. 183–190, 1988.
- [65] L.A. Zadeh, "A Fuzzy-Set-Theoretic Interpretation of Linguistic Hedges", Journal of Cybernetics, Vol: 2, Issue: 3, pp. 4–34, 1972.
- [66] H.L. Larsen, FL-04 Fuzzy knowledge operators aggregation operators (AAUE Course in Fuzzy Logic lecture note). received via e-mail on 01/01/2016.
- [67] B.O. Saracoglu, "SEGS VI & Topaz Solar Farm SAM Empirical Trough & PVWatts Models Case Studies & Validation", International Journal of Research in Advanced Engineering Technologies, Vol: 1, Issue: 1, pp. 28-41, 2017.
- [68] B.O. Saracoglu, "An Experimental Fuzzy Inference System for the Third Core Module of the First Console on the Global Grid Peak Power Prediction System & Its Forecasting Accuracy Measures' Comparisons with the First and the Second Core Modules", Journal Of Energy Systems, Vol: 1, Issue: 2, pp. 75-101, 2017.
- [69] B.O. Saracoglu, "Comparative Study On Experimental Type 1 & Interval & General Type 2 Mamdani FIS for G^2P^3S ", Global Journal of Researches in Engineering: J General Engineering, Vol: 17, Issue: 2, pp. 27-42, 2017.
- [70] B.O. Saracoglu, "Comparative Study On Experimental 2 to 9 Triangular Fuzzy Membership Function Partitioned Type 1 Mamdani's FIS For G^2EDPS ", Global Journal of Researches in Engineering: J General Engineering, Vol: 17, Issue: 2, pp. 1-18, 2017.
- [71] B.O. Saracoglu, " G^2EDPS 's First Module & Its First Extension Modules", American Journal of Applied Scientific Research, Vol: 3, Issue: 4, pp. 33-48, 2017.
- [72] B.O. Saracoglu, "Solar star projects SAM version 2017.9.5 PVwatts version 5 model case study & validation", International Journal of Energy Applications and Technologies, Vol: 5, Issue: 1, pp. 13-28, 2018.

- [73] Google Earth Blog, <http://www.gearthblog.com/wp-content/uploads/2015/06/Imagery-Updates-Large-May-27th-2015.jpg>
- [74] Google Earth, <https://www.google.com/earth/> accessed until 14/10/2015.
- [75] G. Hansen, D. Stone, Assessing the observed impact of anthropogenic climate change, Nature Climate Change, 2015.
- [76] M.T. van Vliet, D. Wiberg, S. Leduc, and K. Riahi, Power generation system vulnerability and adaptation to changes in climate and water resources, Nature Climate Change, 2016.

Information Systems for Repair Alternatives and Initial Cost Estimation of Damaged Building Structures

Can Balkaya*‡

*Department of Civil Engineering, Faculty of Engineering and Architecture, Nişantaşı University, Istanbul, Turkey.
(can.balkaya@nisantasi.edu.tr)

‡Corresponding Author; Can Balkaya, Department of Civil Engineering, Nişantaşı University, Istanbul, Turkey,
Tel: +90 212 210 1010, Fax: +90 212 210 1010, can.balkaya@nisantasi.edu.tr

Received: 13.02.2018 Accepted: 05.03.2018

Abstract- The evaluation of existing structures for repair and strengthening results in the application of the most economical and effective repair techniques. The main focus is the existing buildings in seismic areas. The method of repair or strengthening depends on the damaged structural system, structural (life safety) issues, applicable seismic building code requirements, restrictions in available methods, and architectural and construction requirements. The consideration of new techniques, previous technical information on repair methods, experience of experts, and updated cost information are important in the evaluation. The most cost-effective schemes cannot be determined by choosing the most economical means to repair each component; an integrated approach is necessary. Also, recently the use of computers and networks to share the information are increasing. A knowledge-based information system has been developed for the integrated solutions. The level of damage is determined from the damage and structural information. In the evaluation, major damage conditions are grouped as ground damage, foundation damage and superstructure damage, and then these groups are divided into subgroups. Each repair method is represented by a specific format to determine the damage information index. The developed software is a self-modifying and learning system as a result of the data stored for common types of damaged buildings. The use of information systems results in rapid and effective initial cost estimation of repair methods.

Keywords Earthquake damage, Repair methods, Information systems, Building structures

1. Introduction

The main purposes in an earthquake damage evaluation are the correct determination of damage conditions and the level of repair, and the correct application of repair methodology and current techniques. The repair evaluation results in the application of the most economical and effective repair techniques considering life safety and structural issues according to code requirements. The damaged member can be repaired so that it provides service to the structure equivalent to that before the earthquake. However, this repair oversimplifies the minimum requirement for repairing most structural earthquake damage, since code changes and seismicity issues make this task much more complex. The structural engineer is responsible for the repair or retrofitting of the damaged building according to current codes and life safety requirements.

The evaluation and retrofitting of existing structures for seismic behaviour have recently focused on ASCE [1], and Japanese and Turkish research studies [2]. Current earthquake codes generally require higher earthquake forces than earlier ones. For this reason, there is a need for some additional codes to be applied for existing structures depending on their importance and functions of the structures such as residential buildings, hospitals, fire stations, schools, and historical buildings, etc. There are some guidelines for the seismic evaluation and seismic capacity, and retrofitting of existing buildings, ASCE [1], ATC-21 [3], Ohkubo [4]. Approaches for the evaluation of existing buildings that could be different than the code requirements to be applied for new constructed building structures have been discussed by Balkaya [5]. Approaches and research needs for the assessment of existing structures have been emphasized by Melhechers [6].

In addition to code issues, the most cost-effective repair schemes cannot be determined by choosing the most economical means to repair each component, but rather by applying an integrated approach to this evaluation. In the present study, a knowledge-based information system has been developed for the evaluation of earthquake damaged buildings. Major damage conditions are grouped as aesthetic, functional and structural damage, or a combination of these. The preferred checklist of applicable schemes for the repair evaluation is prepared in table form in a cost effective and level of strengthening order.

2. Evaluation of Damage Conditions

Damage conditions are divided into three main groups: ground damage, foundation damage, and superstructure damage. Then each group is divided into progressive subgroups as shown in Fig. 1. Each specific repair method is defined by using five group numbers (**D-GM-SL-MC-SMN**). From Fig. 2 these group numbers are for Damage (**D**) as G (Ground Damage), F (Foundation Damage), S (Superstructure Damage) or R (Removal and Replacement); General Method (**GM**); Specific Location (**SL**); Material Code (**MC**); and Specific Method Number (**SMN**). Damage conditions are considered for the evaluation of repair methods with their group numbers.

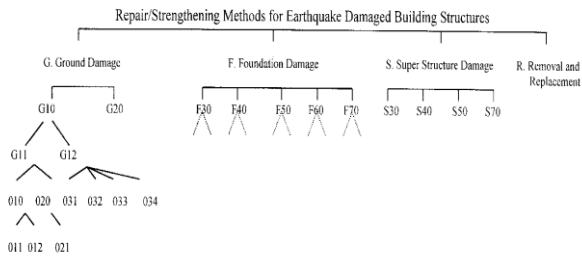


Fig. 1 Group numbering of repair methods

As an example, let S stand for the repair evaluation of superstructure damage. The general method expand number 40 is for the retrofitting method. Thus S40 is the retrofitting of the superstructure damage. If the superstructure damage is in the columns then using the specific location number 40 for column, the damage index becomes S40-40-...-.... For column strengthening by using reinforced concrete, the material code and specific method numbers are 20 and 210, respectively. Therefore, the damage index for a column strengthening method is S40-40-20-210. A typical screen for the developed system is shown in Fig. 2.

Fig. 2 Group numbering of repair methods

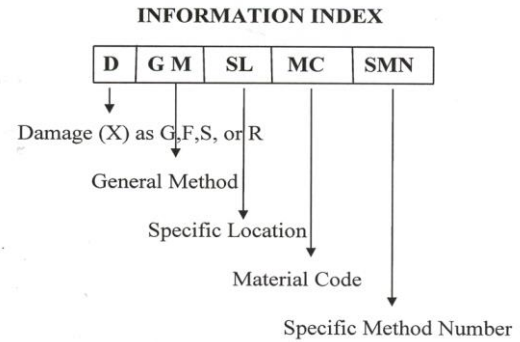


Fig. 3 Specification of repair methods

2.1 Determination of Level of Repair

The determination of the nature of the earthquake damage is important for damage evaluation. Thus for selecting repair methods, the condition assessment plays an important role in determining the distress level of a damaged building. Condition Assessment steps for the earthquake damage buildings are as follows:

Step 1. General Information about the Damaged Building: plan view, type of structural system, irregularities in plan and section, number of floors, type of floor system, foundation systems, construction joints with neighbouring buildings, type and quality of construction materials, wall indices (wall plan area on one floor to total floor area, etc.). An example of general information sheet used in the developed program about the investigated building is shown in Fig. 4.

Fig. 4 General information about the investigated building

Step 2. General Damage Categorization: Damage conditions are categorized as structural and nonstructural. Structural damage state ranges from cracking to collapse of structural members. However, nonstructural damage is a result of deflections or cracking of secondary elements such as brick walls. Damage ranking is done according to the level of damage depending on the structural function, location, crack size and type of cracks.

Damage ratings of buildings are calculated considering all structural and nonstructural members such as columns, beams, shearwalls, floor systems, footings and non-structural members. Using the damage rating information in the databases, final ratings are evaluated as no damage, or slightly, moderate or heavily damaged buildings. This information is used to determine the level of repair/strengthening for selecting repair methods.

Building codes or repair guidelines may affect the level of repair. A damaged structure may require strengthening above its pre-earthquake condition due to these additional requirements. The strengthening of existing buildings using current codes is another issue, especially if they were designed according to earlier codes. The knowledge-based program can be used by considering the level of repair/retrofitting obtained from damage ranking and wall indices without performing any structural safety evaluation. However, the final repair or retrofitting of the structural system depends on structural analyses and design, and must satisfy the current building/earthquake code requirements. Currently, FEMA 274 [7], ASCE [1], UBC [8] (for new constructed building structures), and Turkish Earthquake Codes [9] are considered in the seismic design.

3. Seismic Performance Evaluation

Seismic performance of the investigated buildings for illustration purposes can also be estimated based on the previous investigated data according to wall indices before performing structural safety evaluation. Total area of the walls in the construction area of the plan in both x and y directions separately as wall indices can be obtained by using 'Shiga's Graph' in Fig.5 taken from the Progress Report on Damage Investigation after 1999 Kocaeli Earthquake conducted by Architectural Institute of Japan [2]. Wall indices are the sum of horizontal sectional area of columns (A_c) and the shear walls (A_w) in the first floor. The weight of the building (W) was calculated from sizes of beams, columns, slab, and arrangement of partition walls. If the data were not available, it was assumed that to be 8 kN/m² with non-structural elements.

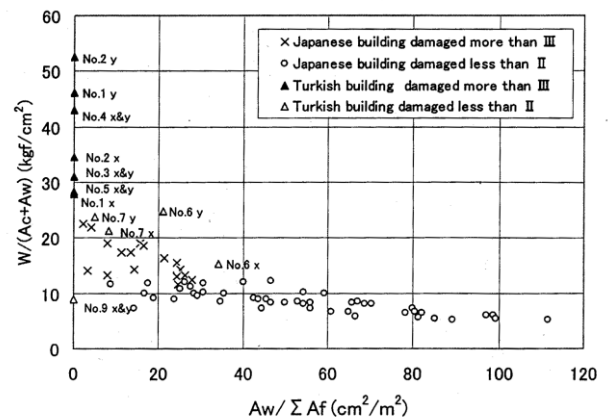


Fig. 5 Shiga's Graph

The marks plotted with 'x' or 'o' in the figure express the Japanese buildings suffered heavy damage or slight damage in 1972 Miyagiken-oki Earthquake respectively. Similarly, 'Δ' and 'Δ' express the Turkish buildings heavy or slight damage in 1999 Kocaeli Earthquake respectively. Buildings plotted in the upper left zone of this graph are judged to have relatively low seismic performance.

The seismic evaluation of 160 branch buildings either belonging to or rented by a commercial bank in Turkey was investigated by Middle East Technical University (METU) after 1999 Turkish Earthquakes. The seismic performance of buildings were initially assumed from the wall indices in both x and y directions. Different than the moderately damaged buildings, in this research, wall indices are calculated for the nondamaged existing building structures as for x-direction: (Shearwalls in x-direction + 0.50 x Column Area in x-direction + 0.10 x Brick Walls Area in x-direction)/Total Building Floor Area. Wall index in y-direction is calculated similarly. In addition to these indices, structural analyses were performed according to Turkish Earthquake Code [9] as an aid to judging the structural capacity.

Capacity spectrum of existing structures are considered [10], with different level of safety [7]. 3-D effects and collapse mechanism are studied in the structural configuration considering existing damaged structural elements and material properties. The main purpose is to see the possible collapse mechanisms to satisfy the minimum code requirement for the life safety.

4. Knowledge Based Information Systems

Information systems are not limited to the accumulation of new methods. This also involves relating something new to what we already know. Domain knowledge is obtained partly from conventional sources; that is textbooks, research papers, reference manuals on repair alternatives [11] and field experience from previous earthquakes. Knowledge based information systems is probably the most time-consuming activity in the evaluation of damaged buildings with an integrated approach.

Knowledge based information has been used to find the appropriate integrated solutions, or minimum solutions satisfying the constraints. The constraints in the evaluation of repair alternatives are the available funds, the minimum level of repair, restrictions in the method, building code requirements, availability of materials and skilled labour, construction requirements and construction time. Integrated solutions are necessary for effective solution methods.

As an example, evaluation of the treatment methods for soils under foundations (G10) is given in Table 1. Similarly, improvement methods and their evaluations for embankment and slope stability (G20) are shown in Table 2. Improvement methods are considered such as in-place soil strengthening, geometric changes and replacement of soil, retaining reinforcement, drainage improvements, and in-place compaction.

Table 1. Evaluation of treatment methods for foundation

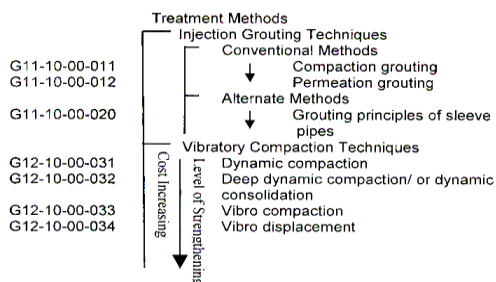
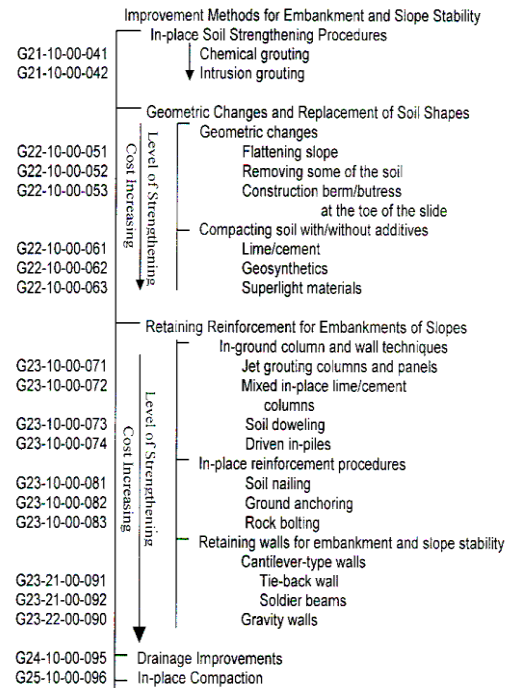


Table 2. Evaluation of improvement methods for embankment and slope stability



The computer software has been written for the evaluation of earthquake damaged building structures. The flowchart in Fig. 6 shows the main steps. In this flowchart, the first step is the determination of the structural and damage information in the field. The level of repair is to be estimated by using damage ranking information, and structural information. Note that all this information are obtained in the field work. By using knowledge based information system databases the level of seismic performance has also been estimated. The next step is to select the repair/retrofitting method by using the built-in database of the program according to the level of repair and cost information. The program lists the repair methods in a cost effective-way with their relative level of strengthening. The computer software also evaluates the cost of the repair method by interacting with current cost databases in the evaluation of repair methods. Structural analyses have been performed externally in the final preparation of design calculation and projects. The last step is to select the most appropriate and economical repair methods among the integrated paths.

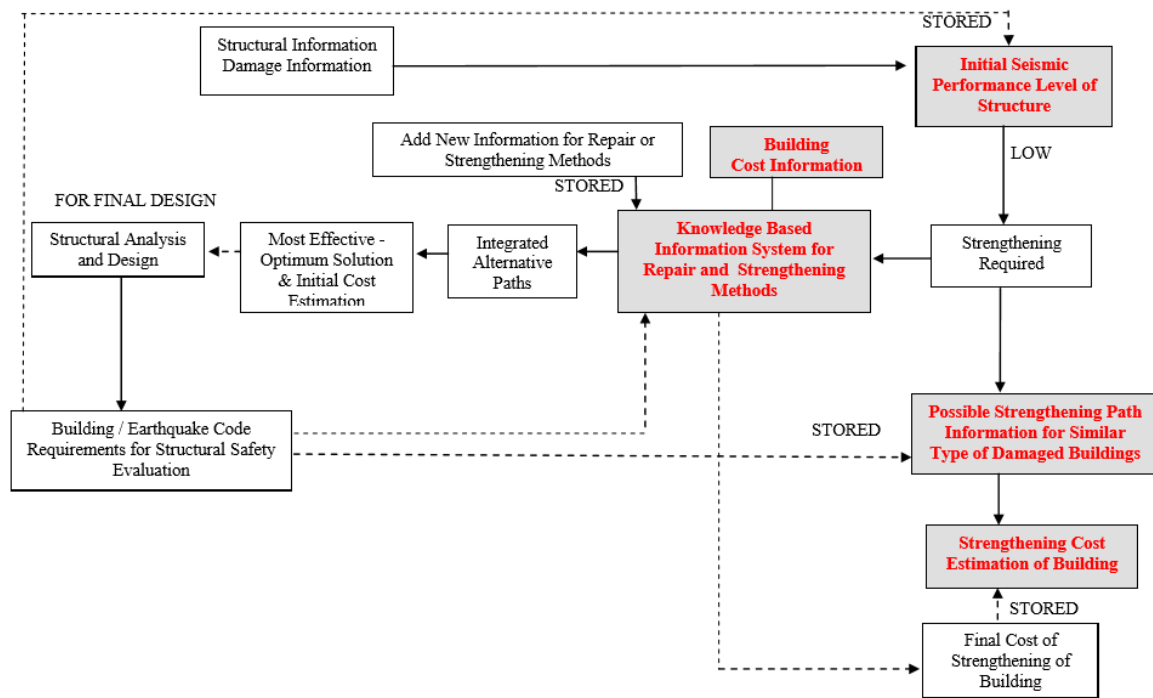


Fig. 6 Evaluation of earthquake damaged building structures

5. Integrated Approach

In the integrated approach, the selection of the most appropriate repair methodology depends on economics and minimum code requirements. An effective solution is obtained considering the optimum solution between the level of strengthening and economy satisfying at least the minimum code requirements or required level of risk considering life safety. However, there will be some problems related to construction techniques and construction equipment, existing architectural constraints, environmental effects, and existing foundation systems. Because of these problems, a particular repair method has not been considered in the integrated path solutions.

5.1 Cost Estimation

Accurate estimate of cost requires the availability of reliable cost and performance data. Considering existing and new construction methods and materials, cost estimation becomes difficult when considering different possibilities. In addition, labour and material costs keep changing. Thus, cost data is collected and organized into a format that makes the cost information instantly accessible through computers. On the other hand, the available old cost information of a repair method has to be taken the basis for a new rapid estimate by considering inflation rates. In this study, Means Building Construction Cost Data [12], and the Turkish Ministry of Public Works Unit prices [13] are used as cost databases. The software gives the total repair costs of building according to available integrated paths by using the latest unit prices. Detail cost estimation has been evaluated by

entering quantity, labour, equipment, etc. Once the analysts establish detailed description of the repair method to be undertaken, then for new cases, the repair cost of that method has been determined only changing some quantities rather than working on the task of the method.

The emphasis in the following case study is how to estimate the total repair/retrofitting cost of similar types of damaged building structures by using stored path information. In this case study, 92 reinforced concrete buildings moderately damaged after the 27 June 1998 Adana-Ceyhan Earthquake with different number of floor levels and total construction area ranging from 500 m² to 7000 m² were studied. These buildings are mostly in earthquake region I (highest earthquake hazard region) in Turkey, and retrofitting projects were prepared by METU. In the retrofitting of the buildings, the retrofitting methods are similar such as column jacketing by using steel, infilled shearwalls inside the reinforced concrete frame, and epoxy injection. Depending on the damage level of the building infilled shearwalls were replaced, amounting to 1-1.5 % of the building basement floor area. Total repair costs corresponding to the selected final integrated path are shown in Fig. 7. Depend on structural type, percentage of infilled wall area, type and level of strengthening, earthquake region, repair cost could be estimated the data stored by using the correlation as shown in Fig. 7. This cost only includes the structural retrofitting cost calculated from structural retrofitting projects. The cost of architectural repair after structural retrofitting and taxes are not included.

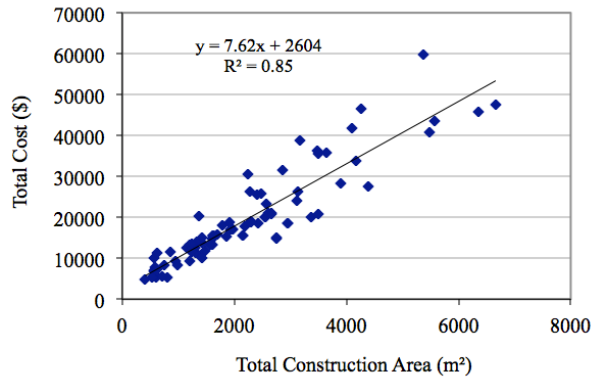


Fig. 7 Repair cost estimation for moderately damaged R/C buildings

5.2 Structural Safety Evaluation

The main objectives for the safety evaluation are to prevent a total collapse of the building or some of its parts, and minimize the danger to life safety as well as avoid financial losses. Structural analyses can be performed before and/or after as a part of the repair alternative evaluation depending on the engineering recommendation for initial rapid cost estimation. The structural configuration, structural type, and the damage level of the building, existing soil and material properties are parameters in the rapid structural safety evaluation. In the final decision, the selected alternatives have been rated to satisfy code requirements. Therefore, structural analyses are performed by using SAP90 [14] finite element analysis program. If the building is designed according to former design codes, the level of damage is determined by first analysing the existing building with current code requirements, and considering seismic performance, capacity spectrum and collapse mechanisms for live safety. Seismic performance, structural capacity, allowable stress levels, drift limitations, and other code requirements have been checked. If retrofitting is necessary, then the retrofitted building is reanalysed by using SAP90 or any general purpose structural analysis program.

There are many repair methods for strengthening the existing structural system. If the damage ratings of the building were moderate or heavily damaged, general structural system strengthening can be preferred rather than

repair of the many individual load carrying members (reducing their force levels). For structural system strengthening, shear walls may be added as infilled walls inside the RC frame or the outside of the building connected with existing frames, new frames, steel braces, and member strengthening as column jacketing, beam strengthening, or a combination of these approaches [7]. If the strengthening cost of heavy damaged building is approximately 40-50% greater than the total cost of building considering the service life, the demolition and reconstruction of the building may be preferred.

The main purpose of the following case study is to illustrate how to estimate the seismic performance of existing building structures. 160 branch buildings of a commercial bank are investigated for the earthquake safety evaluation and preparation of strengthening projects (if necessary) by METU. The 86% of the investigated buildings are the reinforced concrete structures. The structural systems of these are 54% of R/C frame types and 32 % of the R/C frame-shearwall types. Building distributions according to seismic areas are shown in Fig. 8. Note that the earthquake region I is the highest seismic region in Turkey. Wall indices are calculated by using the formula in Seismic Performance Evaluation Part for nondamaged existing buildings in seismic areas. Wall indices in both x any y directions are shown in Fig.9 for the investigated 160 buildings. Structural analyses were also performed for the structural capacity and the Turkish Earthquake Code requirements [9].

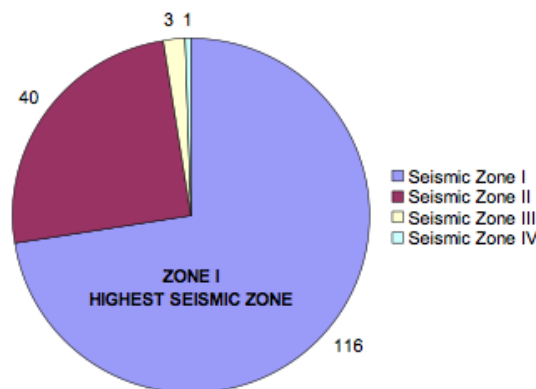


Fig. 8 Investigated building distribution in seismic regions

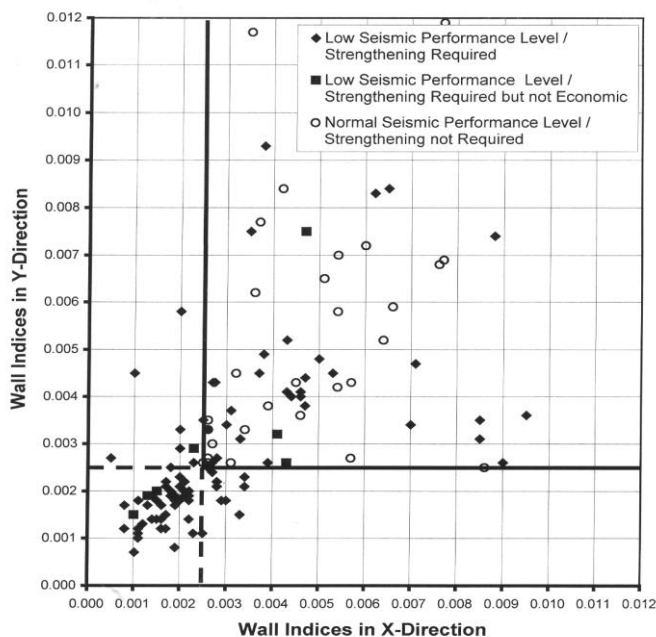


Fig. 9 Wall indices for seismic performance of investigated buildings

As a result of this research, it is observed that when the wall indices in x or y directions are less than 0.0025 the seismic performance of the building can be assumed as low seismic performance level and that building needs a strengthening. If the wall index in only one direction is less than 0.0025 means that the strengthening will be mostly in that direction due to low seismic performance in the corresponding earthquake loading direction.

5.3 Selecting the Most Cost Effective Path

One of the investigated buildings has been presented to show the integrated approach in the evaluation. The superstructure has been taken from Wasti and Sucuoğlu [15] moderately damaged reinforced concrete buildings after the 1 October 1995 Dinar earthquake. In the field, structural and seismic condition assessments were done by a team from METU. The building is a four-story reinforced concrete building, and has no irregularity in plan and elevation. Roof and slabs are flat plates. The damage was observed mainly at the ground level. There is no permanent deformation or

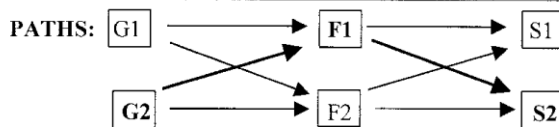
partial collapse in the building. There is slight structural damage in the structural system above the ground level. SAP90 [14] and Turkish Earthquake Code [9] were used in the structural analysis and design of retrofitted buildings.

The damaged building has been analysed [16] in three stages: ground damage, foundation damage and superstructure damage. For each repair group, two alternative repair methods are studied and compared for the evaluation. Cost estimates for repair methods are calculated according to Ministry of Public Work Unit Prices [13]. The integrated paths and their evaluation are shown in Table 3. The total cost estimation for each path is converted to USD.

Note that the permeation grouting is found to be more expensive than compaction grouting because it is done more slowly in Table 3. In the knowledge-based information system described in Table 1 it is also indicated that permeation grouting is an expensive procedure. Thus by using knowledge based system there is no need to calculate this path. However it is only considered as an alternative to illustrate the procedure.

Table 3. Integrated paths and their evaluation

G. Ground Damage Repair	Damage 25%	Relative Level of Strengthening	Cost
G1. Permaion Grouting		1.2	2110 \$
G2. Compaction Grouting		1.0	782 \$
F. Foundation Damage Repair	50%		
F1. Sister Wall		1.0	3365 \$
F2. Replacement of Wall		1.2	6557 \$
S. Superstructure Damage Repair 25%			
S1. Column Strengthening by Steel Casing		1.1	500 \$
S2. Column Strengthening by Reinf. Concrete		1.0	304 \$



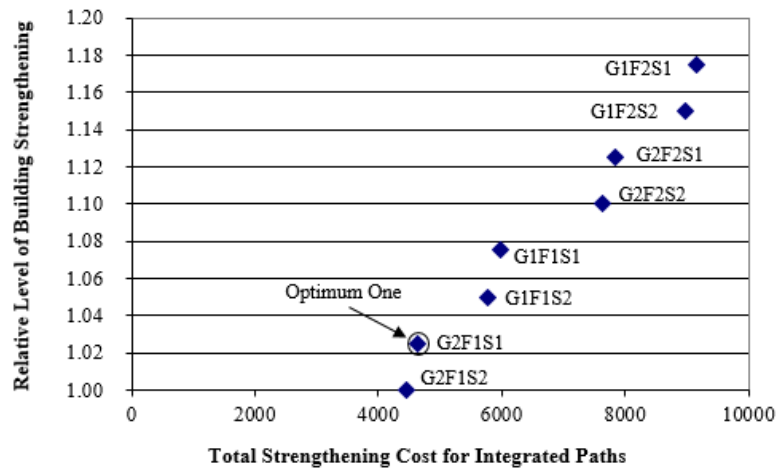


Fig. 10 Integrated path evaluation – cost versus strengthening level

Integrated suitable paths among alternative methods are selected to find the total cost estimation of the damaged building. There are two alternatives for each ground damage (G1, G2), foundation damage (F1, F2) and superstructure damage (S1, S2). Therefore the available integrated paths are: G1 F1 S1, G1 F2 S1, G2 F1 S1, G2 F2 S2, G1 F1 S2, G2 F1 S2, G1 F2 S1, G2 F2 S1. The final path shown as bold (G2 F1 S2) is selected from Table 3 among the repair methods considering structural safety evaluation, level of strengthening, construction requirements, and economy.

Among the integrated paths approximately 100 percent difference between the lowest and the highest cost of the building repair has been occurred. The level of strengthening by using that specific method is also ranked according to the damaged conditions of the investigated building. In this case study, because of heavy damage in the ground and foundation, the damage ranks are assumed for ground, foundation and superstructure as 25%, 50%, and 25% respectively. For each method the relative level of strengthening is indicated in Fig. 10. Then the level of strengthening for the building is defined as the multiplication of main group damage percentages by selected the level of strengthening. As an example the path G1 F1 S1 is corresponding to a relative level of strengthening of $0.25 \times 1.2 + 0.50 \times 1.0 + 0.25 \times 1.1 = 1.075$. Although the final selected path G2 F1 S2 is corresponding to the level of strengthening, 1.0, it means that integrated path also satisfies the minimum code requirements. The final path information corresponding to (G2 F1 S2) has been stored with damage repair information index as: G11-10-00-011, F40-31-00-206, S40-40-20-211 to be used for the similar types of damaged buildings.

6. Conclusion

There are many different approaches for the evaluation of repair methods for earthquake damaged buildings. Costs, codes, and repair techniques vary with time and place. To find the most economical and effective repair or strengthening method with current cost estimates,

a knowledge-based information system has been developed using conventional information for building structures.

It is a challenging task to provide information systems for large numbers of damaged buildings that need to be rehabilitated after earthquakes before accruing of new earthquakes as well as to minimize time for evaluation of repair alternatives. Thus, knowledge-based information systems provide a powerful and most useful tool in selecting cost-effective methods for repair and strengthening of building in seismic areas.

The program is self-modifying for new repair methods, and is a part of a learning system and behaves as an expert system as a result of the data stored for common types of damaged buildings. The repair cost and seismic performance of the building for the level of repair can be estimated by using stored information. Developed information system program interacts with the current cost databases The most cost-effective alternative has been obtained by using integrated approaches. Knowledge based systems are found very effective in the application of integrated approaches.

Acknowledgement

Computer applications for the present study were conducted by Süleyman İlikkan, a former graduate student at the Middle East Technical University.

References

[1] ASCE (2000). Seismic evaluation of existing buildings (draft). Fourth Ballot.
 [2] Progress report on damage investigation after Kocaeli Earthquake (1999). Architectural Institute of Japan, Bogazici Univ., Istanbul Tech. Univ., Middle East Tech. Univ.
 [3] ATC-21 (1988). Procedures for postearthquake safety evaluation of buildings. Applied Technology Council, California.

- [4] Ohkubo, M. (1991). Current Japanese system on seismic capacity and retrofitting techniques for existing reinforced buildings and post-earthquake damage inspection and restoration techniques. University of California, San Diego, SSRP-02.
- [5] Balkaya, C. (2000). Earthquake safety evaluation of existing building structures. *Advances in Civil Engineering*, 4 th International Congress 2000; 4:1577-1587 (in Turkish).
- [6] Melchers, R.E. (2001). 'Assessment of Existing Structures- Approaches and Research Needs.' *Journal of Structural Engineering*, ASCE, 127(4), 406-411.
- [7] FEMA 274 (1997). NEHRP commentary on the guidelines for the seismic rehabilitation of buildings.
- [8] UBC (1994). International Conference of Building Officials.
- [9] Ministry of Public Works and Settlement (1998). Specifications for structures to be built in disaster areas. Ankara, Turkey.
- [10] Freeman, A. Sigmund (1998). Development and use of capacity spectrum method. 6 th U.S. National Conference on Earthquake Engineering, 1-12.
- [11] Balkaya, C. (1994). Evaluation of repair alternatives. Reference manual on earthquake damage repair. G.G. Marino Engineering Consultants, Champaign, IL, Chapter 8.
- [12] Means Building Construction Cost Data (1995). RS Means Company, Inc.
- [13] Ministry of Public Works Unit Prices (1997). Ankara, Turkey, (in Turkish).
- [14] Wilson, E.L., Habibullah, A (1989). SAP90-Structural analysis programs. Computer and Structures, Inc.
- [15] Wasti, S.T., Sucuoğlu, H. (1999). Rehabilitation of moderately damaged R/C buildings after the 1 October 1995 Dinar Earthquake. Report No: METU/EERC 99-01, Middle East Technical University, Ankara, Turkey.
- [16] Ilıkkın, S. (1998). Information systems for the evaluation of repair alternatives of earthquake damaged building structures. M.Sc. thesis presented to Middle East Technical University, Ankara, Turkey.

Investigation of Natural Frequency for Continuous Steel Bridges with Variable Cross-sections by using Finite Element Method

Hüseyin Sağlık*, Bilge Doran*, Can Balkaya**‡

*Department of Civil Engineering, Yıldız Technical University, Istanbul, Turkey.

**Department of Civil Engineering, Faculty of Engineering and Architecture, Nişantaşı University, Istanbul, Turkey.

(huseyinsaglik20@gmail.com, doranbilge@gmail.com, can.balkaya@nisantasi.edu.tr)

‡Corresponding Author; Can Balkaya, Department of Civil Engineering, Nişantaşı University, Istanbul, Turkey,

Tel: +90 212 210 1010, Fax: +90 212 210 1010, can.balkaya@nisantasi.edu.tr

Received: 25.01.2018 Accepted: 05.03.2018

Abstract- This paper mainly focuses on the natural frequencies of composite steel I-girder continuous-span bridges with straight haunched sections. The finite element analysis is performed to model dynamic behaviour of bridges by using CSIBridge package. Continuous-span bridges (two to six) with straight haunched section are considered. All the dimensions used for generating bridge models are designed according to AASHTO LRFD Standards (2014). Effect of various parameters such as span length, the depth ratios between haunched cross-section to mid-span cross-section (r), the length ratio between haunched section to span (α), span configuration and steel girder arrangement on natural frequencies are investigated by numerically generating one hundred fifty three bridge models. “ r ” and “ α ” values are set to be 0.5 - 2.0 and 0.1 - 0.5. The analysis results are given and discussed for the natural frequency of continuous-span composite steel bridges with straight haunched section.

Keywords Composite steel bridges, Natural frequency, Finite element analysis, Straight haunched, Non-prismatic cross-section

1. Introduction

Dynamic response has long been recognized as one of the significant factors affecting the service life and safety of bridge structures, and both analytical and experimental research has been performed [1]. Natural frequency of bridge structure is one of the most important parameter to determine dynamic response. To account for the dynamic effect of moving vehicles, static live load on bridges have been modified by a factor called “the dynamic load allowance” or “the impact factor” in bridge design specifications. The Ontario Highway Bridge Design Code (1983) (OHBDC) [2] is described to dynamic effect of moving vehicles as an equivalent static effect in terms of the natural frequency of the bridge structure. Australian Code (1992) (Austroads) [3] proposed similar dynamic load allowance to regard dynamic effect.

The AASHTO Standard Specifications (2002) [4] and AASHTO LRFD Specifications [5] limit the live load deflection depend on span length. Previous research by

Roeder et al. [6] has shown that the justification for the current AASHTO live-load deflection limits are not clearly defined. Moreover, the bridge design specifications of other countries do not commonly employ deflection limits. Instead, vibration control is often achieved through a relationship between natural frequency, response acceleration and live-load deflection. In the Ontario Highway Bridge Design Code and Australian Code, live-load deflection limits are ensured by relationship with first flexural natural frequency for bridge structures. Therefore, it is important to demonstrate the influence of different variables on the natural frequency.

Frequently, beams are deepened by haunches near the supports to increase the support moment, which results in a considerable reduction of the span moment. Consequently, midspan depth can be reduced in order to obtain more clearance and/or less structural height [7]. Non-prismatic beam members are used commonly in bridge structures and less frequently in building structures [8]. It is especially true for continuous bridges. Despite many studies have been conducted to show influence of different variables on the natural frequency of continuous bridges with uniform

cross-section, investigation for dynamic behaviour of bridges with variable cross-section is limited.

El-Mezaini et al. [7] discussed the general behaviour of non-prismatic members. The behaviour of non-prismatic members differs from that of prismatic ones due to the variation of cross section along the member and the discontinuity of the centroidal axis or its slope. Behaviour of non-prismatic members having T section was discussed by Balkaya [8]. However, the dynamic behaviour of composite continuous-span bridges having non-prismatic members was not considered. Gao et al. [9] studied on continuous concrete bridge with variable cross-section that has parabolic shape was used and proposed an empirical formulation to estimate fundamental frequency. Formulation includes two main parameters: “k” ratio defined as the ratio between side span and central span and “r” ratio defined as the height ratio between mid-span cross-section and the support cross-section but their studies focused on a narrow range of parameters.

The primary objective of this paper is to determine and demonstrate the influence of different variables on the dynamic behaviour of continuous bridges with straight haunched cross-section by finite element analysis (FEA) procedure using CSIBridge software [10]. Analysis results for sample bridges have been discussed.

2. Finite Element Model of Straight Haunched Continuous Bridge Structures

In this section, the procedure of FEA models with using CSIBridge [10] and assumptions are provided. Four-node shell element with six degrees of freedom at each node was used to model concrete slab as well as steel I girders. These elements consist of both membrane and plane-bending behaviour. For diaphragm members, two-node truss members were used as ‘V’ shape for all models to ensure the lateral stability. AASHTO specifications require full composite action between concrete slab and steel girder at the serviceability limit state [11]. Therefore, rigid-body behaviour was used to develop full composite action between steel I girder top flange and concrete slab so that corresponding nodes move together as a three-dimensional

rigid body. Diaphragm members were connected to steel girders top and bottom flanges by hinged connection.

Material properties of bridge structure are listed in Table 1.

The finite element mesh was arranged to ensure good aspect ratio. To provide full composite action behaviour, steel I girder and concrete slab were divided into fine mesh that each node directly overlapped and connected as rigid-body. Typical 3-D model mesh for continuous-span composite steel bridges with straight haunched section is shown in Fig.1.

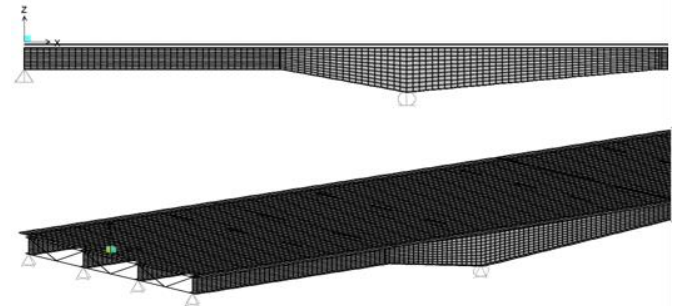


Fig.1. Typical 3-D finite element model mesh system for generated bridges

The supports were used as pin constraint that prevents three translational displacements at one support and roller constrain that prevents vertical and transverse displacement at the other supports rather than modelling piers and abutments. All constraints were placed along the bottom flanges at support locations.

Previous studies [11-12] show that parapet effect on vertical frequency of bridges maybe neglected. In these studies, maximum effect of parapet was found 4.8% between FEA model with and without parapet for Colquitz River Bridge in Canada. Therefore, parapets were neglected in this study.

General geometry of continuous bridges and notations are shown with using typical four-span bridge in Fig.2. Span lengths are selected as the same for all mid-spans (L_m) and are always bigger than side span lengths (L_s). The depth ratios between haunched cross-section to mid-span cross-section which is called ‘r’ and the length ratio between haunched section width to span which is called ‘ α ’ are shown in Fig. 2.

Table 1. Material properties of bridge structure

Components	Elastic Modulus [Mpa]	Shear Modulus [MPa]	Minimum Yield/Tensile Stress (F_y/F_u) [MPa]	Concrete Compressive Strength (F_c) [MPa]	Poisson Ratio	Thickness [m]
Concrete Slab (Shell)	33000	13750	-	30	0.2	0.2
Steel Girders (Shell)	210000	80769	355/510	-	0.3	-
Diaphragm Beams	210000	80769	355/510	-	0.3	-

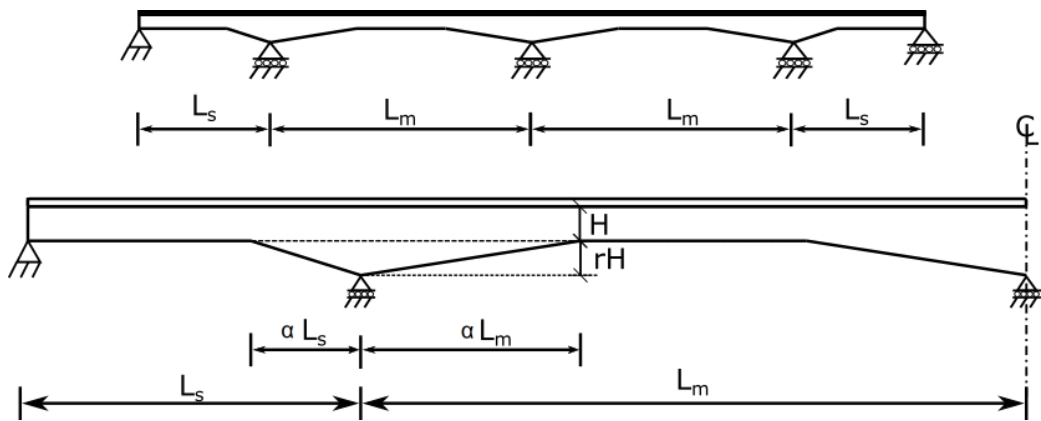


Fig.2. General geometry and notations of continuous-span bridges with straight haunched section

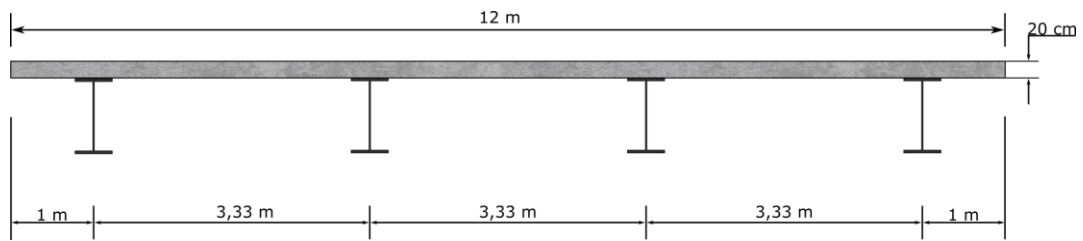
2.1 Variables

To investigate the effect of various parameters such as span arrangements, maximum span length, γ ratio (L_s/L_m), r and α ratios on natural frequency of continues-span bridges, total of 153 models are analysed. All dimensions used for generated bridge models are designed according to AASHTO LRFD Standards [8]. The dimensions of cross sections are determined with using 6.10.2.1.2-1, 6.10.2.2-1, 6.10.2.2-2, 6.10.2.2-3,6.10.2.2-4 limitations from AASHTO LRFD Standards; e.g. for four-span continuous bridges having maximum span length, r ratio and the ratio between steel I girder depth to span length are respectively equal to 30m, 2 and 0.03, the full depth of steel I girder is equal to 2.7m. According to limitations of AASHTO LRFD Standards, web depth of steel I girder (D), web thickness (t_w), flange thickness (t_f), full width of the flange (b_f) were respectively used as 2.63m, 0.0185m, 0.035m, 0.45mm. Concrete slab thickness (that also satisfy to AASHTO LRFD Standards, Section 9.7.1.1) and width are respectively used with same dimensions as 0.2m and 12m for all numerical models. Typical cross-section types are shown in Fig.3.

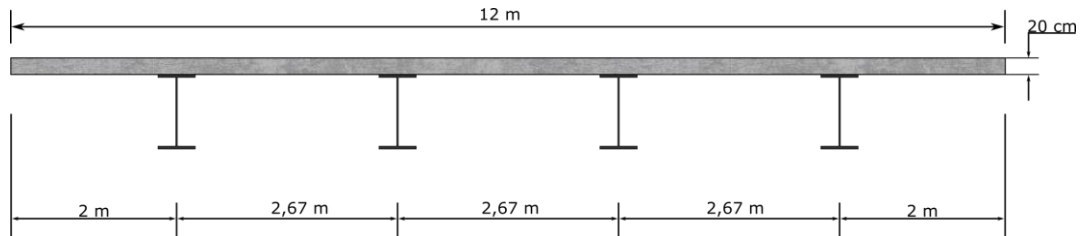
Cross-frames are designed as V-type. UNP380 steel profile was used as V-type cross-frames for all models. Colquitz

River Bridge in Canada [12] that has almost same concrete slab width and thickness is used to design steel profile type of cross-frame. Despite arbitrary 25 ft. (7.62m) spacing limit for cross-frames and diaphragms was given by AASHTO Standard Design Specification, there isn't any limitation for spacing of cross-frames or diaphragms at AASHTO LRFD Standards. Therefore, 7.5m spacing of cross-frames is used so that the span lengths used for study can be equally divided and close to given spacing limit in [4]. Analysis cases are summarized in Table 2 for continuous-span bridges with straight haunched cross section.

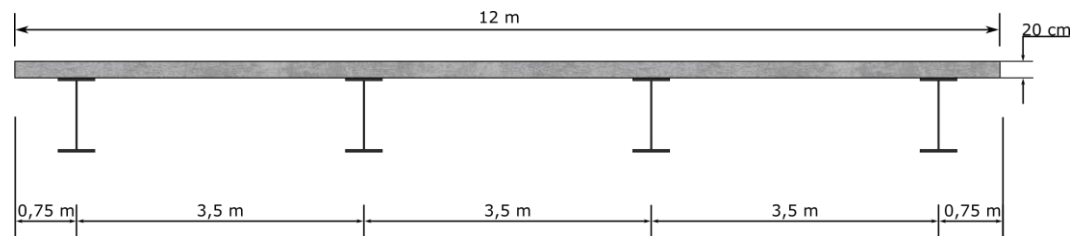
For Case A and B in Table 2; each L_m lengths are used according to given parameters. For Case C; total of 66 models are designed to investigate the relation between effect of r and α ratios on the natural frequency. Every r or α ratios are used as the other parameters given Table 2 are constant; e.g. while r ratios is equal 0.6 and the other parameters are constant as given, α ratios are used as 0.1, 0.2, 0.3, 0.33, 0.4 and 0.5. For Case D; each γ ratio is used with given L_m lengths for three, four, five and six-span continuous bridges. For Case E; five different cross-sections (Fig.3) are used according to given constant length and ratios in Table 2.



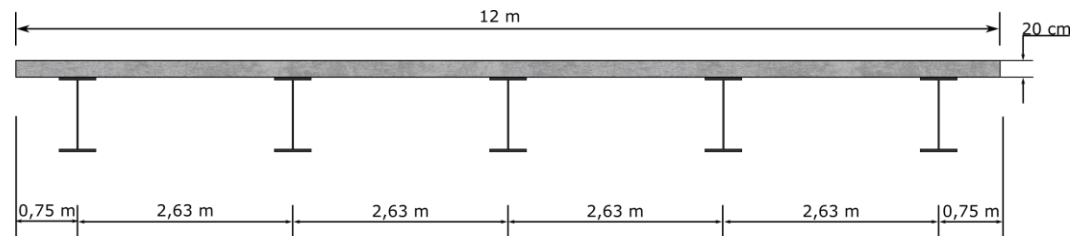
(a) Cross-Section-1 (CS-1)



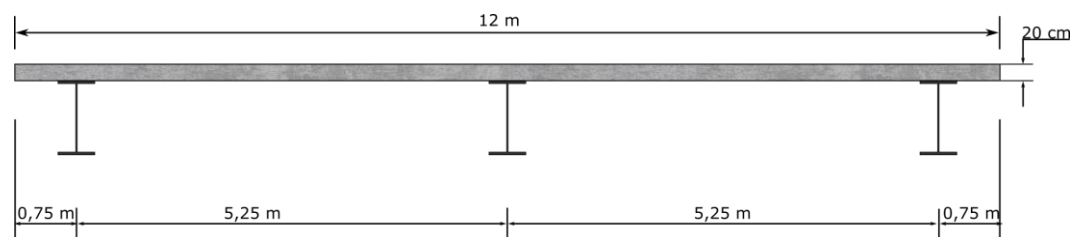
(b) Cross-Section-2 (CS-2)



(c) Cross-Section-3 (CS-3)



(d) Cross-Section-4 (CS-4)



(e) Cross-Section-5 (CS-5)

Fig.3. Cross sectional arrangements for mid-spans of bridges

Table 2. Analysis cases for straight haunched continuous bridges

Case	Span length, L_m (m)	H/ L_m ratio	r ratio	α ratio	γ ratio	Cross Section Type	Span Configuration
A	15, 30, 45, 60, 75, 90	0,03	1	0,33	-	3	simple span
B	15, 30, 45, 60, 75, 90	0,03	1	0,33	1	3	two-span
C	30	0,03	0,5 0,6 0,7 0,8 0,9 1,00 1,20 1,40 1,60 1,80 2,00	0,1 0,2 0,3 0,33 0,4 0,5	0,5	3	four-span
D	15, 30, 45, 60, 75, 90	0,03	1	0,33	0,25 0,33 0,5 0,6 0,67 0,75 0,8 0,83 1	3	three-span four-span five-span six-span
E	30	0,03	1	0,33	0,5	1, 2, 3, 4, 5	four-span

3. Dynamic Analysis Results

The effects of r , α and γ ratios, maximum span length, cross-section configuration and span configuration on natural frequency are discussed and presented here.

3.1 Effect of r and α ratios:

To investigate the effects of r and α ratios on the natural frequency of steel I-girder continuous-span bridges with straight haunched sections, four-span continuous bridges are used with the span configuration as 15m-30m-30m-15m. The r and α ratios are respectively varied from 0.5 to 2.0. and 0.1 to 0.5 (Table 2) as shown in Fig. 4.

As “ r ” ratios increase, there is a clear increment mostly follows curve for the natural frequency while α ratios and all

other variables are constant. As shown in Fig. 5, curves are converged to second-order equation. These increments of natural frequencies are valid for almost all α ratios but α is equal to 0.1. As α is equal to 0.1, there is a clear decreasing of natural frequencies after $r = 1.0$. While the r values increase from 1.0, natural frequencies decrease with second-order curve due to the relation between mass increment and natural frequency. Natural frequency can be more influenced by mass increment than stiffness increments as a result of haunched section which is generated in very narrow haunched length (Fig.5a). Additionally, the increment of frequency is more obvious for the case between $\alpha = 0.5$ and $r = 1.0$ and 1.2 respectively. Increment of frequency rate is 3.35%. Differences of frequencies relative to given “ r ” and “ α ” values are given as Table 3.

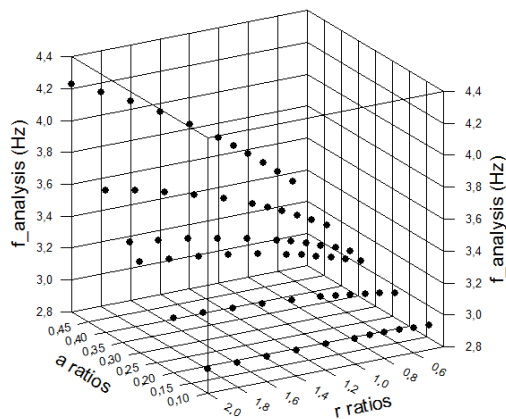


Fig.4. Natural frequencies versus “r” and “α” ratios

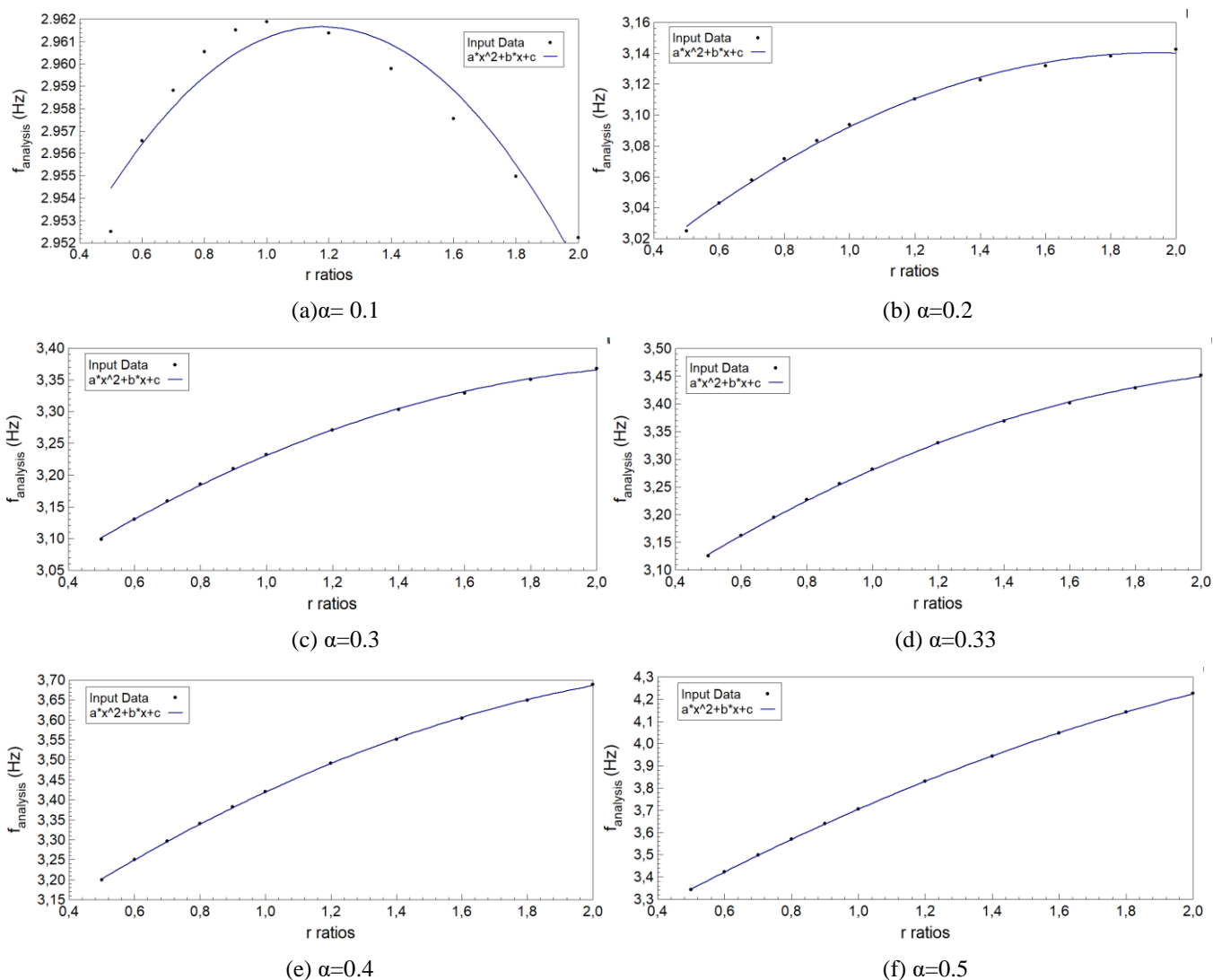


Fig.5. Natural frequencies versus “r” ratios corresponding to constant “α” for four-span straight haunched continuous bridges

Table 3. Differences of natural frequencies relative to given r ratios corresponding α ratios

No	r ratio	α ratio	Freq.	D %*	No	r ratio	α ratio	Freq.	D %*	No	r ratio	α ratio	Freq.	D %*
1	0.5	0.1	2.953	0.137	23	0.5	0.3	3.099	1.028	45	0.5	0.4	3.199	1.580
2	0.6		2.957	0.076	24	0.6		3.130	0.916	46	0.6		3.250	1.440
3	0.7		2.959	0.050	25	0.7		3.159	0.844	47	0.7		3.297	1.344
4	0.8		2.96	0.041	26	0.8		3.186	0.765	48	0.8		3.341	1.240
5	0.9		2.962	0.012	27	0.9		3.210	0.692	49	0.9		3.382	1.145
6	1.0		2.962	0.033	28	1.0		3.232	1.197	50	1.0		3.421	2.044
7	1.2		2.961	0.038	29	1.2		3.271	0.977	51	1.2		3.491	1.740
8	1.4		2.960	0.075	30	1.4		3.303	0.795	52	1.4		3.552	1.481
9	1.6		2.958	0.087	31	1.6		3.329	0.643	53	1.6		3.604	1.258
10	1.8		2.955	0.093	32	1.8		3.351	0.516	54	1.8		3.650	1.067
11	2.0		2.952	-	33	2.0		3.368	-	55	2.0		3.689	-
12	0.5	0.2	3.025	0.590	34	0.5	0.33	3.125	1.178	56	0.5	0.5	3.343	2.372
13	0.6		3.043	0.497	35	0.6		3.162	1.058	57	0.6		3.422	2.202
14	0.7		3.058	0.445	36	0.7		3.195	0.981	58	0.7		3.498	2.078
15	0.8		3.072	0.386	37	0.8		3.227	0.895	59	0.8		3.570	1.948
16	0.9		3.083	0.334	38	0.9		3.256	0.816	60	0.9		3.640	1.827
17	1.0		3.094	0.539	39	1.0		3.282	1.428	61	1.0		3.706	3.355
18	1.2		3.110	0.398	40	1.2		3.329	1.184	62	1.2		3.831	2.961
19	1.4		3.123	0.288	41	1.4		3.369	0.979	63	1.4		3.944	2.617
20	1.6		3.132	0.202	42	1.6		3.402	0.806	64	1.6		4.047	2.316
21	1.8		3.138	0.135	43	1.8		3.429	0.661	65	1.8		4.141	2.051
22	2.0		3.142	-	44	2.0		3.452	-	66	2.0		4.226	-
<i>*Difference relative to r ratio; D % = [(f(xi+1)-f(xi))/f(xi+1)]*100 Peak values are shown as bold</i>														

While “r” ratios and all other parameters are constant, the effect of “ α ” ratio on the natural frequency is investigated as shown Fig. 6. As α values increase, the natural frequencies of bridges also increase with curves which converge to second-order equation. The increment of natural frequency is more

obvious for the case between r =2.0 and α = 0.4 and 0.5 respectively. Increment of frequency rate is 14.57 %. The differences of frequencies between cases are shown in Table 4.

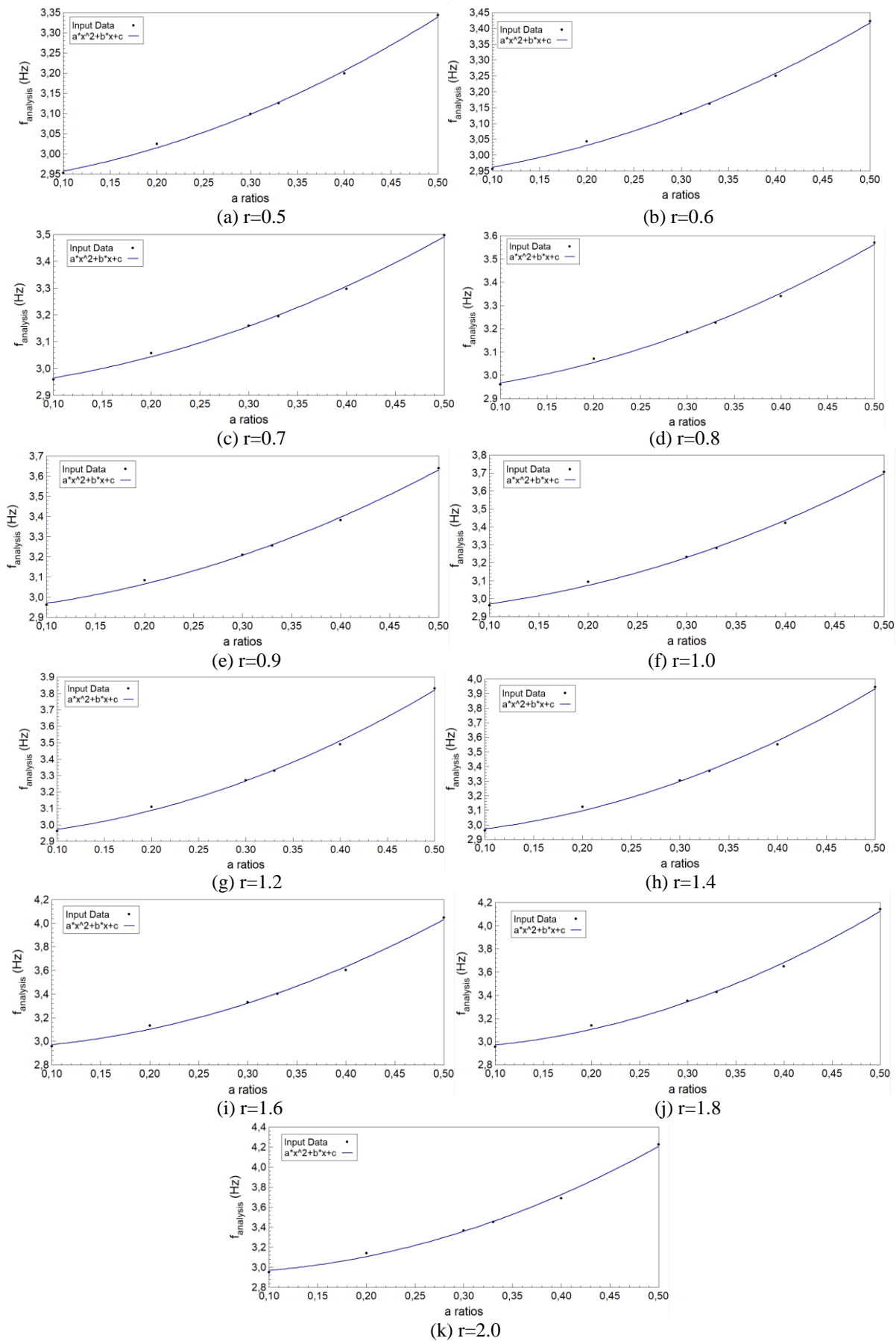


Fig.6. Natural frequencies versus “ α ” ratios for four-span straight haunched continuous bridges

Table 4. Differences of natural frequencies relative to given α ratios corresponding r ratios

No	r ratio	α ratio	Freq.	D %*	No	r ratio	α ratio	Freq.	D %*	No	r ratio	α ratio	Freq.	D %*
1	0.5	0.1	2.953	2.455	25	0.9	0.1	2.962	4.117	49	1.6	0.1	2.958	5.891
2		0.2	3.025	2.433	26		0.2	3.083	4.110	50		0.2	3.132	6.307
3		0.3	3.099	0.858	27		0.3	3.210	1.418	51		0.3	3.329	2.168
4		0.33	3.125	2.368	28		0.33	3.256	3.889	52		0.33	3.402	5.961
5		0.4	3.199	4.497	29		0.4	3.382	7.618	53		0.4	3.604	12.296
6		0.5	3.343	-	30		0.5	3.640	-	54		0.5	4.047	
7	0.6	0.1	2.957	2.918	31	1.0	0.1	2.962	4.452	55	1.8	0.1	2.955	6.197
8		0.2	3.043	2.879	32		0.2	3.094	4.481	56		0.2	3.138	6.775
9		0.3	3.130	1.008	33		0.3	3.232	1.543	57		0.3	3.351	2.334
10		0.33	3.162	2.775	34		0.33	3.282	4.228	58		0.33	3.429	6.437
11		0.4	3.250	5.312	35		0.4	3.421	8.344	59		0.4	3.650	13.469
12		0.5	3.422	-	36		0.5	3.706	-	60		0.5	4.141	-
13	0.7	0.1	2.959	3.351	37	1.2	0.1	2.961	5.050	61	2.0	0.1	2.952	6.440
14		0.2	3.058	3.308	38		0.2	3.110	5.165	62		0.2	3.142	7.181
15		0.3	3.159	1.151	39		0.3	3.271	1.774	63		0.3	3.368	2.481
16		0.33	3.195	3.164	40		0.33	3.329	4.861	64		0.33	3.452	6.866
17		0.4	3.297	6.103	41		0.4	3.491	9.736	65		0.4	3.689	14.574
18		0.5	3.498	-	42		0.5	3.831	-	66		0.5	4.226	-
19	0.8	0.1	2.960	3.759	43	1.4	0.1	2.960	5.507					
20		0.2	3.072	3.718	44		0.2	3.123	5.773					
21		0.3	3.186	1.288	45		0.3	3.303	1.982					
22		0.33	3.227	3.535	46		0.33	3.369	5.437					
23		0.4	3.341	6.871	47		0.4	3.552	11.053					
24		0.5	3.570	-	48		0.5	3.944	-					
<p>*Difference relative to r ratio; $D \% = [(f(xi+1)-f(xi))/f(xi+1)] *100$ Peak values are shown as bold</p>														

3.2 Effect of Maximum Span Length:

The effects of maximum span lengths on natural frequencies of steel I-girder continuous-span bridges with straight haunched sections are investigated. For this purpose; single, two, three, four, five and six continuous-span bridges which have α and r ratios respectively equal to 0.33 and 1, are considered. Maximum span lengths of those bridges have been selected as 15, 30, 45, 60, 75 and 90 m. As shown in Fig. 7 and Fig. 8, while maximum span lengths (L_{max}) increase, frequencies of continuous bridges clearly decrease. Span configuration's effect on natural frequency decreases with increment of span length. In other words, as maximum span lengths values increase, the natural frequencies of

bridges that have different span configuration tend to close each other. This is also observed by Barth [10]. In general, frequencies of continuous bridges having same maximum span length decrease with increment of span number. However, Fig. 8 shows that frequency of three span bridges have higher natural frequencies than the others.

Especially three-span continuous bridges show dispersion on frequencies even though bridges have same maximum span lengths. This dispersion can be result of side span's effect on natural frequency. As side spans are generated in wide range that is from 0.25 portion of middle span to 1.0, middle span is considered as maximum span length for three span continuous bridges and middle span's dynamic contribution decreases with different range of side spans.

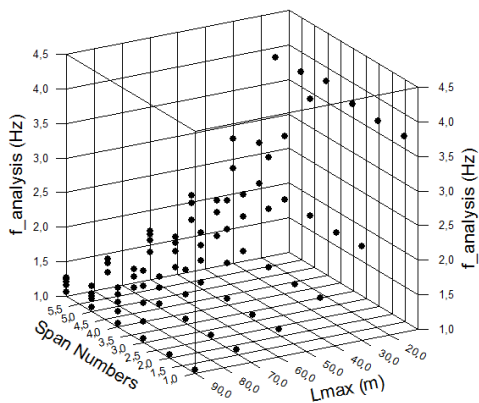


Fig.7. Natural Frequencies versus span number and L_{max}

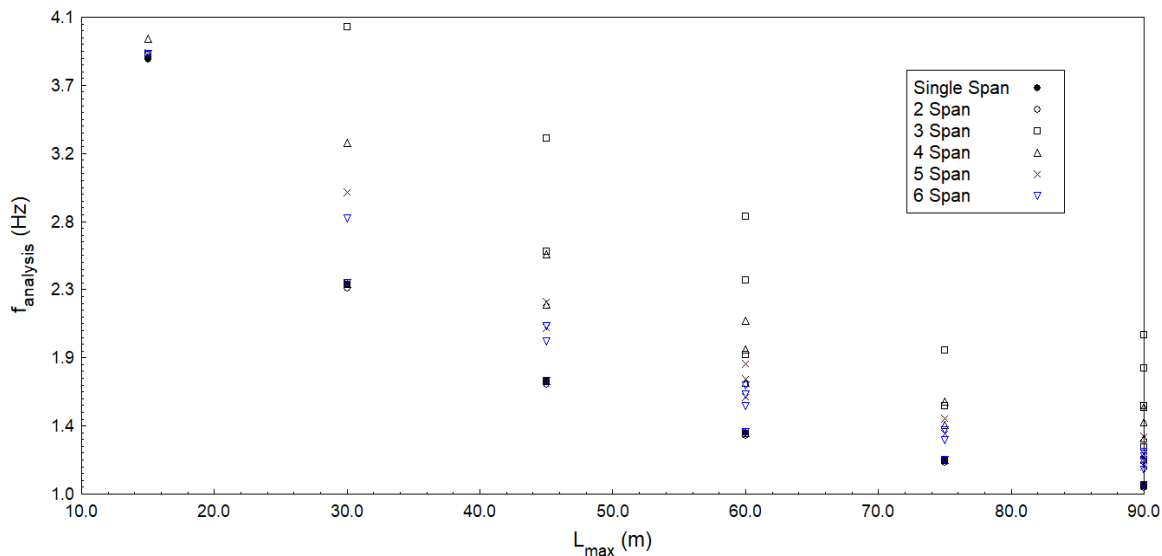
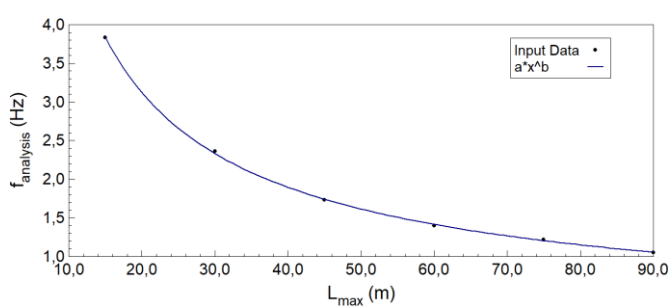
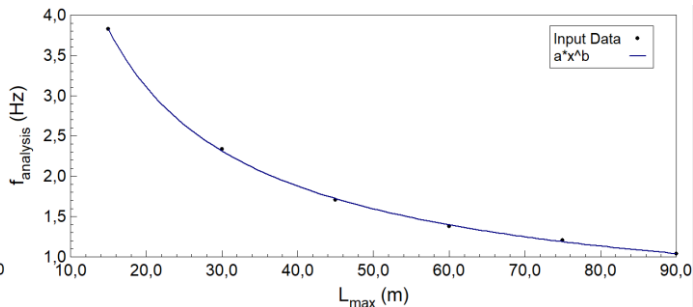


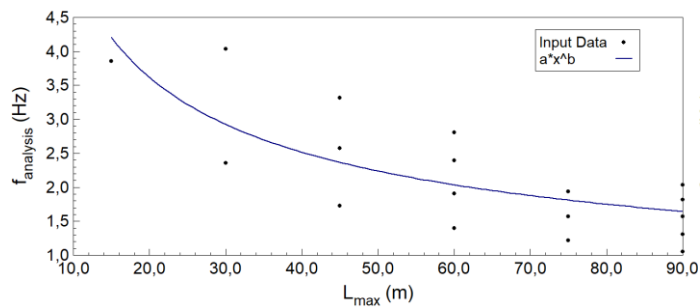
Fig.8. Distribution of natural frequencies versus span numbers and maximum span lengths



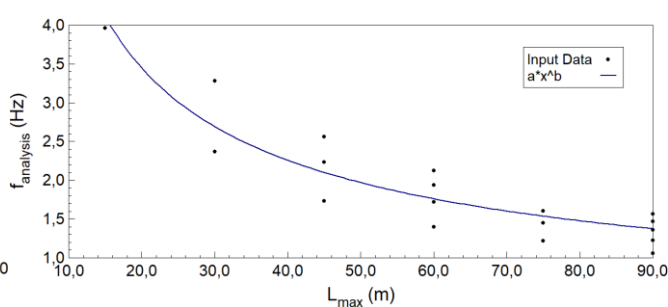
(a) Simple Span



(b) 2 Span



(c) 3 Span



(d) 4 Span

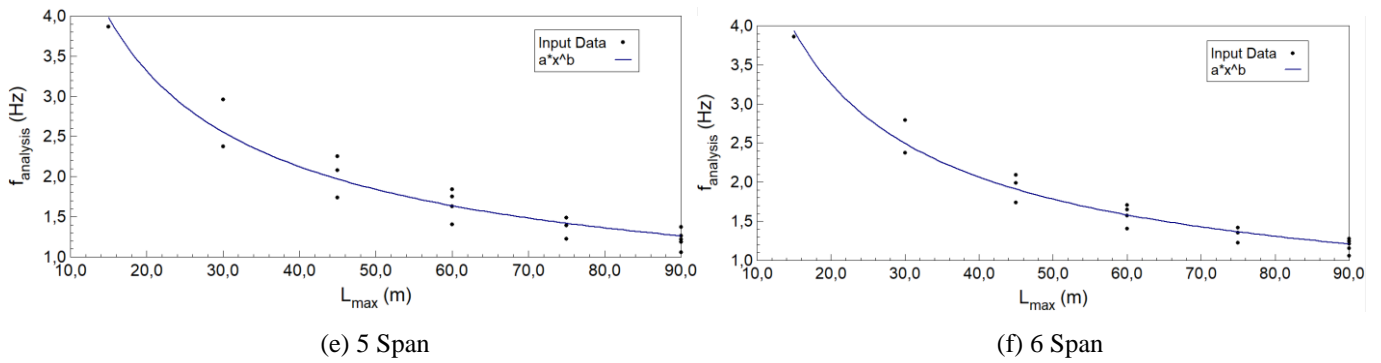


Fig.9. Natural frequencies versus maximum span lengths for different span numbers of straight haunched continuous bridges

According to Fig. 9, as maximum span lengths increase, the natural frequencies decrease with following curve. For almost all curves, ‘a.x^b’ curve gives the best fitting. Curve fitting parameters a and b, are given in Table 5 for different span arrangements

Table 5 Curve fitting parameters

a	b	Span Arrangement
26.947	-0.720	single-span
27.377	-0.726	two-span
17.336	-0.523	three-span
21.494	-0.611	four-span
22.557	-0.640	five-span
23.381	-0.658	six-span

3.3 Effect of γ Ratio:

The effect of γ ratio on natural frequencies of steel I-girder continuous-span bridges with straight haunched sections is investigated. To determine effect of γ ratios on the natural frequencies; three, four, five and six continuous-span bridges are generated with using γ ratios between 0.25 to 1.0. For all considered bridge models, α and r ratios are respectively taken as 0.33 and 1.

Additionally, the relation between γ ratio and natural frequency of bridge is shown Fig. 10 considering maximum span lengths for all types of span numbers. According to Fig. 10, it seems that natural frequency of bridge decreases while γ ratio increases with constant maximum span length of bridge. Typically, decreasing of natural frequencies follow to straight line.

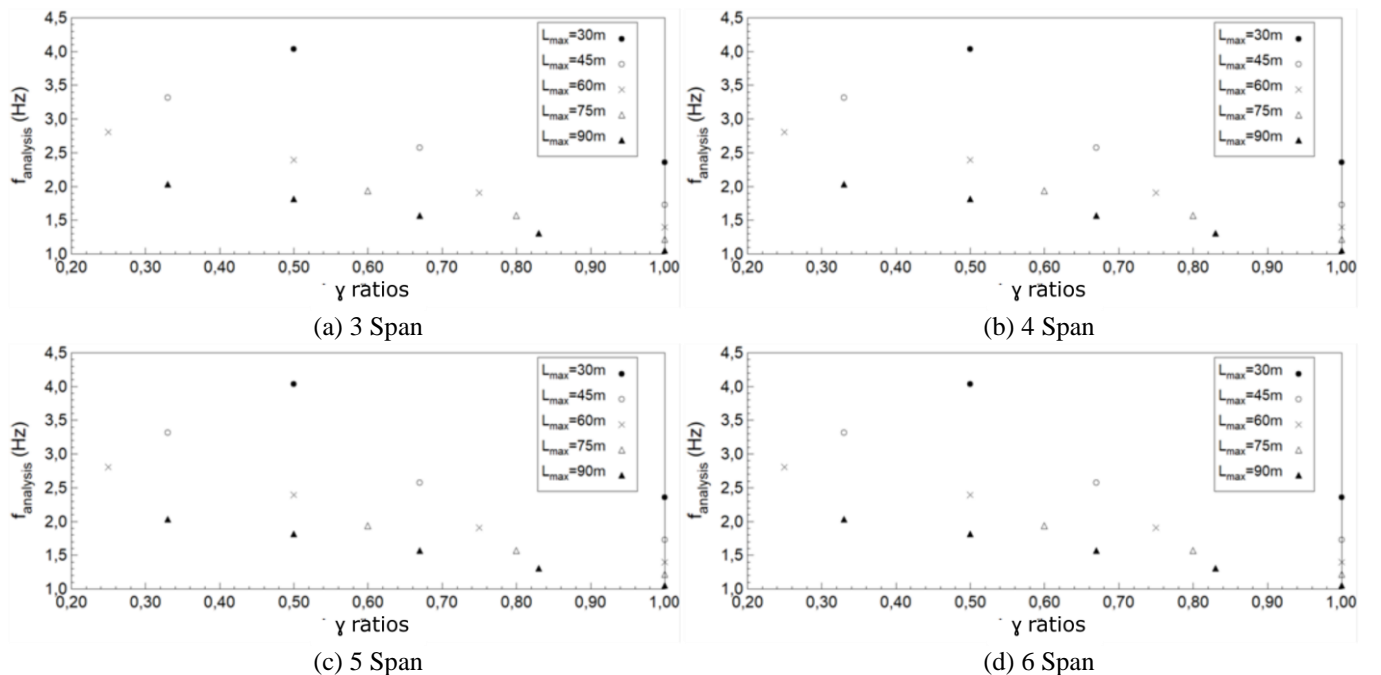


Fig.10. Natural Frequencies versus γ ratios

3.4 Effect of Cross-Section Arrangement:

To investigate cross-sectional effect on the natural frequency, five different steel bridges with variable cross-section are generated. For all generated bridges; α and r ratios are respectively taken as 0.33 and 1.0 as shown in Table 2, Case E. 15m-30m-30m-15m span arrangement is used. Concrete slab thickness and width are respectively used with same dimensions as 0.2 m and 12 m in all numerically modelled continuous bridges.

The natural frequencies of CS-1, CS-2, CS-3, CS-4 and CS-5 respectively equal to 3.289, 3.280, 3.282, 3.510 and 2.963.

CS-1, CS-2 and CS-3 have equal steel girder. Girder spacing and diaphragm lengths of CS-2 are smaller than CS-1 and CS-3. The natural frequencies of CS-1, CS-2 and CS-3 are slightly changed with changing steel girder space. Maximum difference of natural frequencies is obtained as 0.26 % between CS-1 and CS-2. With decreasing diaphragm lengths and therefore decreasing mass can affect to this small increment on the natural frequency.

CS-3, CS-4 and CS-5 which have same distance to concrete edge, are used to obtain effect of girder number on the natural frequency. Vertical rigidity of CS-4 should be more

than the other models and accordingly, CS-4 has biggest frequency value, as CS-5's frequency is the smallest. The maximum difference of the natural frequency is obtained as 18.5 % between CS-5 having 3 steel I-girders and CS-4 having 5 steel I-girders.

3.5 Effect of Support Condition:

From two-span to six-span continuous bridges are used to investigate support condition on the natural frequency of continuous-span bridge. The pin constrains that prevent three translational displacements are used at edge supports for continuous bridges. Roller constrains that prevent vertical and transverse displacements are used at the middle supports. General geometry is shown on typical four-span continuous bridge with straight haunched section in Fig.11.

For all models include two, three, four, five and six-span continuous bridges are analysed with two different support conditions (Fig. 2 and Fig. 11). The natural frequencies of bridges having two pin constrains at edge supports are smaller than the natural frequencies of bridges having one pin constrains at starting support. The maximum difference is observed as 15 % in all analysed cases of continuous bridges with different span arrangements.

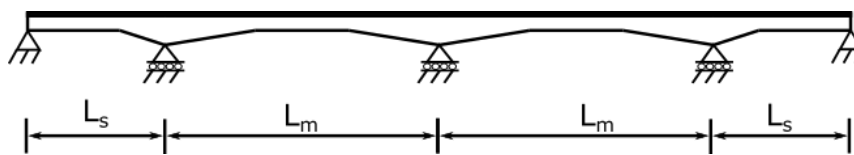


Fig.11. Geometry of continuous-span bridges with two pin constrains at starting and ending supports

4. Summary and Conclusions

This paper investigates the effect of various parameters on the natural frequency of continuous-span composite steel I-girder bridges with straight haunched section. 153 numerical models are analysed by using 3-D finite element models by using CSIBridge. The following conclusions can be drawn based on the results of the analyses:

1. While other parameters are constant; as r values increases, the natural frequency of continuous bridge increases. Likewise, the natural frequencies of continuous bridges increase with increment of α values. As given Table 3, the maximum difference is found as 3.35 % under the condition which α values are constant and r values are variable. Otherwise, the maximum difference is found as 14.57 % under the condition which r values are constant and α values are variable as shown Table 4.
2. Maximum span length of bridge has important effect on the natural frequencies of continuous-span bridges. In general, the natural frequency of bridge decreases with following curve while maximum span length increases. For all curves, 'a.x^b' expression gives best fitting. Depend on results, a

and b values has been produced corresponding span arrangement.

3. Effect of the ratio between middle span length and side span length (γ) on the natural frequency is also important factor. Natural frequencies of bridges that have same span number, linearly decrease with increasing γ ratios.
4. The natural frequencies of bridges can be changed by using different steel girder numbers and girder spacing. The steel girder numbers are more efficient on the natural frequency than steel girder spacing. The difference is obtained as 0.26 % due to effect of steel girder spacing with the same number of steel I-girders while the difference is obtained up to 18.5 % due to the effect of steel girder numbers decreasing from 5 steel I-girders to 3 steel I-girders.
5. Finally it is observed that the edge supports conditions of continuous bridges have also effect on the natural frequency. As ending support condition is changed from roller to pinned support, difference is obtained up to 15 % in studied cases with different span arrangement.

References

- [1] Wolek AL, Barton FW, Baber TT and Mckeel WT Jr., "Dynamic fields testing of the route 58 Meherrin river bridge", Charlottesville (VA): Virginia Transportation Research Council; 1996.
- [2] Ontario Highway Bridge Design Code, 2nd. Edition, Ontario Ministry of Transportation and Communications, Downsview, Ontario, Canada, 1983.
- [3] 92 Austroads bridge design code, Section two-code design loads and its commentary, Austroads, Haymarket, Australia, 1992.
- [4] AASHTO. Standard specifications for highway bridges, 17th. Ed. Washington, DC: American Association of State Highway and Transportation Official, 2002.
- [5] AASHTO. LRFD bridge design specifications, 7th. Ed. Washington, DC: American Association of State Highway and Transportation Official, 2014.
- [6] Roeder CW, Barth KB and Bergman A., "Improved live-load deflection criteria for steel bridges. Final report NCHRP" Seattle (WA): University of Washington", 2002.
- [7] El-Mezaini N., Balkaya Can and Citipitioglu E., "Analysis of frames with nonprismatic members.", ASCE, Journal of Structural Engineering, 117(6), 1573-1592, 1991.
- [8] Balkaya Can, "Behavior and modeling of nonprismatic members having T-sections" ASCE, Journal of Structural Engineering, 127(8), 940-946, 2001.
- [9] Gao Qingfei, Wang Zonglin and Guo Binqiang, "Modified formula of estimating fundamental frequency of girder bridge with variable cross-section", Key Engineering Materials Vol 540 pp 99-106, 2013.
- [10] CSIBridge 2017 v19, Integrated 3D Bridge Analysis Software, Computer and Structures Inc., Berkeley, California.
- [11] Barth KE and H. Wu., "Development of improved natural frequency equations for continuous span steel I-girder bridges.", Engineering Structures 29 (12): 3432-3442, 2007.
- [12] Warren J. Ashley, Sotelino Elisa D. and Cousins Thomas E., "Finite element model efficiency for modal analysis of slab-on-girder bridges", 2009.

A General Approach to Accreditation of Environmental Laboratories in Turkey

Perihan Akan*[‡], Ozlem Muge Testik **

* Department of Environmental Engineering, Faculty of Engineering, Hacettepe University, 06800 Ankara, Turkey

** Department of Industrial Engineering, Faculty of Engineering, Hacettepe University, 06800 Ankara, Turkey

(apakan@hacettepe.edu.tr, ozlemaydin@hacettepe.edu.tr)

[‡] Corresponding Author; Perihan Akan, Hacettepe University, 06800 Ankara, Turkey, Tel.: +90 312 2977800

Fax: +90 312 2992053, apakan@hacettepe.edu.tr

Received: 27.03.2018 Accepted: 04.06.2018

Abstract- In this study, the accreditation of environmental parameters and types of laboratories accredited by ISO 17025 Standard were compared. In Turkey, environmental laboratories were classified as public, private and university laboratories. Furthermore, environmental parameters considered in this study are water quality parameters and air quality parameters. In current study, 43 water quality parameters in university and 47 water quality parameters in public and private institutions were examined with regard to accredited laboratories in Turkey. Accredited water quality parameters in public and private institutions as different from universities are Total Solid, Ammonia/Ammonia Nitrogen, Total Nitrogen, and Total Kjeldahl Nitrogen. As for air quality parameters, the number of air quality parameters accredited in public and private institutions is approximately twice as air parameters accredited in universities (42 and 26, respectively). The most accredited water parameter is pH, with total of 65, where 44 of them are private, 11 are public and 10 are university laboratories. Chemical Oxygen Demand (COD) and Suspended Solid (SS) are placed in the second order with total of 56. Here, 39 private, 10 public and 7 university laboratories are accredited in terms of COD and 40 private, 10 public and 6 university laboratories are accredited in terms of SS. Conductivity is next remarkable parameter with total of 53 institutions (37 private, 8 public and 8 university laboratories). In air parameters, the most accredited one is the SO₂, with total of 52 institutions (49 private, 2 public and 1 university laboratory).

Keywords Laboratory accreditation, environmental quality parameters, ISO 17025, quality management system.

1. Introduction

It is a well-known fact that environmental pollution is considered, water pollution and air pollution first come to mind. The most important and first step to be able to identify the pollution factors, to estimate the dimensions of the pollution and to take precautions is to monitor the pollutants in the medium. The monitoring of the environmental pollutants plays a significant role in the development and implementation of environmental policies. Water quality must be monitored and assessed for the treatment of water resources contaminated by agricultural or industrial activities and also for the protection of natural water resources, which are essential to human and other living organisms. The protection of public health, the providing of aesthetic or social goals of water quality, the determination of the

effectiveness of the regulations to be taken for the protection and control of water quality can be listed as the objectives of water quality management [1]. The air like the water is necessary to life. Living organisms would like to be assured that the air that they consumed will not result in harm effects on them [2]. Hence, air pollutants released into the atmosphere must be monitored and evaluated [3]. The accredited laboratories proving that test and analysis results are reliable by third parties and institutions must be preferred for the monitoring of concentrations of pollutants bringing about severe environmental problems such as water pollution and air pollution and the measurement of the environmental parameters employed as an indicator in the control mechanism of the pollutants [4].

Laboratory accreditation can be described as a formal recognition by an authoritative body of the technical competence of a laboratory to perform tests or calibrations. This recognition is given by an accreditation body, which plays role as a third party between the laboratory and its clients, and intends to provide confidence between them. One of the fundamental goals in the presence of accreditation systems is the need to remove technical barriers to international trade, *i.e.* that a product once tested in an accredited laboratory should not need to be retested by the client, since another accredited laboratory in another country would find a similar result [5, 6].

Accreditation provides an independent conformation of organizational competence having policies in place, a quality management system and audit systems to support self-regulation [7]. Laboratory accreditation evaluates the competencies of all types of laboratories with regard to performing specific tests and calibrations. ISO and the International Electro-Technical Commission (IEC) introduced ISO/IEC 17025 standard, which is significantly related to documenting the process of any analysis performed by a laboratory, owing to the increasing significance of accreditation and international recognition. ISO 17025 consists of the quality management system and technical requirements of the accreditation process [8, 9]. The quality management system of a laboratory is associated with the guarantee of the consistency of test results and their conformity with defined criteria. As for technical requirements for ISO 17025 standard, environment, equipment, reagents, culture media and reference materials, sampling and sample handling, test methods, and quality of performance are considered [10]. The variability of test results and the frequency of errors can be reduced by implementing and monitoring a comprehensive laboratory quality management system [11]

In recent years, many studies are focused on the importance of laboratory accreditation on especially accuracy of experimental results. The summary of the previous studies performed for the assessment of laboratory accreditation in a variety of topics is listed in the following: Morris and Macey [12] investigated the performance of environmental laboratories with two different studies including the 1997 study implemented between 1994 and 1996, and the 2001 study implemented between 1997 and 1999 in Canada. Biochemical Oxygen Demand (BOD), Total Suspended Solids (TSS), Chloride (CL), Dissolved Iron (DFE), Fecal Coliforms (FCOL) were examined environmental parameters. They concluded that in both studies, accredited laboratories outperformed non-accredited laboratories in all measures. Lopez et al., [13] examined the perceived value of accreditation among individuals who have successfully achieved the Intersocietal Accreditation Commission (IAC) echocardiography accreditation. In their study, an electronic survey was sent to accredited facilities soliciting demographic data along with questions regarding the perceived value of accreditation related to 15 quality indicators. In the result of the study, more than 90 % of respondents reported that maintaining accreditation was important for improved quality and better reimbursement. Middlebrook [14] compared the accredited laboratories with

non-accredited laboratories in terms of performance in proficiency testing. In this study, comparisons were made of z-scores between accredited and non-accredited laboratories for the data as a whole, as well as for subsets of the data partitioned into groups such as inorganic tests, organic tests and microbiological tests. The study exhibited that the difference between accredited and non-accredited laboratories was much greater than unsatisfactory results were compared.

Furthermore, the general conclusion of the study showed that accredited laboratories continually outperform non-accredited laboratories as a group. Cortez [5] implemented a case study investigating if accredited laboratories perform better than others in a proficiency testing. In this study, 33 parameters including pH, conductivity, alkalinity, bicarbonate, hardness, Ca^{2+} , Mg^{2+} , Na^+ , K^+ , Cl^- , SO_4^{2-} , F^- , SiO_2 , NO_3^- , NO_2^- , NH_4^+ , PO_4^{3-} , Fe, Mn, Cu, Zn, Al, Ba, Sr, Cd, Cr, Ni, As, Sb, Se, Hg, Ag, and Pb were examined. The 76 participating laboratories represented all types of laboratories from governmental and regulatory bodies, to public, private, industrial and university laboratories investigated. The results of the study showed that accredited results have a significantly higher percentage of satisfactory results.

2. Materials and Methods

In this study, the status of the accreditation of environmental parameters was evaluated and types of laboratories accredited by ISO 17025 Standard were compared. In Turkey, laboratories were classified as public, private and university laboratories for analysis. In current study, 43 water quality parameters in universities and 47 water quality parameters in public and private institution were examined with regard to accredited laboratories in Turkey. These parameters are pH, conductivity, BOD, Chemical Oxygen Demand (COD), Dissolved Oxygen (DO), Hardness, Temperature, Color, Alkalinity, Ammonia, Ammonia Nitrogen, Calcium (EDTA Method), Chlorophyll, Residual Chlorine, Chloride, Chromium, Magnesium, Nitrate/Nitrite Nitrogen, Nitrite/Nitrite Nitrogen, Light Transmittance, Total Solid (TS), Suspended Solid (SS), Ammonium, Ammonium Nitrogen, Total Nitrogen, Phosphate/Orthophosphate Phosphorous, Total Phosphorous, Total Kjeldahl Nitrogen (TKN), Sulfate, Escherichia coli (E. coli) and Coliform Bacteria Count, FCOL, Total Dissolved Solid, Oil-Grease, Turbidity, Total Organic Carbon, Arsenic (As), Cadmium (Cd), Lead (Pb), Iron (Fe), Copper (Cu), Calcium (ICP-MS Method), Zinc (Zn), Aluminum (Al), Manganese (Mn), Nickel (Ni), Silver (Ag), Sodium (Na), Potassium (K).

Accreditation water quality parameters in public and private institution as different from universities are Total Solid, Ammonia, Ammonia Nitrogen, Total Nitrogen and TKN. Furthermore, the number of air quality parameters accredited in public and private institutions is approximately twice as air parameters accredited in universities (42 and 26

respectively). Sulfur dioxide (SO₂), Volatile Organic Carbon (VOC), Particulate Matter (PM10), Hydrogen Cyanide (HCN), Sootiness, Moisture, Carbon monoxide (CO), Carbon Dioxide (CO₂), Oxygen (O₂), Heavy metals (As, Cd, Cr, Cu, etc.) were some of air quality parameters examined in this study.

3. Results

In this study, 184 university laboratories, 11 public and 71 private institution laboratories were examined in terms of their accreditation status in environmental quality parameters. Unfortunately, only 26 universities in Turkey have accredited laboratories and also only 10 of them are accredited in terms

of environmental parameters. In this study, 43 water quality parameters and 26 air quality parameters in university laboratories and 47 water quality parameters and 46 air quality parameters in public and private institution laboratories were investigated in accordance with their accreditation status. According to data obtained from TAA, 24 of the private corporation laboratories are not accredited in terms of water parameters and 12 of them are not accredited in terms of air parameters, too. Similar to universities, only one public institution has accredited laboratory with regard to air quality parameters. The current status of water and air quality parameters of the universities and public institutions having accredited laboratories in Turkey are shown in Table 1 and Table 2.

Table 1. Accreditation status of university laboratories.

University	Number of Accredited Water Quality Parameters	Number of Accredited Air Quality Parameters
Dokuz Eylul	43	26
Aksaray	39	0
Mugla Sıtkı Kocman	35	0
Anadolu	26	0
Bogazici	25	0
Balıkesir	24	0
Trakya	14	0
Kahramanmaraş Sutcu Imam	10	13
Mersin	2	0
Dicle	2	0

Among universities shown in Table 1, Dokuz Eylul, Aksaray and Mugla Sıtkı Kocman University are very successful in the accreditation of environmental parameters especially water quality parameters. Dokuz Eylul University is superior than other 9 universities in both accredited water and air quality parameters. The Scientific and Technological Research Council of Turkey called as its abbreviation (TUBITAK). TUBITAK has the most accreditation laboratories in terms of environmental parameters. Similar to universities, only one public institution (TUBITAK) has accredited laboratory with regard to air quality parameters in accordance with Table 2.

Table 2. Accreditation status of public institution laboratories.

Accreditation Status of Public Institution Laboratories	Number of Accredited Water Quality Parameters	Number of Accredited Air Quality Parameters
The Scientific and Technological Research Council of Turkey	36	17
Antalya Water and Sewage Authority General Directorate	35	0
Denizli Metropolitan Municipality	32	0
Antalya Metropolitan Municipality	28	0
Kayseri Metropolitan Municipality	27	0
Ministry of Environment and Urbanization	26	0
Izmir Water and Sewage Authority General Directorate	25	0
Istanbul Environmental Management Industry and Trade Company	21	0
Mugla Water and Sewage Authority General Directorate (MUSKI)	7	0
Istanbul Metropolitan Municipality	4	0
MUSKI Bodrum Environmental Laboratory	4	0

There are 82 institutions (71 private and 11 public) accredited in terms of environmental parameters in Turkey. All 11 institutions are accredited in all of water quality parameters while all 71 private institutions are not accredited

that. Only 44 (62%) of private institutions with accredited laboratories are accredited in terms of water quality parameters. Hence, it can be said that to be successful in accreditation of water quality parameters for some private

institutions, while some ones have become accredited only on a few water quality parameters. Table 3 exhibits the number of water parameters in accordance with accredited institutions [4].

All 11 institutions are accredited in all of water quality parameters while all 71 private institutions are not accredited that. Only 44 (62%) of private institutions with

accredited laboratories are accredited in terms of water quality parameters. Hence, it can be said that to be successful in accreditation of water quality parameters for some private institutions, while some ones have become accredited only on a few water quality parameters. Table 3 exhibits the number of water parameters in accordance with accredited institutions [4].

Table 3. The number of water parameters in terms of accredited institutions.

Parameters	Number of Accredited Institutions			Total
	Private	Public	University	
pH	44	11	10	65
COD	39	10	7	56
SS	40	10	6	56
Conductivity	37	8	8	53
Oil-Grease	37	8	4	49
BOD	35	7	5	47
Temperature	38	2	2	42

The most accredited water parameter is pH, with total of 65, where 44 of them are private, 11 are public and 10 are university laboratories. COD and SS are placed in the second order with total of 56. Here, 39 private, 10 public and 7 university laboratories are accredited in terms of COD and 40 private, 10 public and 6 university laboratories are accredited in terms of SS. Conductivity is the next remarkable parameter with total of 53 institutions (37 private, 8 public and 8 university laboratories) [4]. As

for air quality parameters accredited in university and institution laboratories in Turkey, the most accredited one is the SO₂, with total of 53 (49 private, 2 public and 2 university laboratories) as shown in Table 4 [16]. Air parameters compared to water quality parameters accredited in various institutions accredited only two university laboratories (Dokuz Eylul University and Kahramanmaraş Sutcu Imam University).

Table 4. The number of air parameters in terms of accredited institutions.

Parameters	Number of Accredited Institutions			Total
	Private	Public	University	
SO ₂	49	2	2	53
Sootiness	49	1	2	52
CO and CO ₂	48	2	2	52
O ₂	46	1	2	49
NO _x	46	1	2	49
PM ₁₀	45	1	2	48
Humidity	42	1	2	45

4. Conclusion

In this study, the status of the accreditation of environmental parameters was evaluated and types of laboratories as public, private and university laboratories accredited by ISO 17025 Standard were compared in terms of the number of accredited environmental quality parameters. In accordance with the result of this study, only three (Dokuz Eylul University, Aksaray University and Mugla Sıtkı Kocman University) of 184 universities in 2016-2017 academic year are more successful in accreditation of water quality parameters, while only one university laboratory (Dokuz Eylul University) shows accreditation in all air quality

parameters. Moreover, pH, COD, SS, conductivity, oil-grease, BOD, temperature are the most accredited water quality parameters, respectively and also SO₂, sootiness, CO as well as CO₂ are the remarkable air quality parameters in terms of accreditation status of especially private institution laboratories. In literature, along with the importance of accredited laboratories has been increasing every passing day, the number of studies covering the accreditation status of particularly environmental laboratories is not enough to identify the contents of studies implemented in this area. In this context, this study will shed light on the literature.

Acknowledgements

This study was presented as an extended abstract in 2nd International Conference on Air, Water, and Soil Pollution and Treatment (DOI: 10.11159/awspt17.119).

References

- [1] P.H. McGauhey, 'Engineering management of water quality', McGraw-Hill, University of California, Berkeley, 1968.
- [2] P. A. Vesilind, S. M. Morgan, L. G. Heine, 'Introduction to environmental engineering', 3rd ed. Cengage Learning, USA, 2010.
- [3] J. R. Mihelcic, J. B. Zimmerman, 'Environmental engineering fundamentals, sustainability, design', 2nd ed. Wiley, USA, 2014.
- [4] P. Akan, O. M. Aydin Testik, "Examination of the accreditation status of water quality parameters" The Turkish Journal of Occupational/ Environmental Medicine and Safety, vol.2. pp. 1-9, 2017.
- [5] L. Cortez, "The implementation of accreditation in a chemical laboratory. Trends in Analytical Chemistry" Trends Analyt. Chem. vol. 18, pp. 638-643, 1999.
- [6] ISO/IEC Guide 2: Standardisation and related activities - General vocabulary, Geneva, 1996.
- [7] B.W. J. Rankin, C. Welsh, "Accreditation", Encyclopedia of Forensic Sciences, 2nd ed., pp. 515-518, 2013.
- [8] E. Sadikoglu, T. Temur, "The Relationship Between ISO 17025 Quality Management System Accreditation and Laboratory Performance", Quality Management and Practices, Chp13, pp. 221-230, InTech Publisher, 2012.
- [9] "TS EN ISO/17025:2005 General requirements for the competence of testing and calibration laboratories " <http://www.iso.org/standard/39883.html> Accessed 26th March 2018
- [10] M. Upmann, R. Stephan, "Laboratory Accreditation", Encyclopedia of Meat Sciences, vol. 2, pp. 667-674, 2014.
- [11] T. F. Peter, P. D. Rotz, D. H. Blair, A. A. Khine, R. R. Freeman, M. M. Murtagh, "Impact of laboratory accreditation on patient care and the health system", Am. J. Clin. Pathol. vol. 134, pp. 550-555, 2010.
- [12] A. Morris, D. Macey, "Laboratory Accreditation: Proof of Performance for Environmental Laboratories-2001 study", Accred Qual Assur, vol. 9, pp. 52-54, 2004.
- [13] L. Lopez, M. B. Farrell, J. Y. Choi, K. M. Cockroft, H. L. Gornik, G. V. Heller, S. D. Jerome, W. J. Manning, "Accreditation is perceived to improve echocardiography laboratory quality: results of an intersocietal accreditation commission survey" Journal of Diagnostic Medical Sonography vol. 33 (3), pp.163-171, 2017.
- [14] K. Middlebrook, "Do accredited laboratories perform better in proficiency testing than non-accredited laboratories?" Accred Qual Assur, vol. 22, pp.111-117, 2017.
- [15] Turkish Accreditation Agency, http://www.turkak.org.tr/turkaksite/Default_eng.aspx Accessed: 26th March 2018.
- [16] P. Akan, O. M. Aydin Testik, "Investigation of Accreditation Status of Environmental Parameters in Turkey", Proceedings of the 2nd World Congress on Civil, Structural, and Environmental Engineering, DOI: 10.11159/awspt17.119, 3-4 April 2017.

Investigation on Industry 4.0 and Virtual Commissioning

Akin Aras*, Murat Ayaz**‡, Engin Özdemir***, Nurettin Abut*

* Department of Electrical Engineering, Kocaeli University, 41380 Kocaeli, Turkey

**Department of Alternative Energy Resources Technology, Kocaeli University, 41380 Kocaeli, Turkey

***Department of Energy Systems Engineering, Kocaeli University, 41380 Kocaeli, Turkey

(akin.aras@siemens.com, murat.ayaz@kocaeli.edu.tr, eozdemir@kocaeli.edu.tr, abut@kocaeli.edu.tr)

‡Corresponding Author; Murat Ayaz, Kocaeli University, 41380 Kocaeli, Turkey, Tel: +90 (262) 371 23 95,

Fax: +90 (262) 371 47 75, murat.ayaz@kocaeli.edu.tr

Received: 03.04.2018 Accepted:24.05.2018

Abstract - The human being had been busy with mostly agricultural economy for a long history when the steam was considered as a resource of kinetic energy. Using the steam machine in textile industry for the first time in the UK at the beginning of the 18th century, would be called as “Industrial Revolution” many decades later. Respectively, second industrial revolution with the invention and utilizing of electricity, then third industrial revolution with the rise of electronics and automation followed this period. And today, we have been facing with the fourth industrial revolution via internet of things, augmented reality, learning machines, etc. One of the key technologies that are improved in this period is virtual commissioning. The aim of this contribution is to suggest a definition to the Industry 4.0 with its historical precursors, and to give a focus on virtual commissioning technology as an output of the fourth industrial revolution.

Keywords: Industry 4.0, Big data, Virtual Commissioning, Siemens, Process Simulate, Simulation

1. Introduction

When the “Industry 4.0” concept was verbalized in Hannover Fair in 2011 for the first time [1], the historical improvement of the industry became an interesting topic again. Since this statement was used, many people from various fields have focused on the main milestones of the industry to understand the meaning of the fourth industrial revolution and to give a satisfying definition to this period.

The first industrial revolution emerged with the invention of the steam machine and its utilization in textile industry in the UK, in early 18th century. The second one can be stated as the invention and utilization of electricity and the emerging of the serial production lines in parallel to this. The third one can be defined as the electronic control systems to be used in serial production lines as PLCs, robots, etc. And with the utilization of the huge data that is generated by the smartened things, the world has been talking about the Industry 4.0.

Many new technologies have emerged during this new period. [2,3] They are Internet of things, smart factories, 3D printers, augmented realities, wearable technologies, etc. [3] Virtual commissioning is one of these shining technologies.

In traditional commissioning, the automation program is tested on the real machine or production line. Virtual commissioning has emerged as an answer to the necessity of a technique that brings cost and time efficiency in commissioning process, and shortens the time to market. [4]

In the first part of this contribution, the Industry 4.0 concept is analyzed in historical process and is tried to be defined in technological aspects. In the next part, its gainings and effects are observed. In the last part, virtual commissioning is explained with its advantages as cost and time efficient, and more flexible alternative to the traditional commissioning approaches. Besides, Siemens Process Simulate and VR system with ABB RobotStudio and HTC Vive are observed at the end, as simplified, flexible and state of the art virtual commissioning solutions.

2. Industry 4.0

At the beginning of the 18th century, the first steam machines, a sample can be seen in Fig. 1, had been invented and were used in textile industry. As soon as the steam machines took the place of the human muscle force, the labour force that was earlier working in agriculture shifted into mechanized production eventually.

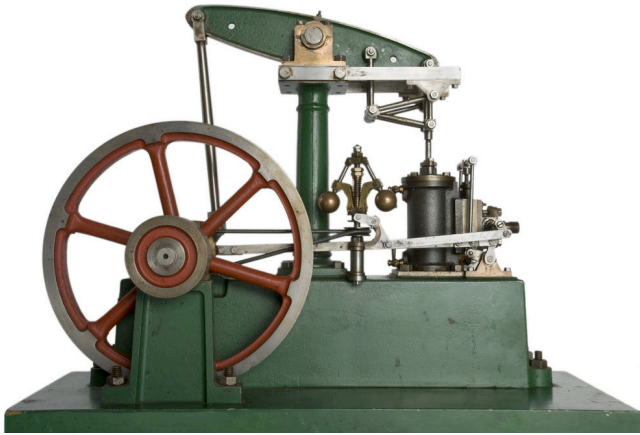


Fig. 1. Steam Machine [5]

This situation caused migration from rural to urban areas and led the powerful states researching raw materials in order to produce even more. This period is named as industrial revolution in world history.

Almost 100 years later, via the invention of electricity and the integration of the electrical machines, a sample can be seen in Fig. 2, to industry, serial production lines emerged. As a result of people to work in serial production lines, the production outcomes increased rapidly. Thus, more industry products were released to market in less time. The topics such as decreasing costs and increasing reachability of the products affected the societies as well. As a cycle effect, the increasing populations of the urban areas caused more labour force and more industry products to emerge. This period that the industry was transformed with the electricity is named as second industrial revolution.

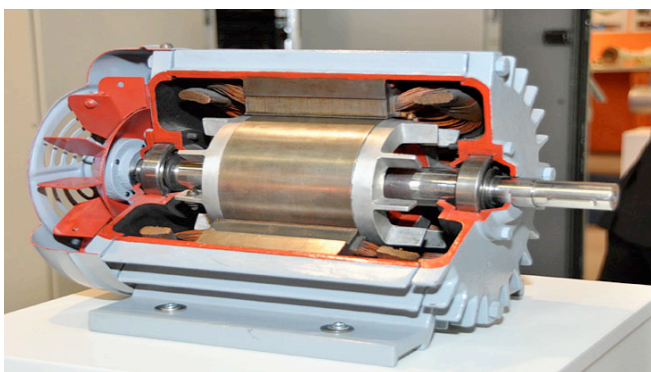


Fig. 2. Electrical Machine [6]

Along with the electronics was improved in 20th century and the PLCs, some sample models can be seen in Fig. 3, were integrated into industry 40-50 years ago from today, the automation era began. As a benefit of the PLCs to be used in the industry, the serial production lines became more

controllable and flexible. This situation led the quantity and the diversity of the industry products to increase. At the same time the requirement to the human muscle force decreased, the need of the technical knowledge and skills increased. This period that the automation systems transformed the industry is named as third industrial revolution.



Fig. 3. Programmable Logic Controllers (the one in the front is an I/O module) [7]

In automated serial production lines, huge information is generated by various sources such as sensors, valves, motors and robots. This unprocessed information is called as big data. The processing and reuse of this big data and beyond this, the pursuit of transforming all things to be able to produce data, gave birth to the fourth industrial revolution. In this regard, "Industry 4.0" statement was used in Hannover Fair in 2011 for the first time.

According to a study [3], the integration of Internet of Things to the manufacturing environments is forcing the fourth industrial revolution. The cyber-physical systems allow the companies to incorporate their machinery, warehouse and production systems under one unique network. This facilitates the smart machines and production facilities to exchange information autonomously and to control their jobs independently. In Industry 4.0 concept, the smart factories let the smart products to be produced with more flexibility, considering not only the market demands but also the individual customer requirements. The core factor behind this dynamic business model is the big data that is generated in the manufacturing environment.

2.1. Big Data

The key point of fourth industrial revolution is creating value from the huge information that is generated by various objects.

Along with the analyze and reuse of the data that is generated from the things, new research and application fields emerged that are recently named as "smart factories", "cyber-physical systems", "augmented reality", "autonomous robots", "additive manufacturing", "cloud computing", "Internet of Things" and further can be seen in Fig. 4.

As stated by Ninan et al. [8], almost all objects are likely to be turned to source of data by Internet of Things technologies. According to them, the sequence of activities to

create value from information can be defined as the Information Value Loop Fig. 5.

2.2. Changing Business Lines

This value created data changes the industry and also the society in various aspects. In this period of the industry to be transformed, many business lines have been disappeared while new business lines have been appeared.

In automation era, the robotic systems rapidly invaded in the places of the nonskilled work force by performing the repetitious jobs in manufacturing. However new specialties that emerged in this period like automation, robotics, mechatronics provided new job fields. In Industry 4.0 era, the smart systems will be likely taking the places of the skilled work force those are performing repetitious jobs in manufacturing and in offices as well, such as complex assembly, quality control, planning, etc. Same as in automation era, this repetitious job killing process have led new specialties to emerge like:

- 3D manufacturing engineering: Along with the improvement of 3D printers, the additive manufacturing entered into focus in various industries. This technology necessitates specialized technical people.
- Big Data Analyst: Since the core topic of Industry 4.0 is big data, the requirement of specialized people for analysing this data has emerged.

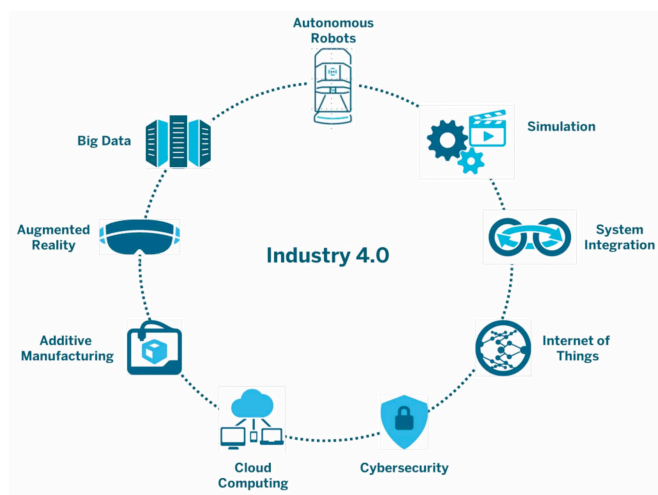


Fig. 4. Industry 4.0 components [9]

According to this loop, an act is defined by sensors and information is created by this way. Then this information is communicated via network and is aggregated by standards. Augmented intelligence techniques allow the information to be analyzed. At the end of the loop, improved action is reached by augmented behaviour techniques.

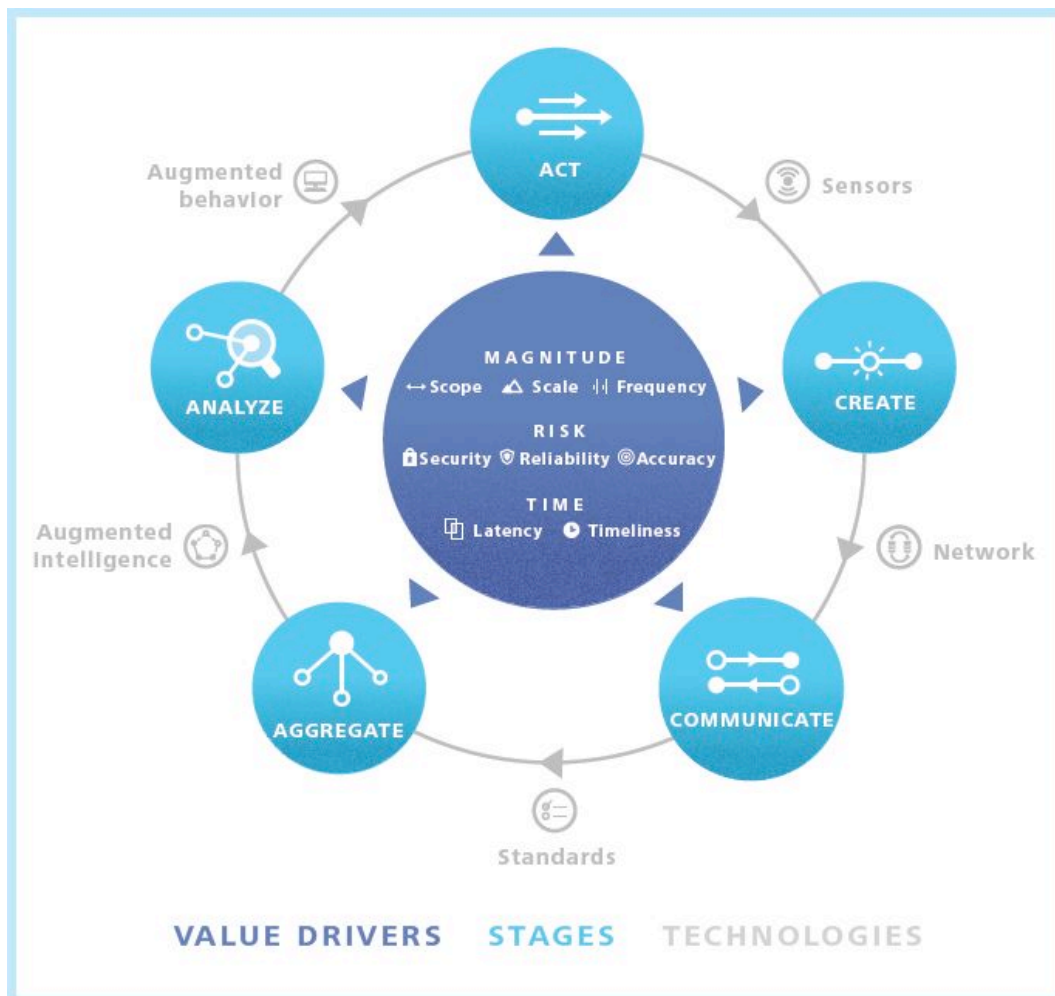


Fig. 5. Information Value Loop [8]

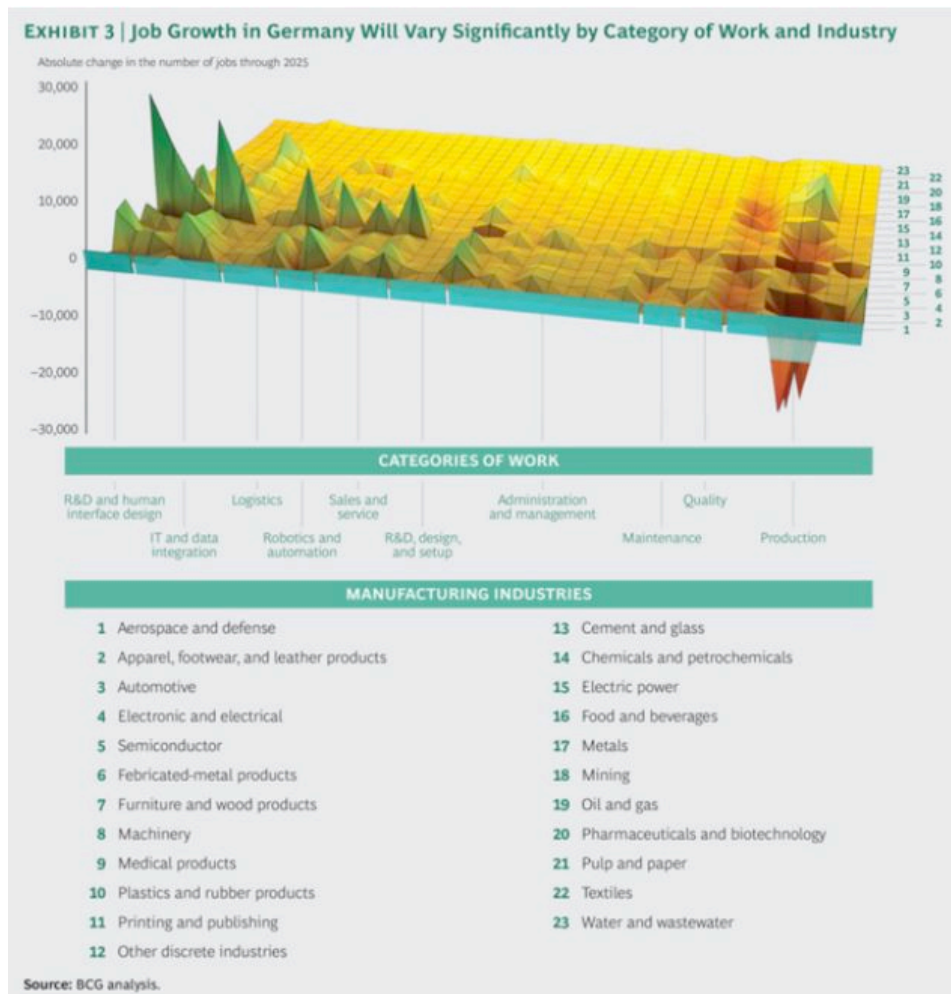


Fig. 6. Shifting in the Jobs in Industry 4.0 Era [10]

- Robotics engineering: Since robots have already invaded in manufacturing industry, along with the advanced dynamics technologies, the robots have been taking their places in society step by step in logistics, warehouse operations, personal assistance, etc. These functions point out the requirement for specialized robotics experts.

- Drone pilot: Drones have already been used in photography and film industries, logistics, security, etc. Although this field is very new, drone pilot jobs are likely to be more popular.

- Simulation engineering: Utilizing the big data, the manufacturing systems can be simulated. This technology has led virtual commissioning as it is explained in a detailed way in this article.

In order to reveal the shifting in jobs in Industry 4.0 era [10], the below graphic in Fig. 6 would be beneficial.

2.3. Revenue, Cost and Efficiency Benefits of Industry 4.0

Along with the transformation of big data to smart knowledge, there have been outstanding revenue, cost and efficiency benefits of the fourth industrial revolution.

A study [11] demonstrates that Industry 4.0 is increasing the revenue by digitizing the products and

services, creates new digital products, utilizing big data analytics as service, personalizing products and etc. Besides this, Industry 4.0 is increasing the efficiency of the systems by utilizing big data analytics for real-time quality control, increasing the flexibility and adaptability of production, using predictive algorithms to increase the equipment efficiency and etc.

Considering these benefits of Industry 4.0, the Virtual Commissioning is one of the technologies that stepped forward in this new period. In the next part, virtual commissioning systems for serial productions lines are explained and virtual communication software is observed.

3. Virtual Commissioning

Virtual commissioning for the serial production lines stepped forward as one of the innovations that were brought by the fourth industrial revolution. In traditional approach, the automation program is prepared and after that, the production line is mechanically installed in real environment. Subsequent to this, the automation program is tested on the site components (sensors, motors, valves, etc.) via PLC and thus the commissioning of the production line is performed. In this process, the errors in the automation program and mechanical design are detected and fixed. At

the same time, the product prototype quality is aimed to be reached to the requested level for the serial production.

According to a study [12], the commissioning period takes up to 25% and correcting errors in the automation program takes up to %15 of the time that is used for plant engineering and construction. As a possible solution to these problems the authors propose virtual commissioning.

In virtual commissioning concept, the process is performed in the computer environment via a real PLC or soft PLC. The purpose in this process is to detect and fix the errors in early phase. In order to realize this, the simulation model of the production line is prepared in simulation software including all of the components (sensors, motors, valves, etc.) that will be used. By means of the automation program to be communicated with the simulation software, the process of the machine or the production line is virtually observed and all program and design bugs can be fixed in this virtual environment.

An experimental study in virtual commissioning [13] shows the advantages of this technique to the traditional commissioning. The study was performed with two groups, each of them containing 30 people. One group used virtual commissioning for programming a machine. The other group did not use virtual commissioning and the results were compared. The tested system was a tin can be moulding press and the PLC was Siemens S7-300 model that uses 10 actuator outputs and 17 sensor inputs. The first group prepared the PLC program and then tested it on the real machine. The second group made the programming and testing on a virtual model. They performed real commissioning after verifying their program on the virtual model. The second group achieved a %75 shortened commissioning times. This result mainly caused by the improved accuracy of the program at the virtual commissioning period and shows the advantages of this technique. However, the virtual model was ready at the beginning of the second group's work so the time required for preparing the virtual model was not taken into consideration. In the conclusion, the authors indicate the necessity of a simplified and accelerated virtual model building approach. [14]

As a simplified and flexible solution to virtual modeling and commissioning, Siemens Process Simulate software is observed in the following section.

3.1. Siemens Process Simulate

Process Simulate, sample screenshots can be seen in Fig. 7 and Fig. 8, is software that is developed by Siemens and it is used to digitalize and verify the manufacturing processes in 3D environment [16].

In this software, manufacturing systems can be comprehensively designed and validated via advanced 3D environment. In order to simplify and accelerate the virtual commissioning process on Siemens Process Simulate, these steps are defined in a study [17] to be followed respectively: Characterizing the system, computer aided design, virtual environments, testing the virtual

environments, and virtual environments as a monitoring system.

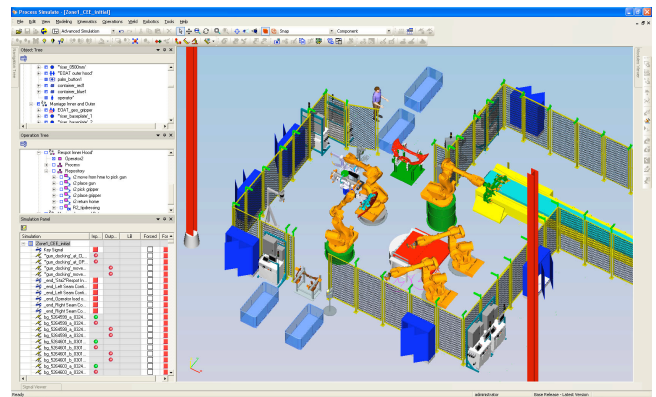


Fig. 7. Siemens Process Simulate – 1 [15]

These steps can be detailed like that: characterizing the system means to specify the working principles of the system. Then the system is needed to be designed in a CAD program like NX (Siemens PLM Software) or CATIA. Any CAD programs can be used for the design; however, the file then should be inserted in NX at the end, in order to convert it into. JT extension file. Then the design can be put into Process Simulate because it only needs JT file to be able to convert it to a COJT file. Then the virtual environment should be created via defining the movements. In this process, the internal logic blocks are also defined. Then the PLC program is prepared. The PLC program can be connected to Process Simulate using PLCSIM. The PLCSIM is software that allows the PLC programs to be simulated and tested. After the PLC program works properly on simulation, then it is downloaded to the PLC and tested on the real environment. And when it works properly on the real system, the simulation can be used as a monitoring system. The connection between the PLC and the Process Simulate is done via Siemens OPC software. Then the authors suggest utilizing these five steps to establish a simulation methodology for the manufacturing processes.

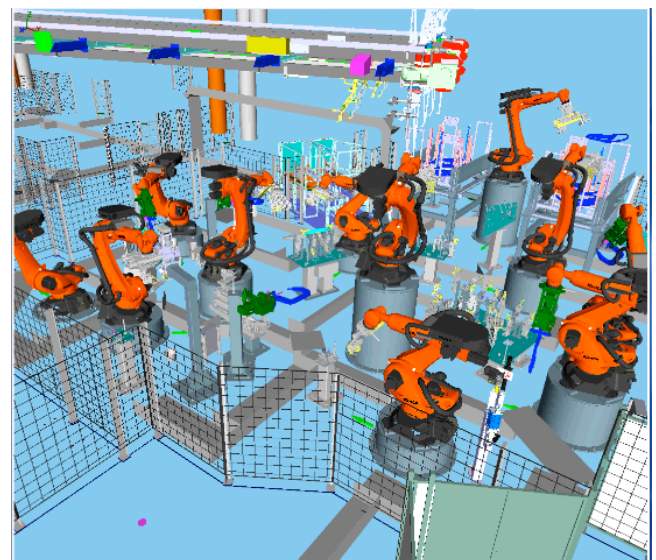


Fig. 8. Siemens Process Simulate - 2

4. ABB RobotStudio and HTC Vive VR System

ABB RobotStudio is software that allows robotic production lines to be designed and simulated on computer environment. Offline robot programming also can be performed in this software. Using HTC Vive VR system with this software, the robotic production lines can be virtually realized. The block diagram in Fig. 9 shows the hardware scope of the VR system.

HTC Vive is a virtual reality system. HTC Vive VR system consists of three main components. They are the main stations, controllers and headset as shown in Fig. 10. The headset and the hand controllers are tracked devices. With the help of the main stations, they can locate themselves in the virtual world.

Once the robotic production line is simulated in ABB RobotStudio, HTC Vive virtual reality system can be connected to the simulation. So that it gives the opportunity to feel as if you are in the virtual world of the simulated line. With the movement of the headset and the hand controllers as it can be seen in Fig. 11 and Fig. 12, the person can move in the ABB RobotStudio virtual environment and observe any point that the controllers are aimed. The laptop screens in Fig. 11 and Fig. 12 shows the change in the point of view, according to the movement of the controllers with the person.

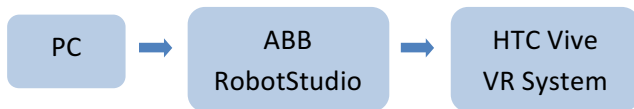


Fig. 9. Block diagram of VR simulation system



Fig. 10. HTC Vive main components [18]

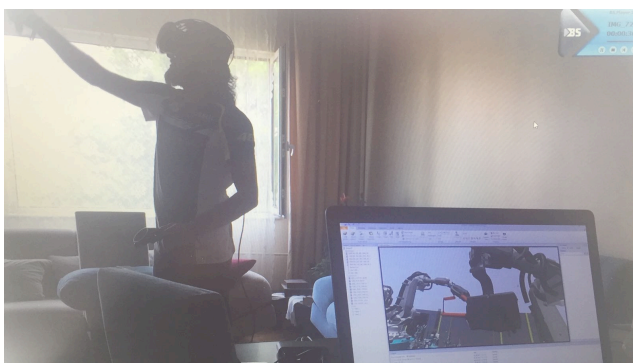


Fig. 11. VR System Application -1

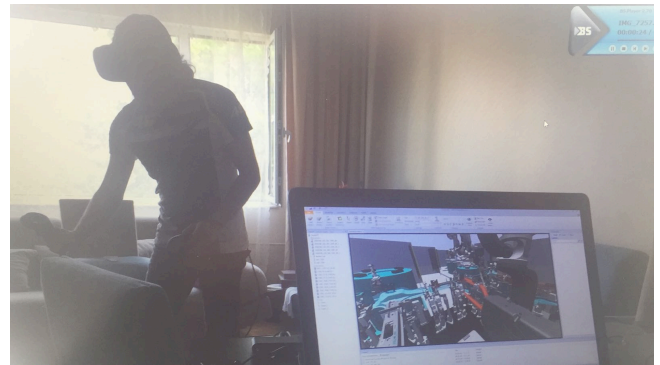


Fig. 12. VR System Application -2

5. Conclusion

In this contribution, Industry 4.0 concept and its components are explained with their effects on production lines. Via the observation of the virtual commissioning technology with different software, it is shown that this technology is cost and time efficient, and more flexible alternative to the traditional commissioning approaches.

Acknowledgements

The author gratefully acknowledges the support of Mr. Haluk Ozcan from Robo Automation for sharing valuable information about virtual commissioning.

The author also gratefully thanks to Mr. Gokhan Oguz from MekaSim Engineering for the support about ABB RobotStudio and HTC Vive VR system.

References

- [1] S. Alçın, “Endüstri 4.0 ve İnsan Kaynakları”, Popüler Yönetim Dergisi, vol. 63, p. 47, 2016.
- [2] T. Stock, G. Seliger, “Opportunities of Sustainable Manufacturing in Industry 4.0”, Procedia CIRP, vol. 40, ss. 536-541, December 2016.
- [3] Plattform Industrie 4.0, Recommendations for implementing the strategic initiative INDUSTRIE 4.0 - Final report of the Industrie 4.0 Working Group, Acatech, April 2013.
- [4] P. Puntel-Schmidt, A. Fay, “Levels of Detail and Appropriate Model Types for Virtual Commissioning in Manufacturing Engineering”, IFAC-PapersOnLine, vol. 48-1, pp. 922-927, February 2015.
- [5] <http://www.whoinventedfirst.com/invented-steam-engine/>
- [6] <http://www.bilgibaba.org/yazi/elektrik-motoru-nedir-nasil-calisir>
- [7] https://w3.siemens.com/mcms/programmable-logic-controller/en/advanced-controller/pages/default_alt.aspx
- [8] S. Ninan, B. Gangula, M. von Alten, B. Snidermann, “Who owns the road? The IoT-connected car of today- and tomorrow”, Deloitte University Press, August 2015.

- [9] <https://www.semiwiki.com/forum/content/6341-industry-4-0-manufacturing-processes.html>
- [10] <https://www.bcg.com/publications/2015/technology-business-transformation-engineered-products-infrastructure-man-machine-industry-4.aspx>
- [11] R. Geissbauer, J. Vedso, S. Schrauf, "Industry 4.0: Building the digital enterprise", www.pwc.com/industry40, April 2016.
- [12] M. F. Zäh, G. Wünsch, "Schnelle Inbetriebnahme von Produktionssystemen", *wt Werkstattstechnik online*, vol. 95, pp. 699-704, September 2005.
- [13] M. F. Zäh, G. Wünsch, T. Hensel, A. Lindworsky, "Nutzen der virtuellen Inbetriebnahme: Ein experiment - Use of virtual commissioning: An experiment", *ZWF Zeitschrift fuer Wirtschaftlichen Fabrikbetrieb*, vol. 101, pp. 595-599, October 2006.
- [14] P. Hoffmann, R. Schumann, T. Maksoud, G. Premier, "Virtual Commissioning of Manufacturing Systems: A Review and New Approaches for Simplification", 24th European Conference on Modelling and Simulation, Kuala Lumpur, pp. 175-181, 01-04 June 2010.
- [15] <https://www.cardsplmsolutions.nl/en/plm-software/tecnomatix/process-simulate-23/screenshots>
- [16] <https://www.plm.automation.siemens.com/en/products/tecnomatix/manufacturing-simulation/assembly/process-simulate.shtml>
- [17] L. Guerrero, V. López, J. Mejía, "Virtual Commissioning with Process Simulation (Tecnomatix)", *Computer-Aided Design and Applications*, vol. 11, pp. 11-19, July 2014.
- [18] <https://www.usgamer.net/articles/htc-vive-virtual-reality-systemdeluxe-audio-strap-549-black-friday-sale>.

A Novel Method for Increasing the Noise Immunity of Military Radio Systems via Self-Tuned Phased Array Antennas

Yalçın İsayev *, Mustafa Emre Aydemir **‡,

Ahed İsayev *, L.H. Mammadova*

* War College of Armed Forces of the Azerbaijan Republic Azerbaijan Military High School after H.Aliev, Azerbaijan

** Department of Computer Eng., Faculty of Engineering, Istanbul Gelisim University, Avcılar, Istanbul, Turkey

(yalchin.isaev.73@mail.ru, meaydemir@gelisim.edu.tr, ahadisayev@mail.ru, nazrinb97@mail.ru)

‡ Corresponding Author; Mustafa Emre Aydemir, Department of Computer Eng., Faculty of Engineering, Istanbul Gelisim University, Avcılar, Istanbul, Turkey, Tel: +90 212 422 70 00

Fax: +90 212 422 74 01, meaydemir@gelisim.edu.tr

Received: 17.04.2018 Accepted: 08.06.2018

Abstract- The noise immunity of radio systems is one of the most important topics in military science. In this article, the methods for increasing the noise immunity of military-purpose radio systems in connection with increasing the accuracy and reliability requirements of transmitted and received information using modern information technologies have been investigated. A novel analysis method to increase the noise immunity of radio systems for military purposes has been presented.

Keywords Additive interference, antenna patterns, active-noise interference, correlation, spatial selection

1. Introduction

The detection and tracking of military targets by radar is realized in presence of various noise that are created by means of electronic warfare or natural sources. Therefore, both at development and target applications of radar systems, safety precautions for noise immunity must be taken, which can be masking, misinforming or combined, that acts on both main and side directional lobes of radar antenna [1].

The results of the evaluations of noise immunity can be used as a base for determination of interference and its parameters. On the other hand, the results of these investigations are needed during development of noise-protected radars.

2. Active Masking Immunity and Safety Principles

It is known that, when the coming f and heterodyne f_h frequencies enter the mixer detector then the string of $|nf \pm mf_h|$ frequencies is formed at the output. If some of these frequencies coincide with intermediate f_{mid} one on which following stages of receiver are adjusted, then it is amplified and the receiving channel is created. In real conditions, when $f_h \gg f_{mid}$, contingent receiving channels are formed on the input frequencies [1]:

$$f_{mn} = \frac{1}{n}(mf_h \pm f_{mid})$$

The characteristics of directivity of pickup and transmitting antennas for out-of-band emission, side emission and receiving channels differ for main emission and receiving channels by much level of side lobes.

In many cases, in the same district the transmitter of radio electronic emits out-of-band and contingent signals, but receiving means also have contingent receiving channels. If main and contingent receiving channel coincide accidentally with main or contingent emission channels and the power of emission signal is high, then there is bilateral masking interference.

The electromagnetic compatibility provides an exclusion of bilateral interference. The electromagnetic compatibility is implemented by filtration of side emissions in transmitting sets, by heterodyne frequencies in receiving stages taking into an account right using propagation conditions, features of terrain, choice of radio-electronic means working regimes.

3. Possible principles for masking active interference

The defence activity from masking active interference can be effective in for case the signal suppression does not occur due to narrow range of receiver. Here, some activities can be applied using frequency, spatial, polarization selection etc. At sufficient dynamic range of receiver, the condition of target detection in masking stationary active interferences of type of white noise is:

$$E_{input} \geq \theta (N_0 + N_{ind}) \quad (1)$$

where E_{input} is energy of received signal on radar detector input; θ is an observability coefficient at given detection or measurement factors; N_0 is a spectral density of internal noisy of receiver; N_{ind} is a spectral density of masking interference on receiver input. If r_{max} is the limiting range of radar then we take radiolocation equation at presence of interference:

$$\frac{EG_G A}{(4\pi r_{max}^2)^2} = \prod \left(N_0 + \sum_{i=1}^m \frac{1}{4\pi} \frac{P_{ni} G_{ni} A_i^*}{r_{ni}^2 \Delta f_{ni}} \gamma_i \alpha_i \right) \quad (2)$$

This equation is also called as “anti-radar one”. As we can see from (1) and (2), the increasing of probing signal energy increases a range of action in interferences in proportion to $\sqrt[4]{E}$ in mode of external cover and to \sqrt{E} in mode of self-recover. The increasing of transmission antenna power gain to target direction allows to increase a range of action in interferences also in proportion to $\sqrt[4]{E}$ in mode of external cover and to \sqrt{E} in mode of self-recover [1].

The decreasing of polarization coefficient γ can decrease interference. The decreasing of observability coefficient θ also help to solve this problem. In whole, the action range in mode of self-recover is inversely proportional to $\sqrt{\gamma}$ and $\sqrt{\theta}$. Finally, the decreasing of relativity level of side lobes of directional pattern A'/A (or even, the formation of gaps in main lobe to direction of interferences source) allows to increase the action range in mode of external cover by proportional to $\sqrt[4]{A'/A}$.

The increasing of the coefficient of antenna power gain to target direction concentrates useful energy and

slows down space survey if such concentration will be provide for all directions. In present, methods of controlling survey with sequential analysis have been developed, when the time of antenna directed to target depends on detection conditions in particular on interference conditions. The application of transmitting antenna with electronic control of ray beam in form of phased array [2] has wide possibilities.

It is known, that receiving antenna is usually in tune with some specified polarization of receivable signal: linear, circular, elliptical. Antennas with controlled polarization. If the polarization of antenna is alligned with polarization of reference then the effect of interference is maximum. For instance, the interference effect will be maximum for vertical polarization if there is a receiver on the vertical vibrator. For circular polarization with field vector clockwise rotation, the the impact effect will be maximum if the antenna is alligned for same kind of polarization. Knowing this, the we can retune antenna on orthogonal polarization that is on the horizontal polarization or on the circular polarization with counterclockwise rotation.

For the elliptically polarized wave also the elliptically polarized oscillation is orthogonal, but with displaced polarization of 90^0 . For all indicated noise attenuation is present. As, since (even for not controlling polarization on emission) the reflected from real targets signal polarization is casual, then there are possibilities to weaken a interference more than signal.

For increasing of a noise immunity it is rational to decrease the coefficient of observability θ for account of optimal receiving. If the disturbance is a stationary noise such as white disturbance, then the decreasing of θ is implemented by receiving optimization for such disturbance. The filtering is done at the receiving stage by using the optimal frequency characteristic, that is, optimal frequency selection. The spot jammings (with less frequency range), as a rule, are more effectivite, but are hard to implement. The spot jamming creation is much more difficult in the case of rapid frequency tuning of radar, at multifrequency or wide broadband probing signal etc. [3]. If the frequency band of disturbance is much narrower than bandwidth of receiving signal, then resulting noise is not considered as white. In this case the frequency characteristic with rejection in interference frequency range is optimal, that is, it is rational to use various kind of tuned rejector filters for disturbance ripples, and it leads to essential decreasing of observability coefficient θ [4].

The improving of spatial selection is a major method for all kinds of active disturbance in radar protection. It is implemented in order to taper of main lobe and decrease the levels of side lobes of antenna diagram up to 25 dB and less relatively to maximize the main lobe in normalized antenna diagram. In result, tapering of sector of effectivety suppression and decreasing of compression ratio of the detection zone of radar is implemented [3]. For improving of spatial selection of

signal on disturbance, background noise must come from same direction. The methods of coherent and non-coherent compensation of disturbance oscillations can be used. To do this, subsidiary antennas can be used (phased-array antenna type) [6].

4. Receiver Models

The system including main and two subsidiary antennas is shown on the Fig. 1. Each antenna has own receiving channel. The corresponding receiving channels oscillations are input into adder. Here, complex transfer ratios K_1 and K_2 are regulated on amplitude and phases at least in two subsidiary channels.

If the complex characteristics of channels directivity have shapes $F_0(\Theta)$, $F_1(\Theta)$ and $F_2(\Theta)$, then the cumulative complex characteristic of directivity can be presented as:

$$F_{\Sigma}(\Theta) = F_0(\Theta) + K_1 F_1(\Theta) + K_2 F_2(\Theta) \quad (3)$$

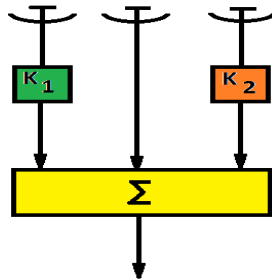


Fig. 1. The system with two subsidiary receiving channels for dips formation in resulted antenna diagram.

For the angle coordinates of disturbance sources Θ_1 and Θ_2 we can reach formation of dips in resulted characteristic of directivity for these directions. K_1 and K_2 are defined as:

$$F_0(\Theta_1) + K_1 F_1(\Theta_1) + K_2 F_2(\Theta_1) = 0, \quad (4a)$$

$$F_0(\Theta_2) + K_1 F_1(\Theta_2) + K_2 F_2(\Theta_2) = 0. \quad (4b)$$

Due to coherent compensation of disturbance in directivity characteristic, spatial disturbance appears on both main and side lobes. When receiving antennas as phased ones are used, application of compensated methods becomes widely available.

The selection of coefficients in multichannel charts can be realized using the principle of correlation feedback. The chart with two inputs, on which the voltages with same frequency and complex amplitudes $U_0(t)$ and $U_1(t)$ (for example, main and subsidiary antennas), is shown on Fig. 2. On the summer a voltage is formed:

$$U_{\Sigma}(t) = U_0(t) - KU_1(t) \quad (5)$$

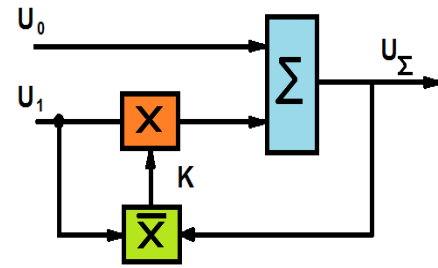


Fig. 2. The chart correlation feedback.

There is a feedback circuit in output of summer to controlling element (multiplier in circuit of first voltage supply). The device of correlation moment calculation $\overline{U_{\Sigma} U_1^*}$ is included in this circuit. The latter with accurate within χ is used as controlling multiplier K supplied on the controlled element. From two equations $K = \chi \overline{U_{\Sigma} U_1^*}$ and (5), we can find

$$K = \frac{\chi \overline{U_0 U_1^*}}{1 + \chi |\overline{U_1}|^2} \quad (6)$$

$$U_{\Sigma} = U_0 - \frac{\chi \overline{U_0 U_1^*}}{1 + \chi |\overline{U_1}|^2} U_1. \quad (7)$$

When $\chi \rightarrow \infty$ and enough U_0 and U_1 correlation (for example, at $U_1 = CU_0$, where $C = \text{constant}$) the full compensation occurs, that is U_{Σ} becomes zero. As known, the multiplication of complex amplitudes can be realized, for example, by frequency transformation; the averaging can be realized by integration in bandlimited filter [2].

The disturbance compensation effect is provided if each of circuit inputs is involved in correlation feedback (Fig. 3). The voltage U_0 is applied in output of summer at the absence of correlation (when controlling voltage K_0 becomes zero), the weighting voltage α is applied on it. Then, equations are:

$$U_{\Sigma} = (-K_0 + \alpha) U_0 - KU_1 \quad (8)$$

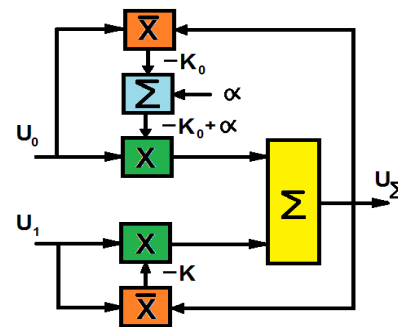


Fig. 3. The compensation chart with correlation feedback on the both inputs.

$$K_0 = \chi \overline{U_{\Sigma} U_0^*} \quad (9)$$

$$K = \chi \overline{U_{\Sigma} U_1^*} \quad (10)$$

Substitute (8) in (9) and (10), gives:

$$K_0 = (1 + \chi|\overline{U_0}|^2) + K \chi \overline{U_1 U_0^*} = \alpha \chi |\overline{U_0}|^2 \quad (11)$$

$$K_0 \chi = \overline{U_0 U_1^*} + K(1 + \chi|\overline{U_1}|^2) = \alpha \chi |\overline{U_1}|^2 \quad (12)$$

At $\chi \rightarrow \infty$, $\alpha = \alpha_0 = \text{const} \neq 0$ and full correlation of voltages U_0 and U_1 when $U_1 = CU_0$, from (8) and (11) we get, that $U_\Sigma \rightarrow 0$, in this case the disturbances are compensated.

Along with compensating of disturbances, in both circuits signal compensation occurs in case the duration of the later is enough for circuit's transformation. In the case of a very short signal, both circuits will be tuned only on disturbance compensation [7]. If there is absence of disturbance, both circuits give K and K_0 which are equal zero. Output voltage of second circuit becomes $U_\Sigma - \alpha U_0$, when disturbances absence each other, the circuit transmits oscillation applied on the main channel. When $\alpha = 1$, both circuits are identical. If $\alpha = \alpha_0$ (Fig. 8), the weighting α_1 is added to voltage of correlation feedback then output effect in conditions of disturbances absence is

$$U_\Sigma = \alpha_0 U_0 + \alpha_1 U_1 \quad (12)$$

On the base of stated, we can recommend the circuit below with the self-tuned phased antenna (Fig. 4)

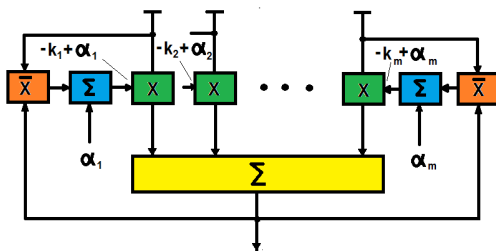


Fig. 4. Multichannel circuit of disturbance compensation using correlation feedback.

In each element of phased antenna, the correlation feedback is used. The correlation feedback is shown in the chart only for the last (left and right) elements. Summands of $\alpha_1, \alpha_2, \dots, \alpha_m$ provide the best effect of signal receiving in absence of disturbance (analogous to component α in Fig. 3). When disturbances come from maximum m directions there are possible formation of side-lobes in directivity characteristic in these directions. As the detailed analysis shows for discrete case, the directivity characteristic is optimized with taking an account disturbances providing the most profitable spatial selection [5].

5. Conclusion

In this paper a novel method to overcome disturbances is proposed. It is necessary to apply disturbance compensation to provide effective interference rejection which depends on character of active disturbances acting on a radar. The results of analysis methods to increase the noise immunity of radio systems for military and civilian purposes have been presented. The possible principles of active disturbances

protection by application of coherent and non-coherent compensation of interference oscillations are investigated. It is shown that improvement of signal to noise ratio may be implemented in presence of spatial selection on background disturbances coming from different directions. It is seen that when the receiving antenna is of phased array type, there are the optimal compensation is implemented.

References

- [1] Daniel W. O'Hagan, Shaun R. Doughty, Michael R. Inggs, Multistatic radar systems, Academic Press Library in Signal Processing, Volume 7, 2018, Pages 253-275,
- [2] Shirman Ya.D. Theoretical basis of radiolocation. - M.: Sov. radio, 1970, p.560
- [3] Ibragimov B.G., Isayev Ya.S. The analysis of parameters of signals of the noise immunity in radio systems // National security and military sciences. Baku, 2015. № 1(1). p. 145 – 149
- [4] Bakulev P. A. Radiolocation systems. –M.: Radiotechnics, 2004, p. 320
- [5] Botov M.I., Vaxirev V.A. Basis of theory of radiolocation systems and complexes. Krasnoyarsk SFU, 2013, p.504
- [6] Shirman Ya.D., Manjos V.N. Theory and technics of development of radiolocation information with the noise immunity. - Moscow: Radio and communications, 1981, p. 406
- [7] Nilov M.A. The multipurpose countermeasures-safe ship radar system with pseudo-continuous sounding. [http://www.raspletin.com/NOC/vko/VKO_3\(3\).pdf](http://www.raspletin.com/NOC/vko/VKO_3(3).pdf)

Analysis of a Soft Switching High Voltage Gain DC/DC Boost Converter for PV Systems

Sarah Al-Hajm*, Mehmet Ucar**‡

* Department of Electrical and Electronics Engineering, Graduate School of Natural and Applied Sciences, Duzce University, 81620, Duzce, Turkey

** Department of Electrical and Electronics Engineering, Faculty of Engineering, Duzce University, 81620, Duzce, Turkey

(sarahyahyasalih@gmail.com, mehmetucar@duzce.edu.tr)

‡ Corresponding Author; Mehmet Ucar, Department of Electrical and Electronics Engineering, Faculty of Engineering, Duzce University, 81620, Duzce, Turkey, Tel: +90 380 542 10 36,

Fax: +90 380 542 10 37, mehmetucar@duzce.edu.tr

Received: 29.04.2018 Accepted: 26.05.2018

Abstract- This paper presents an analysis of a non-isolated soft switching high voltage gain DC/DC boost converter by using a coupled inductor, voltage quadrupler and active clamp circuit for Photovoltaic (PV) systems. The main advantage of this converter, coupled inductor with voltage quadrupler circuit is used to decrease voltage stress in semiconductor switches and providing high voltage gain. Therefore, low voltage valued and low on-resistance $R_{DS(ON)}$ MOSFETs can be used to decrease on-state losses. The reverse recovery and high frequency turn off losses is reduced for achieving Zero-Current Switching (ZCS) in all diodes. Voltage spike caused by leakage inductance of the coupled inductor is minimized by means of the active clamp circuit. Thus, Zero-Voltage Switching (ZVS) turn on of all MOSFET switches are achieved. The Perturb and Observe (P&O) method is utilized in this study to obtain maximum power from the PV system. In order to show the effectiveness of the converter, PSIM simulations are realized under various irradiance cases. The conversion efficiency is obtained about 95.97% at full load from the simulation results.

Keywords DC/DC converter, high voltage gain, coupled inductor, voltage quadrupler, ZCS, ZVS, PV system.

1. Introduction

In the past few decades, distributed generation with renewable energy sources have rapidly developed [1]. Much research has been carried out on renewable energy to get maximum power with high efficiency among renewable energy resources like wind, Photovoltaic (PV), etc. The output PV panel voltage is very low between (25-50 V) due to safety factors and for various applications is required boosting large voltage [2]. Maximum Power Point Tracking (MPPT) methods are commonly used with PV systems to maximize power extraction [3]. The Perturb and Observe (P&O) [4], [5] and the incremental conductance [6] MPPT algorithms are frequently used in the PV systems. These algorithms depend on the voltage-power characteristic, if $(\frac{dP}{dV} < 0)$ right of the maximum power point MPP, while the left of the MPP when $(\frac{dP}{dV} > 0)$ [7].

In conventional boost converters, high losses are found on input side due to large peak current which adverse effects on the magnetic components. Because the large voltage across the switch, the switch conduction losses are increased ($R_{DS(ON)} \propto V_{DS}^2$). The inductor and capacitor resistances increase the losses due to large duty cycle. In addition, diode reverse recovery problem is a disadvantage [8]. For these reasons, the conventional boost converters are not appropriate to use for high voltage gain application. To get a high voltage gain without a high duty cycle, there are several proposed topologies. Among them, the coupled inductor is commonly used [9]. Although achieving high voltage gain with large turns ratio, its leakage inductance cause power losses and high voltage stress on the MOSFETs [10]. Therefore, passive or active clamp techniques are used to recycle leakage energy from the coupled inductor. Passive clamp circuits reform voltage gain, but cause high voltage stress on output diode. Utilizing active clamp circuit, Zero-

Voltage Switching (ZVS) turn on with power switches are obtained [11].

In this paper, coupled inductor based high voltage gain soft switching DC-DC boost converter is analyzed and controlled for PV systems. This converter [11] has main advantages; firstly, the voltage quadrupler circuit is combined with secondary of the coupled inductor to produce high voltage gain. Secondly, at turn on for a MOSFET, coupled inductor transfers the energy to the voltage multiplier circuit. Thus, smaller magnetic component can be used with this converter. Thirdly, all diodes turned off at Zero-Current Switching (ZCS) and therefore reverse recovery losses, high frequency turn off losses are reduced and high voltage spike is eliminated.

2. Proposed System Overview

The proposed system, including soft switching, high voltage gain converter is illustrated in Fig. 1. It involves of an input voltage (V_{PV}) and current (I_{PV}) from PV panel, input capacitor (C_{PV}), a coupled inductor primary side denotes (L_m and L_{kp}) and secondary side denotes (L_{ks}), a clamp circuit (auxiliary switch S_2 and out capacitor C_{o3}), a resonant voltage quadrupler circuit (consist of the diodes D_1, D_2, D_{o1} , and D_{o2} along with capacitors C_1, C_2, C_{o1} , and C_{o2}), parasitic capacitors of MOSFETs (C_{r1} and C_{r2}) and output DC load (R_o). The converter key waveforms as indicated in Fig. 2 and the nine operation interval are briefly described in [11].

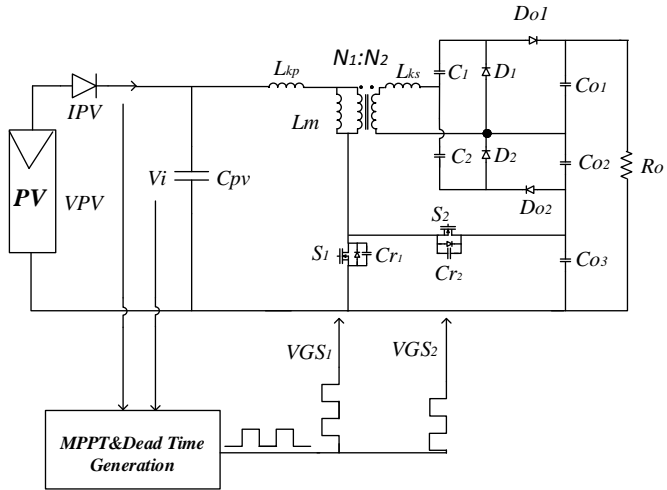


Fig. 1. The proposed system block diagram.

The conversion ratio (M) of the converter is calculated from equation (1). The turn ratio of coupled inductor can be increased without increase MOSFET's voltage stress.

$$M = \frac{V_o}{V_{in}} = \frac{1+2N}{1-D} \tag{1}$$

Soft switching operation of the converter is achieved as the following:

i) For achieving ZVS turn on of MOSFET S_1 there are two conditions: First, the stored magnetizing inductance energy is greater enough to discharge C_{r1} of MOSFET S_1

and charge C_{r2} of MOSFET S_2 . Second, the dead time (ΔT) is enough for charge and discharge the MOSFET parasitic capacitor. For getting ZVS of MOSFETs, magnetizing inductance (L_{mmax}) is obtained from equation (2).

$$L_{mmax} < \frac{V_{in} D_{max} (1-D_{max})}{2(1+2N)I_o f_s} \tag{2}$$

In this study, the magnetizing inductance (L_m) is selected as $9\mu H$, and dead time (ΔT) is determined from equation (3).

$$\Delta T \geq \sqrt{L_m (C_{r1} + C_{r2})} \tag{3}$$

ii) The ZCS turn off of diodes D_1, D_2, D_{o1} and D_{o2} is achieved if the minimum time to turn on MOSFET S_1 is greater than the one-half of resonant period. Therefore, the capacitors C_1 and C_2 are obtained as equation (4).

$$C_1, C_2 < \left(\frac{D_{min}^2 T_s^2}{\pi^2 L_{ks}}, \frac{(1-D_{max})^2 T_s^2}{\pi^2 L_{ks}} \right) \tag{4}$$

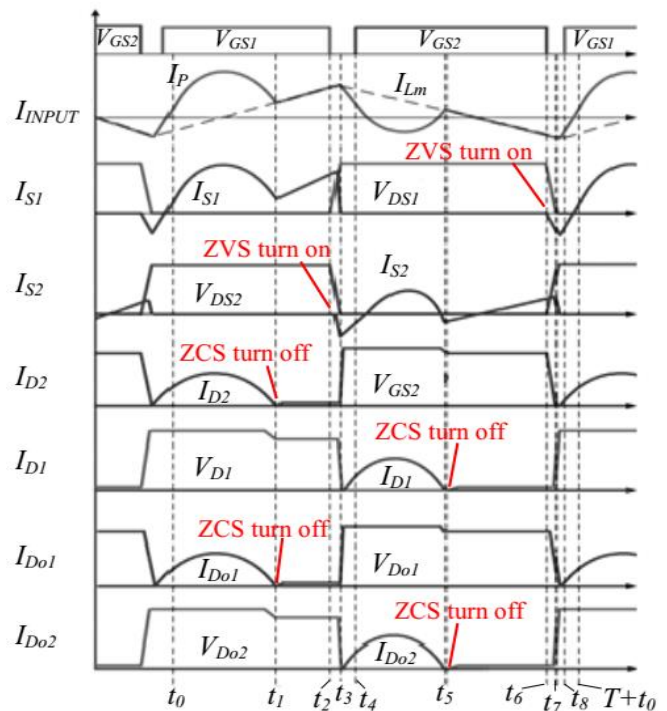


Fig. 2. The converter key waveforms.

In the paper, high voltage gain is obtained without using high duty cycle or large magnetic components, which are main advantages over the conventional converter as indicated in Table 3.

Table 3. Comparison of conventional and analyzed boost converter.

Parameter	Conventional boost converter	Analyzed boost converter
Voltage gain	$\frac{1}{1-D}$	$\frac{1+2N}{1-D}$
Voltage stress of MOSFETs	V_o	$\frac{V_o}{1+2N}$
Voltage stress of diodes	V_o	$\frac{NV_o}{1+2N}$

3. Simulation Results

PSIM based proposed system block diagram is seen in Fig. 3. The Perlght Solar PLM-250M PV panel is used as the input source. The PV panel parameters are given in Table 1. Current-voltage (I-V) curves of the PV panel at different irradiation cases are illustrated in Fig. 4. The ratings of the P_{MPP} values are depicted in this figure under the solar irradiation decreases from 1000 W/m^2 to 200 W/m^2 at constant temperature 25°C . The sensed PV voltage and current are given to MPPT inputs and then Pulse Width Modulated (PWM) signal outputs are obtained to gate signal for main and auxiliary MOSFET switches. The P&O MPPT algorithm is used due to simple operation, tracking efficiency and high reliability. For achieving ZVS for main and auxiliary switches, the time delay between to gate signals is adjusted properly by using dead time generator. The converter specifications are given in Table 2.

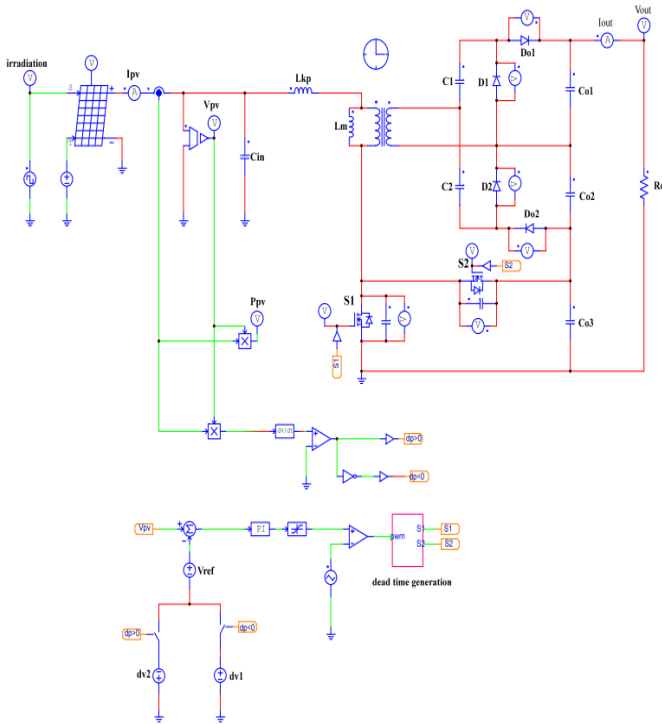


Fig. 3. PSIM based proposed system block diagram.

Table 1. PV panel parameters.

Parameter	Value
PV panel model	PLM-250M
Maximum power (P_m)	250 W
Number of cells (N_s)	60
Maximum power current (I_{pm})	8.20 A
Short circuit current (I_{sc})	8.78 A
Maximum power voltage (V_{pm})	30.50 V
Open circuit voltage (V_{oc})	38 V

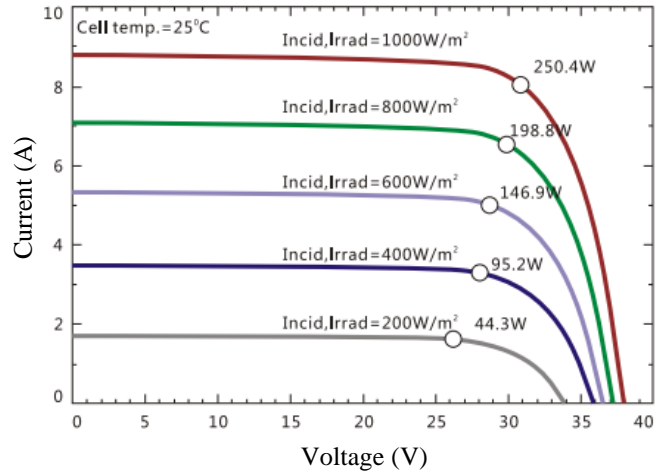


Fig. 4. I-V curves under different solar irradiation.

Table 2. The converter specifications.

Components	Value
Output voltage (V_o)	340 V
Switching frequency (f_{sw})	60 kHz
Power (P)	250 W
Turns ratio (N)	1:2.4
MOSFETs (S_1, S_2)	IRFP4227pbf
Diodes (D_1, D_2, D_{o1}, D_{o2})	MUR1560
Capacitors (C_1, C_2)	$2 \mu\text{F}$
Output capacitors (C_{o1}, C_{o2}, C_{o3})	$100 \mu\text{F}$
Magnetizing Inductance (L_m)	$9 \mu\text{H}$
Leakage Inductance (L_{kp}, L_{ks})	$0.174 \mu\text{H}, 1 \mu\text{H}$

The simulation results for the proposed system are obtained at full load condition. Also, for evaluation performance of the MPPT method, the solar irradiation are changed instantly from 1000 W/m^2 to 600 W/m^2 . Figure 5 shows ZVS turn on of the MOSFETs S_1, S_2 with input signals (V_{GS1}), (V_{GS2}) and primary and magnetizing current of the coupled inductor. In this figure, ZVS turn on of all MOSFETs is clearly depicted. Figure 6 shows ZCS turn off of the diodes D_1, D_2, D_{o1} and D_{o2} . Thus the losses of the diodes caused by the reverse recovery issue is decreased. The ZVS and ZCS soft switching process improves the conversion efficiency of the converter.

The PV panel current (I_{PV}), voltage (V_{PV}) and the converter output current (I_{out}), voltage (V_{out}) waveforms obtained by PSIM simulation are shown in Fig. 7. The range of input and output voltage of the converter is 30 V-340 V. It can be observed that the converter with coupled inductor and resonant voltage multiplier circuit provides high output voltage under different irradiation conditions. The performance of the MPPT method in rapidly changing solar irradiation is confirmed.

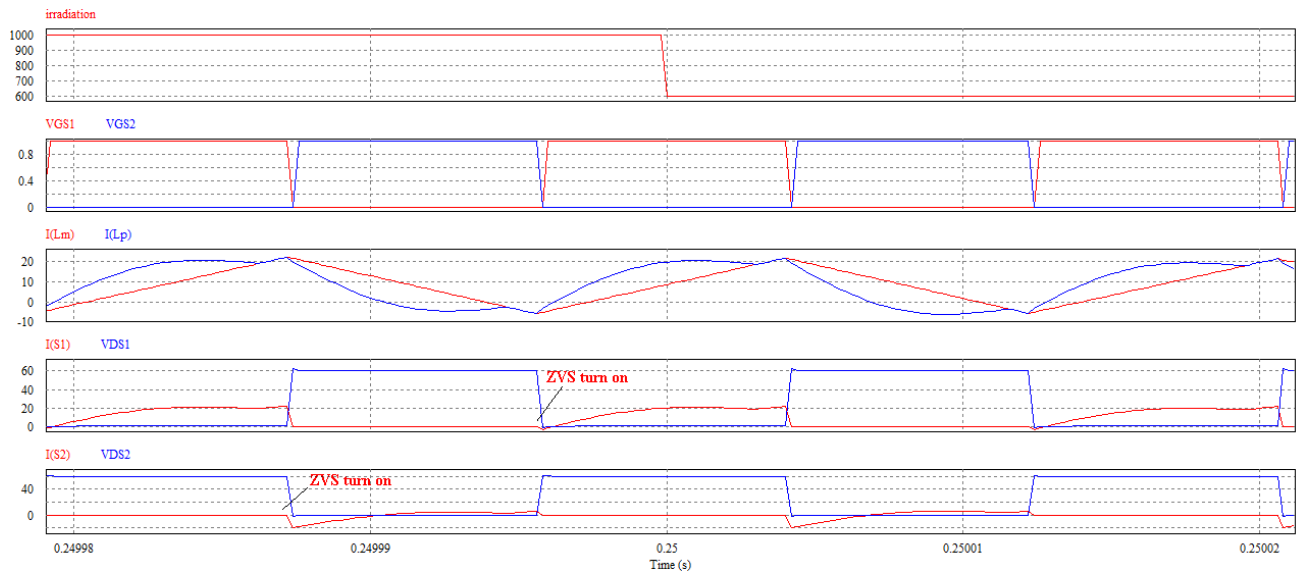


Fig. 5. ZVS turn on of the MOSFETs S_1 , S_2 with V_{GS1} , V_{GS2} and inductor magnetizing and primary current.

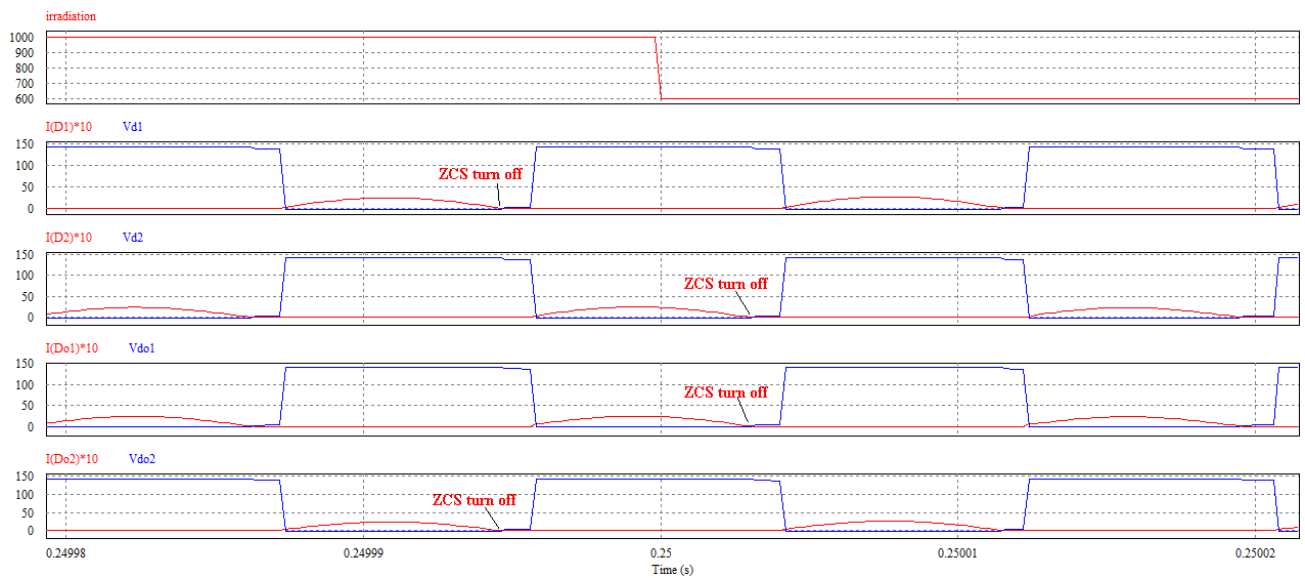


Fig. 6. ZCS turn off of the diodes D_1 , D_2 , D_{o1} and D_{o2} .

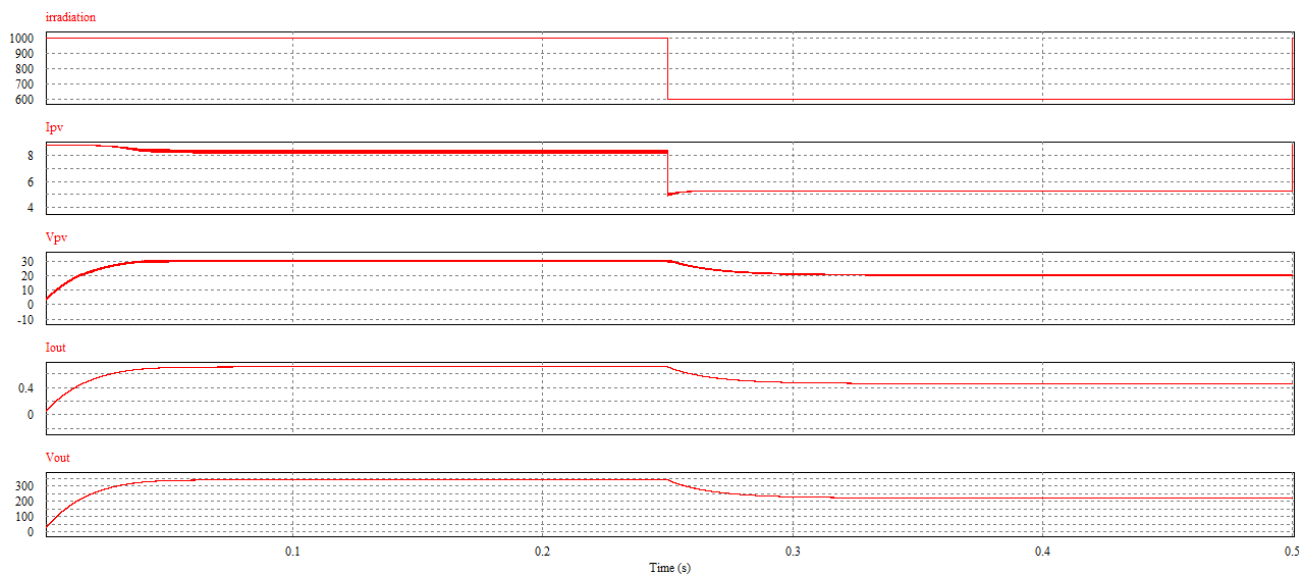


Fig. 7. PV panel I_{PV} , V_{PV} and converter I_{out} , V_{out} waveforms under solar irradiation change.

4. Conclusion

In this paper, the non-isolated high voltage gain DC/DC boost converter with coupled inductor and resonant quadrupler circuit for PV systems is analyzed. The PSIM simulations are realized to confirm the soft switching process of the converter. The high voltage gain is realized without utilizing high duty cycle or large magnetic components which a main advantage over the conventional converters. Thus, the efficiency is improved by the low on-state resistance $R_{DS(ON)}$ MOSFETs and the ZVS turn on of the all MOSFETs. The reverse recovery losses are decreased and the quasi-resonant quadrupler circuit provides the ZCS turn off of all diodes. Therefore, the proposed system is a proper choice for the PV systems.

References

- [1] J. M. Guerrero, F. Blaabjerg, T. Zhelev, K. Hemmes, E. Monmasson, S. Jemei, M. P. Comech, R. Granadino, J. I. Frau, "Distributed generation: toward a new energy paradigm", IEEE Industrial Electronics Magazine, vol. 4, no. 1, pp. 52-64, March 2010.
- [2] S. Hema, A. Arulmathy, V. Saranya and S. Yugapriya, "High voltage gain soft switching converter for solar energy AC and DC applications", International Conference on Power and Embedded Drive Control (ICPEDC), Chennai, 2017, pp. 326-332.
- [3] E. Mamarelis, G. Petrone and G. Spagnuolo, "Design of a sliding-mode-controlled SEPIC for PV MPPT applications", IEEE Transactions on Industrial Electronics, vol. 61, no. 7, pp. 3387-3398, July 2014.
- [4] C. W. Tan, T. C. Green and C. A. Hernandez-Aramburo, "Analysis of perturb and observe maximum power point tracking algorithm for photovoltaic applications", IEEE 2nd International Power and Energy Conference, Johor Bahru, 2008, pp. 237-242.
- [5] F. Boico and B. Lehman, "Study of different implementation approaches for a maximum power point tracker", IEEE Workshops on Computers in Power Electronics, Troy, NY, 2006, pp. 15-21.
- [6] B. Liu, S. Duan, F. Liu and P. Xu, "Analysis and improvement of maximum power point tracking algorithm based on incremental conductance method for photovoltaic array", 7th International Conference on Power Electronics and Drive Systems, Bangkok, 2007, pp. 637-641.
- [7] D. Sera, L. Mathe, T. Kerekes, S. V. Spataru and R. Teodorescu, "On the perturb-and-observe and incremental conductance MPPT methods for PV systems", IEEE Journal of Photovoltaics, vol. 3, no. 3, pp. 1070-1078, July 2013.
- [8] M. Das and V. Agarwal, "A novel, high efficiency, high gain, front end DC-DC converter for low input voltage solar photovoltaic applications", IECON 2012 - 38th Annual Conference on IEEE Industrial Electronics Society, Montreal, QC, 2012, pp. 5744-5749.
- [9] S. Sathyan, H. M. Suryawanshi, M. S. Ballal and A. B. Shitole, "Soft-switching DC-DC Converter for distributed energy sources with high step-up voltage capability", IEEE Transactions on Industrial Electronics, vol. 62, no. 11, pp. 7039-7050, Nov. 2015.
- [10] S. Sathyan, H. M. Suryawanshi, A. B. Shitole and G. G. Talapur, "Soft switched high voltage gain boost integrated flyback converter", IEEE International Conference on Power Electronics, Drives and Energy Systems (PEDES), Trivandrum, 2016, pp. 1-6.
- [11] S. Sathyan, H. M. Suryawanshi, B. Singh, C. Chakraborty, V. Verma and M. S. Ballal, "ZVS-ZCS high voltage gain integrated boost converter for DC microgrid", IEEE Transactions on Industrial Electronics, vol. 63, no. 11, pp. 6898-6908, Nov. 2016.

A Parallel Iterated Local Search Algorithm on GPUs for Quadratic Assignment Problem

Erdener Ozcetin*, Gurkan Ozturk**

* Industrial Engineering Department, Hitit University Engineering Faculty, Corum, Turkey

** Industrial Engineering Department, Eskisehir Technical University Engineering Faculty, Eskisehir, Turkey

(erdenerozcetin@hitit.edu.tr, gurkan.o@anadolu.edu.tr)

‡Corresponding Author; Erdener Ozcetin, Industrial Engineering Department, Hitit University Engineering Faculty,

Corum, Turkey , Tel: +90 364 227 4533,

Fax: +90 364 227 4535, erdenerozcetin@hitit.edu.tr

Received: 25.10.2018 Accepted: 21.06.2018

Abstract- In this study, quadratic assignment problem, which is a hard combinatorial optimization problem, is examined to solve by a new approach. To reach the optimal results by using mathematical programming approaches cannot be possible even for some sorts of small and middle scaled problems in a reasonable time interval. Huge amounts of data are being progressed simultaneously by graphics processing units located on computers' graphics card. Therefore, a parallel iterated local search algorithm has been proposed to solve the quadratic assignment problem by using graphics processing units' simultaneously progressing property. This parallel algorithm and the sequential one on central processing units are tested and compared for test problems in literature. Indeed, it is observed that the parallel algorithm works averagely 6.31 times faster for Skorin problems and 11.93 times faster for Taillard problems faster than sequentially one.

Keywords Quadratic assignment problem (QAP), local search algorithms, graphics processing units (GPU), CUDA.

1. Introduction

Combinatorial optimization is a topic that consists of finding optimal solution from a finite set of alternative solutions ($n!$) that generally studied in applied mathematics and theoretical computer sciences. Quadratic assignment problem (QAP) is a type of combinatorial optimization problem that was introduced by Koopmans and Beckmen in 1957 [1].

As a real life problem QAP can be defined facility planning, circuit designing and assigning the air-crafts to the gates. If we investigate QAP as a facility planning problem, the objective is assigning n facilities to n candidate locations by minimizing a cost function. The mathematical formulation of QAP can be as:

$$\min z = \sum_{i=1}^n \sum_{j=1}^n \sum_{k=1}^n \sum_{l=1}^n f_{ij} d_{kl} x_{ik} x_{jl} \quad (1.1)$$

$$\sum_{i=1}^n x_{ij} = 1 \quad j = \overline{1, n} \quad (1.2)$$

$$\sum_{j=1}^n x_{ij} = 1 \quad i = \overline{1, n} \quad (1.3)$$

$$x_{ij} \in \{0,1\} \quad 1 \leq i, j \leq n \quad (1.4)$$

In this formulation, f_{ij} is the flow between two facilities and d_{kl} is the distance between two candidates. Complexity study of this mathematical model is handled by Sahni and Gonzalez [2] in 1976. They showed that QAP is *NP-Hard* and even finding an ϵ approximate solution is extremely hard.

With the reason of QAP is *NP-Hard*, working with exact methods such as mathematical programming is so difficult. For this reason, researchers are tended to study on meta-heuristics. Although meta-heuristic algorithms do not guarantee to find optimal solution, they can converge to optimal solution much faster than exact methods. There are many studies in literature that subjected solving QAP with meta-heuristics. Simulated annealing is an iteration based meta-heuristic algorithm that developed by Kirkpatrick et al. [3]. Burkard and Rendl [4], Wilhelm and Ward [5] and Abreu et al. [6] used this algorithm for QAP in their studies. Ant colony optimization (ACO) is a population based meta-heuristic algorithm. Stützle and Dorigo [7] and Dorigo et al. [8] implemented this algorithm for QAP. Another population based algorithm is genetic algorithm (GA) that published in QAP literature such as Kochhar et al. [9] and Drezner [10]. Glover [11], developed iteration based tabu search (TS) algorithm to solve problems that oriented to integer programming, in 1989. Main concentration of this algorithm

is to search neighbors with a method to escape local optima. Skorin [12], Taillard [13], Misevicius and Ostereika [14] proposed a TS algorithm for QAP.

Introduction of CUDA by nVIDIA in 2006 can be considered as a turning point of using for computational sciences of Graphics Processing Units (GPUs) [15]. Thousands of applications have been proposed from different disciplines of science since that day. As a reason of complexity of QAP and compatibility of meta-heuristics are lead researchers in this area to work on GPUs. The motivation of starting these studies is to accelerate the algorithms and to decrease the time of solutions, reasonably. On the other hand, there are only several studies that related to combinatorial optimization with meta-heuristics on GPUs. Tsutsui and Fujimoto [16] published a parallel GA on GPUs for QAP and they gained between 3-12 times speed-ups according to Central Processing Unit (CPU) implementation. In another study, same authors [17], applied a hybrid ACO algorithm. They focused on local search to parallelize that the most time consuming part of algorithm and they observed up to 24.6 times speed-ups. Czapsinski [18] proposed multi-start TS algorithm on GPUs to solve QAP. They gained up to 50 times speed-ups for symmetric instances. Again for symmetric instances, Ozçetin and Ozturk [19] handled averagely 17 times up to 51 times speed-ups with a hybrid evolutionary algorithm on GPUs.

2. Iterated Local Search Algorithm

Iterated local search algorithms (ILS) can be defined as a hybrid local search (LS) algorithms that improved with global search procedures. Basically, LS stop when a local optimum solution found. Two procedures are often used to continue searching from the solution found with LS. First one is perturbing the current local minimum. This is the simplest way to start the search from another starting point. Second one is modifying solution according to a mutation based procedure.

In this study, a multi start ILS algorithm is developed for solving symmetric QAP instances efficiently. In the first phase of algorithm the instances is read to two matrices. *D* is the distance matrix of locations and *F* is the flow matrix of facilities. After that, objective function evaluation is calculated for each solution only once. Then, the algorithm starts to search. There are $\frac{n(n-1)}{2}$ alternative changes for each solution, so calculation of objective function for each iteration is a computationally expensive operation. For this reason, during the search objective function evaluation is not considered again. Instead of objective function calculation a delta function is used like in equation 2.1. A solution is defined as a permutation. If we consider about changing a^{th} and b^{th} neighbors in permutation, $\pi(a)$ and $\pi(b)$ will be the values in permutation of *a* and *b*, respectively This candidate changing is done, if and only if δ value is lower than zero.

$$\delta = \sum_{t=1}^n (d_{at} - d_{bt})(f_{\pi(b)\pi(t)} - f_{\pi(a)\pi(t)}) \quad (2.1)$$

Basically, the algorithm has two main operators. One of

them is LS and the other one is mutation operator. Mutation operator is designed to escape the local optimum in a systematic procedure with the cross exchange of two elements in a solution.

3. Parallelization of Algorithm

Some parts of proposed ILS algorithm is available for parallelization. For *p* starting elements objective function evaluation is handled in a parallel fashion like in Figure 1.



Fig 1. Parallelization of elements

For CPU implementation, loops of an objective function evaluation are also a demanding issue for parallelization. It takes n^2 steps for sequential version. This means that there are n^2 multiplication of distance and flow and summation. In parallel version, a kernel is organized to carry out all these multiplications simultaneously.

Another kernel is organized for parallel LS procedure. For *p* elements each neighborhood search is investigated in a parallel manner. Following figure is an example of 2nd and 4th neighbors changing.

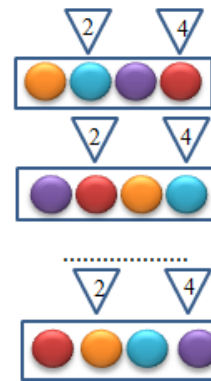


Fig 2. An illustrative example for parallel local search

Let we think about four facilities will be assigned four candidate locations. In this problem T_1, T_2, T_3, T_4 are the elements of flow matrix between facilities *F* and Y_1, Y_2, Y_3, Y_4 are the elements of distance matrix between locations *D*.

Think that we have 3 individual solutions with the permutations Π_1, Π_2, Π_3 , 1-2-3-4, 4-1-3-2 and 1-3-4-2, respectively. For third solution, assignment will be like this: $T1 \rightarrow Y1, T3 \rightarrow Y2, T4 \rightarrow Y3$ and $T2 \rightarrow Y4$. According to this information, multiplications of objective function calculation will be like in Figure 3.

	1	2	3	4	5	6	7	8	9	10	11	12	13	14	15	16	17	18
S	d_{12}	d_{13}	d_{14}	d_{23}	d_{24}	d_{34}	d_{12}	d_{13}	d_{14}	d_{23}	d_{24}	d_{34}	d_{12}	d_{13}	d_{14}	d_{23}	d_{24}	d_{34}
R	f_{12}	f_{13}	f_{14}	f_{23}	f_{24}	f_{34}	f_{41}	f_{43}	f_{42}	f_{13}	f_{12}	f_{32}	f_{13}	f_{14}	f_{12}	f_{34}	f_{32}	f_{42}
A	s_{1r_1}	s_{2r_2}	s_{3r_3}	s_{4r_4}	s_{5r_5}	s_{6r_6}	s_{7r_7}	s_{8r_8}	s_{9r_9}	$s_{10r_{10}}$	$s_{11r_{11}}$	$s_{12r_{12}}$	$s_{13r_{13}}$	$s_{14r_{14}}$	$s_{15r_{15}}$	$s_{16r_{16}}$	$s_{17r_{17}}$	$s_{18r_{18}}$
Obj	$2(A_1 + A_2 + A_3 + A_4 + A_5 + A_6)$						$2(A_7 + A_8 + A_9 + A_{10} + A_{11} + A_{12})$						$2(A_{13} + A_{14} + A_{15} + A_{16} + A_{17} + A_{18})$					

Fig 3. An illustrative example for parallel evaluations

There are $\frac{4(4-1)}{2} = 6$ multiplications for each element's objective function calculation. Each multiplication corresponds to unique thread for GPU and is collected in the array of A . Objective function values is calculated by summarizing the A with parallel reduction via *thrust library*.

For parallel local search same neighborhood search is handled like in Figure 4. Calculation of delta function is computed via a device kernel. First step of neighborhood search for this example, for first individual changing of 1-2 orders in permutation, for second 4-1 and for third 1-3 handled simultaneously. Only second individual's changing is done as a reason of delta value (-240). This procedure continues as the same.

F , D matrices and permutations are allocated on GPU side with *thrust* vectors. For each iteration only solutions are copied. Shared memory and constant memory cannot be used as a reason of capacity. For this reason, only device memory has been used for the implementation on GPUs

Individual	Orders	Facilities	Delta
Π_1	$\pi_1 \pi_2$	1-2	120
	$\pi_1 \pi_3$	1-3	
	$\pi_1 \pi_4$	1-4	
	$\pi_2 \pi_3$	2-3	
	$\pi_2 \pi_4$	2-4	
	$\pi_3 \pi_4$	3-4	
Π_2	$\pi_1 \pi_2$	4-1	-240
	$\pi_1 \pi_3$	4-3	
	$\pi_1 \pi_4$	4-2	
	$\pi_2 \pi_3$	1-3	
	$\pi_2 \pi_4$	1-2	
	$\pi_3 \pi_4$	3-2	
Π_3	$\pi_1 \pi_2$	1-3	180
	$\pi_1 \pi_3$	1-4	
	$\pi_1 \pi_4$	1-2	
	$\pi_2 \pi_3$	3-4	
	$\pi_2 \pi_4$	3-2	
	$\pi_3 \pi_4$	4-2	

Fig 4. Parallel neighborhood search

4. Results

A work station which have 6 cores CPU with 32 GB RAM and a GTX580 chipset GPU is used for comparisons. There are 1000 individual solutions for multi-start. In addition to this, probability of accepting worse solution in mutation operator is 0.4. Grid parameters are used for objective function evaluation n block in grid, n threads in a block and for parallel local search 125 blocks in grid, and 8 threads in a block (This numbers defined with preliminary studies). Number of iterations is not a stopping criterion for these implementations. Stopping criterion is done with gap of solution $(\frac{Avg.Obj.Val-BK}{BK})$ (BK=best known solution).

In tables 1, 2 GAP CPU and GAP GPU columns represent the average gap of ten iterations both on CPU and GPU. CPU(s) and GPU(s) columns represent solution times. In addition, HIT column represents number of hits to best known solution for ten iterations. Finally, speed factor is calculated with $(\frac{CPU(s)}{GPU(s)})$.

Table 1. Skorin Test Problems

Problem	BK	CPU(s)	GPU(s)	GAP CPU	GAP GPU	HIT	Speed Up
Sko42	15812	40.347	2.843	0.0001	0	9/10	14.18x
Sko49	23386	65.814	10.179	0.0005	0.0006	2/10	6.46x
Sko56	34458	66.211	11.161	0.0002	0.0004	1/10	5.93x
Sko64	48498	80.243	18.647	0.0001	0.0003	4/10	4.30x
Sko72	66256	104.15	21.579	0.0013	0.0015	0/10	4.82x
Sko81	90998	118.223	24.813	0.0013	0.0014	0/10	4.76x
Sko90	115534	152.651	31.289	0.0017	0.0019	0/10	4.87x
Sko100a	152002	190.581	36.695	0.0020	0.0022	0/10	5.19x
Avg.		102.27	19.65	0.0009	0.0009		6.31x

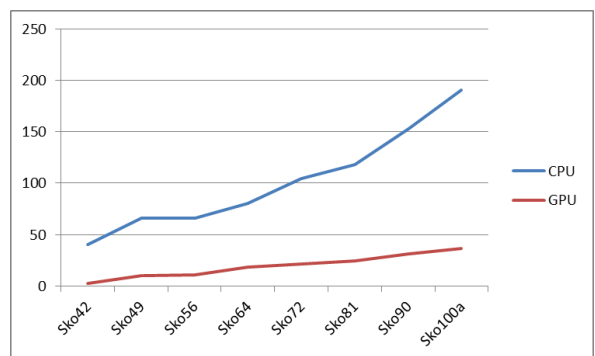


Fig 5. Skorin Speed-Ups

For comparisons all test instances are taken from QAPLIB (<http://anjos.mgi.polymtl.ca/qaplib/>) with best known solutions up to date. Skorin and Taillard test problems are the well-known hardest test instances for QAP.

Table 1 and Fig. 5 are the results for Skorin test problems. Average gap of these problems are 0.0009 both on CPU and GPU implementation. In addition, 6.31x speed-up gained for these problems. For Sko42 problem, execution time of CPU version is 40.347 seconds and GPU version is 2.843 seconds. The speed-up factor for this problem is 14.18x with the 9/10 best known solution hit. Computational results of the proposed ILS for Taillard problems are shown in Table 2 and Figure 6 According to this, average gap for these problems set are 0.0063 on CPU and 0.0068 on GPU, respectively. If we have an eye on execution times, GPU implementation runs 11.93 times faster than CPU implementation. Best speed-up observed with Tai30a problem with a 16.69x (CPU(s)/GPU(s)) factor.

Table 2. Taillard Test Problems

Prob.	BK	CPU(s)	GPU(s)	GAP CPU	GAP GPU	HIT	Speed Up
Tai20a	703482	1.943	0.493	0	0	10/10	3.93x
Tai25a	1167256	14.95	1.165	0	0	10/10	12.83x
Tai30a	1818146	39.849	2.387	0.0003	0.0004	8/10	16.69x
Tai35a	2422002	116.682	10.472	0.0008	0.0008	7/10	11.14x
Tai40a	3139370	179.576	11.398	0.0004	0.0004	0/10	15.75x
Tai50a	4938796	277.076	18.202	0.0093	0.0091	0/10	15.38x
Tai60a	7208572	360.42	32.112	0.0117	0.0135	0/10	11.25x
Tai80a	13515450	453.78	44.188	0.0122	0.0121	0/10	10.29x
Tai100a	21054656	602.98	59.776	0.022	0.025	0/10	10.19x
Avg.		227.47	20.02	0.0063	0.0068		11.93x

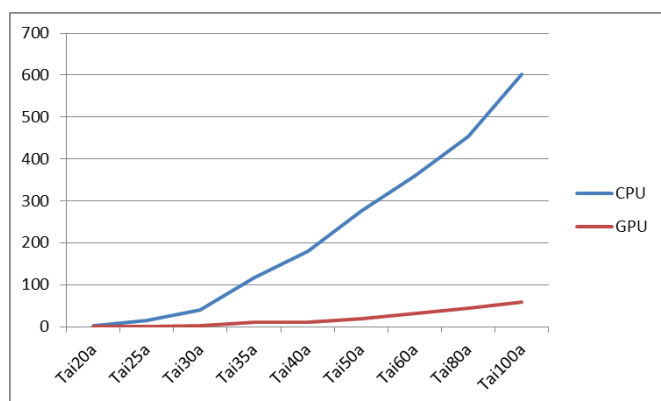


Fig 6. Taillard Speed-Ups

5. Conclusion

Solving combinatorial optimization problems are extremely hard and computationally expensive. For many cases, it can be impossible to solve these problems optimally with exact methods. For these reasons, researchers tend to study with meta-heuristics. Even meta-heuristics converge to approximate solution much more reasonable time, it is still a handicap for large scale instances of combinatorial optimization problems. According to this motivation, we consider about a parallel implementation of ILS algorithm on GPUs. We observed on preliminary studies that our algorithm finds optimal solutions for Escherman and Nuggent problems for all runs in a few seconds. In our results, we prefer to show more difficult problems Skorin and Taillard test instances. Our algorithm converges to best known solution with small gaps. Averagely, 6.31x speed-up gained for Skorin test instances and 11.93x speed-up gained for Taillard test instances. For future studies, GPU implementation of algorithm is available for development. For much more speed-up memory operations can be improved. Finally, this algorithm is also available for other combinatorial optimization problems.

REFERENCES

- [1] T. C. Koopmans ve M. J. Beckmann, "Assignment problems and the location of economic activities," *Econometrica*, vol. 25, pp. 53-76, 1957.
- [2] S. Sahni ve T. Gonzalez, "P-complete approximation problems," *Journal of the Association of Computing Machinery*, vol. 23, pp. 555-565, 1976.
- [3] S. Kirkpatrick, C. Gelat ve M. Vecchi, "Optimization by Simulated Annealing," *Science*, vol. 220, pp. 671-680, 1983.
- [4] R. Burkard ve F. Rendl, "A thermodynamically motivated simulation procedure for combinatorial optimization problems," *European Journal of Operational Research*, vol. 17, pp. 169-174, 1984.
- [5] M. Wilhelm ve T. Ward, "Solving quadratic assignment problems by 'simulated annealing'," *IIE Transactions*, vol. 19, pp. 107-119, 1987.
- [6] N. Abreu, T. Querido ve P. Boaventura-Netto, "A simulated annealing for the quadratic assignment problem," *Rairo-Operations Research*, vol. 33, pp. 249-273, 1999.
- [7] T. Stützle ve M. Dorigo, "ACO Algorithms for the Quadratic Assignment Problem," *New Ideas in Optimization*, McGraw-Hill, 1999.
- [8] M. Dorigo, V. Maniezzo ve A. Colorni, "The Ant System: Optimization by a colony of cooperating agents," *IEEE Transactions on Systems*, vol. 26, pp. 1-13, 1996.
- [9] J. Kochhar, B. Foster ve S. Heragu, "A genetic algorithm for the unequal area facility layout problem," *Computers & Operations Research*, vol. 25, pp. 583-594, 1998.

- [10] Z. Drezner, "A New Genetic Algorithm for the Quadratic Assignment Problem," *Informs Journal on Computing*, vol. 15, pp. 320-330, 2003.
- [11] F. Glover, "Tabu Search - Part I," *ORSA Journal on Computing*, vol. 1, pp. 190-206, 1989.
- [12] J. Skorin-Kapov, "Tabu Search Applied to the Quadratic Assignment Problem," *ORSA Journal on Computing*, vol. 2, pp. 33-45, 1990.
- [13] E. D. Taillard, "Robust taboo search for the quadratic assignment problem," *Parallel Computing*, vol. 17, pp. 443-455, 1991.
- [14] A. Misevičius ve A. Ostreika, "Defining Tabu tenure for the Quadratic Assignment Problem," *Information Technology and Control*, vol. 36, 2007.
- [15] "Developer Centers: CUDA Zone," nVIDIA,. Available: <http://developer.nvidia.com/cuda/what-cuda>.
- [16] S. Tsutsui ve N. Fujimoto, "Solving Quadratic Assignment Problems by Genetic Algorithms with GPU Computation: A Case Study," *GECCO*, Montreal, 2009.
- [17] S. Tsutsui ve N. Fujimoto, "Fast QAP Solving by ACO with 2-opt Local Search on a GPU," *IEEE Section Congress*, San Francisco, 2011.
- [18] M. Czapinski, "An effective Parallel Multistart Tabu Search for Quadratic Assignment Problem CUDA platform," *J. Parallel Distrib. Comput.*, vol. 73(11), pp. 1461-1468, 2013 .
- [19] E. Özçetin ve G. Öztürk, "A Hybrid Genetic Algorithm for the Quadratic Assignment Problem on Graphics Processing Units," *ANADOLU UNIVERSITY JOURNAL OF SCIENCE AND TECHNOLOGY –A Applied Sciences and Engineering*, vol. 17, no. 1, pp. 167-180, 2016.

INTERNATIONAL JOURNAL OF ENGINEERING TECHNOLOGIES-IJET

Guide for Authors

The **International Journal of Engineering Technologies (IJET)** seeks to promote and disseminate knowledge of the various topics of engineering technologies. The journal aims to present to the international community important results of work in the fields of engineering such as imagining, researching, planning, creating, testing, improving, implementing, using and asking. The journal also aims to help researchers, scientists, manufacturers, institutions, world agencies, societies, etc. to keep up with new developments in theory and applications and to provide alternative engineering solutions to current.

The *International Journal of Engineering Technologies* is a quarterly published journal and operates an online submission and peer review system allowing authors to submit articles online and track their progress via its web interface. The journal aims for a publication speed of **60 days** from submission until final publication.

The coverage of IJET includes the following engineering areas, but not limited to:

All filed of engineering such as;

Chemical engineering

- Biomolecular engineering
- Materials engineering
- Molecular engineering
- Process engineering

Civil engineering

- Environmental engineering
- Geotechnical engineering
- Structural engineering
- Transport engineering
- Water resources engineering

Electrical engineering

- Computer engineering
- Electronic engineering
- Optical engineering
- Power engineering

Mechanical engineering

- Acoustical engineering
- Manufacturing engineering
- Thermal engineering
- Vehicle engineering

Systems (interdisciplinary) engineering

- Aerospace engineering
- Agricultural engineering
- Applied engineering
- Biological engineering
- Building services engineering
- Energy engineering
- Railway engineering
- Industrial engineering
- Mechatronics
- Military engineering
- Nano engineering
- Nuclear engineering
- Petroleum engineering

Types of Articles submitted should be original research papers, not previously published, in one of the following categories,

- Applicational and design studies.
- Technology development,
- Comparative case studies.
- Reviews of special topics.
- Reviews of work in progress and facilities development.
- Survey articles.
- Guest editorials for special issues.

Editor-in-Chief and Associate Editors

Editor-in-Chief:

Prof. Dr. Mustafa BAYRAM

Associate Editors:

Assoc. Prof. Dr. Baris SEVIM

Asst. Prof. Dr. Ahmet AKTAS

Asst. Prof. Dr. Yalcin CEKIC

Asst. Prof. Dr. Ali ETEMADI

Ethic Responsibilities

The publication of an article in peer-reviewed “*International Journal of Engineering Technologies*” is an essential building block in the development of a coherent and respected network of knowledge. It is a direct reflection of the quality of the work. Peer-reviewed articles support and embody the scientific method. It is therefore important to agree upon standards of expected ethical behavior for all parties involved in the act of publishing: the author, the journal editor, the peer reviewer, the publisher and the society of society-owned or sponsored journals.

All authors are requested to disclose any actual or potential conflict of interest including any financial, personal or other relationships with other people or organizations within three years of beginning the submitted work that could inappropriately influence, or be perceived to influence, their work.

Submission of an article implies that the work described has not been published previously that it is not under consideration for publication elsewhere. The submission should be approved by all authors and tacitly or explicitly by the responsible authorities where the work was carried out, and that, if accepted, it will not be published elsewhere in the same form, in English or in any other language, including electronically without the written consent of the copyright-holder.

Upon acceptance of an article, authors will be asked to complete a “Copyright Form”. Acceptance of the agreement will ensure the widest possible dissemination of information. An e-mail will be sent to the corresponding author confirming receipt of the manuscript together with a “Copyright Form” form or a link to the online version of this agreement.

Author Rights

As a journal author, you retain rights for a large number of author uses, including use by your employing institute or company. These rights are retained and permitted without the need to obtain specific permission from *IJET*. These include:

- ❖ The right to make copies (print or electronic) of the journal article for your own personal use, including for your own classroom teaching use;

- ❖ The right to make copies and distribute copies (including via e-mail) of the journal article to research colleagues, for personal use by such colleagues for scholarly purposes;
- ❖ The right to post a pre-print version of the journal article on internet web sites including electronic pre-print servers, and to retain indefinitely such version on such servers or sites for scholarly purposes
- ❖ the right to post a revised personal version of the text of the final journal article on your personal or institutional web site or server for scholarly purposes
- ❖ The right to use the journal article or any part thereof in a printed compilation of your works, such as collected writings or lecture notes.

Article Style

Authors must strictly follow the guide for authors, or their articles may be rejected without review. Editors reserve the right to adjust the style to certain standards of uniformity. Follow Title, Authors, Affiliations, Abstract, Keywords, Introduction, Materials and Methods, Theory/Calculation, Conclusions, Acknowledgements, References order when typing articles. The corresponding author should be identified with an asterisk and footnote. Collate acknowledgements in a separate section at the end of the article and do not include them on the title page, as a footnote to the title or otherwise.

Abstract and Keywords:

Enter an abstract of up to 250 words for all articles. This is a concise summary of the whole paper, not just the conclusions, and is understandable without reference to the rest of the paper. It should contain no citation to other published work. Include up to six keywords that describe your paper for indexing purposes.

Abbreviations and Acronyms:

Define abbreviations and acronyms the first time they are used in the text, even if they have been defined in the abstract. Abbreviations such as IEEE, SI, MKS, CGS, sc, dc, and rms do not have to be defined. Do not use abbreviations in the title unless they are unavoidable.

Text Layout for Peer Review:

Use single column layout, double spacing and wide (3 cm) margins on white paper at the peer review stage. Ensure that each new paragraph is clearly indicated. Present tables and figure legends in the text where they are related and cited. Number all pages consecutively; use 12 pt font size and standard fonts; Times New Roman, Helvetica, or Courier is preferred.

Research Papers should not exceed 12 printed pages in two-column publishing format, including figures and tables.

Technical Notes and Letters should not exceed 2,000 words.

Reviews should not exceed 20 printed pages in two-column publishing format, including figures and tables.

Equations:

Number equations consecutively with equation numbers in parentheses flush with the right margin, as in (1). To make equations more compact, you may use the solidus (/), the exp function, or appropriate exponents. Italicize Roman symbols for quantities and variables, but not Greek symbols. Use an dash (–) rather than a hyphen for a

minus sign. Use parentheses to avoid ambiguities in denominators. Punctuate equations with commas or periods when they are part of a sentence, as in

$$C = a + b \tag{1}$$

Symbols in your equation should be defined before the equation appears or immediately following. Use “Eq. (1)” or “equation (1),” while citing.

Figures and Tables:

All illustrations must be supplied at the correct resolution:

- * Black and white and colour photos - 300 dpi
- * Graphs, drawings, etc - 800 dpi preferred; 600 dpi minimum
- * Combinations of photos and drawings (black and white and color) - 500 dpi

In addition to using figures in the text, upload each figure as a separate file in either .tiff or .eps format during submission, with the figure number.

Table captions should be written in the same format as figure captions; for example, “Table 1. Appearance styles.”. Tables should be referenced in the text unabbreviated as “Table 1.”

References:

Please ensure that every reference cited in the text is also present in the reference list (and viceversa). Any references cited in the abstract must be given in full. Unpublished results and personal communications are not recommended in the reference list, but may be mentioned in the text. Citation of a reference as “in press” implies that the item has been accepted for publication. Number citations consecutively in square brackets [1]. Punctuation follows the bracket [2]. Refer simply to the reference number, as in [3]. Use “Ref. [3]” or Reference [3]” at the beginning of a sentence: “Reference [3] was ...”. Give all authors’ names; use “et al.” if there are six authors or more. For papers published in translated journals, first give the English citation, then the original foreign-language citation.

Books

- [1] J. Clerk Maxwell, *A Treatise on Electricity and Magnetism*, 3rd ed., vol. 2. Oxford:Clarendon Press, 1892, pp.68-73.

Journals

- [2] Y. Yorozu, M. Hirano, K. Oka, and Y. Tagawa, “Electron spectroscopy studies on magneto-optical media and plastic substrate interface”, *IEEE Transl. J. Magn. Japan*, vol. 2, pp. 740-741, August 1987.

Conferences

- [3] Çolak I., Kabalci E., Bayindir R., and Sagiroglu S, “The design and analysis of a 5-level cascaded voltage source inverter with low THD”, *2nd PowerEng Conference*, Lisbon, pp. 575-580, 18-20 March 2009.

Reports

- [4] IEEE Standard 519-1992, Recommended practices and requirements for harmonic control in electrical power systems, *The Institute of Electrical and Electronics Engineers*, 1993.

Text Layout for Accepted Papers:

A4 page margins should be margins: top = 24 mm, bottom = 24 mm, side = 15 mm. Main text should be given in two column. The column width is 87mm (3.425 in). The space between the two columns is 6 mm (0.236 in). Paragraph indentation is 3.5 mm (0.137 in). Follow the type sizes specified in Table. Position figures and tables at the tops and bottoms of columns. Avoid placing them in the middle of columns. Large figures and tables may span across both columns. Figure captions should be centred below the figures; table captions should be centred above. Avoid placing figures and tables before their first mention in the text. Use the abbreviation “Fig. 1,” even at the beginning of a sentence.

Type size (pts.)	Appearance		
	Regular	Bold	<i>Italic</i>
10	Authors' affiliations, Section titles, references, tables, table names, first letters in table captions, figure captions, footnotes, text subscripts, and superscripts	Abstract	
12	Main text, equations, Authors' names, ^a		<i>Subheading (1.1.)</i>
24	Paper title		

Submission checklist:

It is hoped that this list will be useful during the final checking of an article prior to sending it to the journal's Editor for review. Please consult this Guide for Authors for further details of any item. Ensure that the following items are present:

- ❖ One Author designated as corresponding Author:
 - E-mail address
 - Full postal address
 - Telephone and fax numbers
- ❖ All necessary files have been uploaded
- Keywords: a minimum of 4
- All figure captions (supplied in a separate document)

- All tables (including title, description, footnotes, supplied in a separate document)
 - ❖ Further considerations
- Manuscript has been "spellchecked" and "grammar-checked"
- References are in the correct format for this journal
- All references mentioned in the Reference list are cited in the text, and vice versa
- Permission has been obtained for use of copyrighted material from other sources (including the Web)
- Color figures are clearly marked as being intended for color reproduction on the Web (free of charge) and in print or to be reproduced in color on the Web (free of charge) and in black-and-white in print.

Article Template Containing Author Guidelines for Peer-Review

First Author*, Second Author**‡, Third Author***

*Department of First Author, Faculty of First Author, Affiliation of First Author, Postal address

**Department of Second Author, Faculty of First Author, Affiliation of First Author, Postal address

***Department of Third Author, Faculty of First Author, Affiliation of First Author, Postal address

(First Author Mail Address, Second Author Mail Address, Third Author Mail Address)

‡Corresponding Author; Second Author, Postal address, Tel: +90 312 123 4567, Fax: +90 312 123 4567, corresponding@affl.edu

Received: xx.xx.xxxx Accepted:xx.xx.xxxx

Abstract- Enter an abstract of up to 250 words for all articles. This is a concise summary of the whole paper, not just the conclusions, and is understandable without reference to the rest of the paper. It should contain no citation to other published work. Include up to six keywords that describe your paper for indexing purposes. Define abbreviations and acronyms the first time they are used in the text, even if they have been defined in the abstract. Abbreviations such as IEEE, SI, MKS, CGS, sc, dc, and rms do not have to be defined. Do not use abbreviations in the title unless they are unavoidable.

Keywords- Keyword1; keyword2; keyword3; keyword4; keyword5.

2. Introduction

Authors should any word processing software that is capable to make corrections on misspelled words and grammar structure according to American or Native English. Authors may get help by from word

processor by making appeared the paragraph marks and other hidden formatting symbols. This sample article is prepared to assist authors preparing their articles to IJET.

Indent level of paragraphs should be 0.63 cm (0.24 in) in the text of article. Use single column layout, double-spacing and wide (3 cm) margins on white paper at the peer review stage. Ensure that each new paragraph is clearly indicated. Present tables and figure legends in the text where they are related and cited. Number all pages consecutively; use 12 pt font size and standard fonts; Times New Roman, Helvetica, or Courier is preferred. Indicate references by number(s) in square brackets in line with the text. The actual authors can be referred to, but the reference number(s) must always be given. Example: "..... as demonstrated [3, 6]. Barnaby and Jones [8] obtained a different result"

IJET accepts submissions in three styles that are defined as Research Papers, Technical Notes and Letter, and Review paper. The requirements of paper are as listed below:

- Research Papers should not exceed 12 printed pages in two-column publishing format, including figures and tables.
- Technical Notes and Letters should not exceed 2,000 words.
- Reviews should not exceed 20 printed pages in two-column publishing format, including figures and tables.

Authors are requested write equations using either any mathematical equation object inserted to word processor or using independent equation software. Symbols in your equation should be defined before the equation appears or immediately following. Use "Eq. (1)" or "equation (1)," while citing. Number equations consecutively with equation numbers in parentheses flush with the right margin, as in Eq. (1). To make equations more compact, you may use the solidus (/), the exp function, or appropriate exponents. Italicize Roman symbols for quantities and variables, but not Greek symbols. Use an dash (–) rather than a hyphen for a minus sign. Use parentheses to avoid ambiguities in denominators. Punctuate equations with commas or periods when they are part of a sentence, as in

$$C = a + b \tag{1}$$

Section titles should be written in bold style while sub section titles are italic.

3. Figures and Tables

3.1. Figure Properties

All illustrations must be supplied at the correct resolution:

- Black and white and colour photos - 300 dpi
- Graphs, drawings, etc - 800 dpi preferred; 600 dpi minimum
- Combinations of photos and drawings (black and white and colour) - 500 dpi

In addition to using figures in the text, Authors are requested to upload each figure as a separate file in either .tiff or .eps format during submission, with the figure number as Fig.1., Fig.2a and so on. Figures are cited as “Fig.1” in sentences or as “Figure 1” at the beginning of sentence and paragraphs. Explanations related to figures should be given before figure. Figures and tables should be located at the top or bottom side of paper as done in accepted article format.



Figure 1. Engineering technologies.

Table captions should be written in the same format as figure captions; for example, “Table 1. Appearance styles.”. Tables should be referenced in the text unabbreviated as “Table 1.”

Table 1. Appearance properties of accepted manuscripts

Type size (pts.)	Appearance		
	Regular	Bold	<i>Italic</i>
10	Authors’ affiliations, Abstract, keywords, references, tables, table names, figure captions, footnotes, text subscripts, and superscripts	Abstract	
12	Main text, equations, Authors’ names, Section titles		<i>Subheading (1.1.)</i>
24	Paper title		

4. Submission Process

The *International Journal of Engineering Technologies* operates an online submission and peer review system that allows authors to submit articles online and track their progress via a web interface. Articles that are prepared referring to this template should be controlled according to submission checklist given in “Guide f Authors”. Editor handles submitted articles to IJET primarily in order to control in terms of compatibility to aims and scope of Journal.

Articles passed this control are checked for grammatical and template structures. If article passes this control too, then reviewers are assigned to article and Editor gives a reference number to paper. Authors registered to online submission system can track all these phases.

Editor also informs authors about processes of submitted article by e-mail. Each author may also apply to Editor via online submission system to review papers related to their study areas. Peer review is a critical element of publication, and one of the major cornerstones of the scientific process. Peer Review serves two key functions:

- Acts as a filter: Ensures research is properly verified before being published
- Improves the quality of the research

5. Conclusion

The conclusion section should emphasize the main contribution of the article to literature. Authors may also explain why the work is important, what are the novelties or possible applications and extensions. Do not replicate the abstract or sentences given in main text as the conclusion.

Acknowledgements

Authors may acknowledge to any person, institution or department that supported to any part of study.

References

- [1] J. Clerk Maxwell, *A Treatise on Electricity and Magnetism*, 3rd ed., vol. 2. Oxford:Clarendon Press, 1892, pp.68-73.
(Book)
- [2] H. Poor, *An Introduction to Signal Detection and Estimation*, New York: Springer-Verlag, 1985, ch. 4. (Book Chapter)
- [3] Y. Yorozu, M. Hirano, K. Oka, and Y. Tagawa, "Electron spectroscopy studies on magneto-optical media and plastic substrate interface", *IEEE Transl. J. Magn. Japan*, vol. 2, pp. 740-741, August 1987. (Article)
- [4] E. Kabalcı, E. Irmak, I. Çolak, "Design of an AC-DC-AC converter for wind turbines", *International Journal of Energy Research*, Wiley Interscience, DOI: 10.1002/er.1770, Vol. 36, No. 2, pp. 169-175. (Article)
- [5] I. Çolak, E. Kabalci, R. Bayindir R., and S. Sagiroglu, "The design and analysis of a 5-level cascaded voltage source inverter with low THD", *2nd PowerEng Conference*, Lisbon, pp. 575-580, 18-20 March 2009. (Conference Paper)
- [6] IEEE Standard 519-1992, Recommended practices and requirements for harmonic control in electrical power systems, *The Institute of Electrical and Electronics Engineers*, 1993. (Standards and Reports)

Article Template Containing Author Guidelines for Accepted Papers

First Author*, Second Author**[‡], Third Author***

*Department of First Author, Faculty of First Author, Affiliation of First Author, Postal address

**Department of Second Author, Faculty of First Author, Affiliation of First Author, Postal address

***Department of Third Author, Faculty of First Author, Affiliation of First Author, Postal address

(First Author Mail Address, Second Author Mail Address, Third Author Mail Address)

[‡]Corresponding Author; Second Author, Postal address, Tel: +90 312 123 4567,

Fax: +90 312 123 4567, corresponding@affl.edu

Received: xx.xx.xxxx Accepted:xx.xx.xxxx

Abstract- Enter an abstract of up to 250 words for all articles. This is a concise summary of the whole paper, not just the conclusions, and is understandable without reference to the rest of the paper. It should contain no citation to other published work. Include up to six keywords that describe your paper for indexing purposes. Define abbreviations and acronyms the first time they are used in the text, even if they have been defined in the abstract. Abbreviations such as IEEE, SI, MKS, CGS, sc, dc, and rms do not have to be defined. Do not use abbreviations in the title unless they are unavoidable.

Keywords Keyword1, keyword2, keyword3, keyword4, keyword5.

1. Introduction

Authors should use any word processing software that is capable of making corrections on misspelled words and grammar structure according to American or Native English. Authors may get help from word processor by making visible the paragraph marks and other hidden formatting symbols. This sample article is prepared to assist authors preparing their articles to IJET.

Indent level of paragraphs should be 0.63 cm (0.24 in) in the text of article. Use single column layout, double-spacing and wide (3 cm) margins on white paper at the peer review stage. Ensure that each new paragraph is clearly indicated. Present tables and figure legends in the text where they are related and cited. Number all pages consecutively; use 12 pt font size and standard fonts; Times New Roman, Helvetica, or Courier is preferred. Indicate references by number(s) in square brackets in line with the text. The actual authors can be referred to, but the reference number(s) must always be

given. Example: "... as demonstrated [3,6]. Barnaby and Jones [8] obtained a different result"

IJET accepts submissions in three styles that are defined as Research Papers, Technical Notes and Letter, and Review paper. The requirements of paper are as listed below:

➤ Research Papers should not exceed 12 printed pages in two-column publishing format, including figures and tables.

➤ Technical Notes and Letters should not exceed 2,000 words.

➤ Reviews should not exceed 20 printed pages in two-column publishing format, including figures and tables.

Authors are requested to write equations using either any mathematical equation object inserted to word processor or using independent equation software. Symbols in your equation should be defined before the equation appears or immediately following. Use "Eq. (1)" or "equation (1),"

while citing. Number equations consecutively with equation numbers in parentheses flush with the right margin, as in Eq. (1). To make equations more compact, you may use the solidus (/), the exp function, or appropriate exponents. Italicize Roman symbols for quantities and variables, but not Greek symbols. Use an dash (-) rather than a hyphen for a minus sign. Use parentheses to avoid ambiguities in denominators. Punctuate equations with commas or periods when they are part of a sentence, as in

$$C = a + b \quad (1)$$

Section titles should be written in bold style while sub section titles are italic.

6. Figures and Tables

6.1. Figure Properties

All illustrations must be supplied at the correct resolution:

- Black and white and colour photos - 300 dpi
- Graphs, drawings, etc - 800 dpi preferred; 600 dpi minimum
- Combinations of photos and drawings (black and white and colour) - 500 dpi

In addition to using figures in the text, Authors are requested to upload each figure as a separate file in either

Table 1. Appearance properties of accepted manuscripts

Type size (pts.)	Appearance		
	Regular	Bold	<i>Italic</i>
10	Main text, section titles, authors' affiliations, abstract, keywords, references, tables, table names, figure captions, equations, footnotes, text subscripts, and superscripts	Abstract-	<i>Subheading (1.1.)</i>
12	Authors' names,		
24	Paper title		

6.2. Text Layout for Accepted Papers

A4 page margins should be margins: top = 24 mm, bottom = 24 mm, side = 15 mm. The column width is 87mm (3.425 in). The space between the two columns is 6 mm (0.236 in). Paragraph indentation is 3.5 mm (0.137 in). Follow the type sizes specified in Table. Position figures and tables at the tops and bottoms of columns. Avoid placing them in the middle of columns. Large figures and tables may span across both columns. Figure captions should be centred below the figures; table captions should be centred above. Avoid placing figures and tables before their first mention in

.tiff or .eps format during submission, with the figure number as Fig.1., Fig.2a and so on. Figures are cited as "Fig.1" in sentences or as "Figure 1" at the beginning of sentence and paragraphs. Explanations related to figures should be given before figure.



Fig. 1. Engineering technologies.

Figures and tables should be located at the top or bottom side of paper as done in accepted article format. Table captions should be written in the same format as figure captions; for example, "Table 1. Appearance styles.". Tables should be referenced in the text unabbreviated as "Table 1."

the text. Use the abbreviation "Fig. 1," even at the beginning of a sentence.

7. Submission Process

The International Journal of Engineering Technologies operates an online submission and peer review system that allows authors to submit articles online and track their progress via a web interface. Articles that are prepared referring to this template should be controlled according to submission checklist given in "Guide f Authors". Editor handles submitted articles to IJET primarily in order to control in terms of compatibility to aims and scope of Journal. Articles passed this control are checked for

grammatical and template structures. If article passes this control too, then reviewers are assigned to article and Editor gives a reference number to paper. Authors registered to online submission system can track all these phases. Editor also informs authors about processes of submitted article by e-mail. Each author may also apply to Editor via online submission system to review papers related to their study areas. Peer review is a critical element of publication, and one of the major cornerstones of the scientific process. Peer Review serves two key functions:

- Acts as a filter: Ensures research is properly verified before being published
- Improves the quality of the research

8. Conclusion

The conclusion section should emphasize the main contribution of the article to literature. Authors may also explain why the work is important, what are the novelties or possible applications and extensions. Do not replicate the abstract or sentences given in main text as the conclusion.

Acknowledgements

Authors may acknowledge to any person, institution or department that supported to any part of study.

References

- [7] J. Clerk Maxwell, A Treatise on Electricity and Magnetism, 3rd ed., vol. 2. Oxford:Clarendon Press, 1892, pp.68-73. (Book)
- [8] H. Poor, An Introduction to Signal Detection and Estimation, New York: Springer-Verlag, 1985, ch. 4. (Book Chapter)
- [9] Y. Yorozu, M. Hirano, K. Oka, and Y. Tagawa, "Electron spectroscopy studies on magneto-optical media and plastic substrate interface", IEEE Transl. J. Magn. Japan, vol. 2, pp. 740-741, August 1987. (Article)
- [10] E. Kabalcı, E. Irmak, I. Çolak, "Design of an AC-DC-AC converter for wind turbines", International Journal of Energy Research, Wiley Interscience, DOI: 10.1002/er.1770, Vol. 36, No. 2, pp. 169-175. (Article)
- [11] I. Çolak, E. Kabalcı, R. Bayindir R., and S. Sagiroglu, "The design and analysis of a 5-level cascaded voltage source inverter with low THD", 2nd PowerEng Conference, Lisbon, pp. 575-580, 18-20 March 2009. (Conference Paper)
- [12] IEEE Standard 519-1992, Recommended practices and requirements for harmonic control in electrical power systems, The Institute of Electrical and Electronics Engineers, 1993. (Standards and Reports)

**INTERNATIONAL JOURNAL OF ENGINEERING TECHNOLOGIES (IJET)
COPYRIGHT AND CONSENT FORM**

This form is used for article accepted to be published by the IJET. Please read the form carefully and keep a copy for your files.

TITLE OF ARTICLE (hereinafter, "The Article"):

.....
.....
.....

LIST OF AUTHORS:

.....
.....
.....

CORRESPONDING AUTHOR'S ("The Author") NAME, ADDRESS, INSTITUTE AND EMAIL:

.....
.....
.....

COPYRIGHT TRANSFER

The undersigned hereby transfers the copyright of the submitted article to International Journal of Engineering Technologies (the "IJET"). The Author declares that the contribution and work is original, and he/she is authorized by all authors and/or grant-funding agency to sign the copyright form. Author hereby assigns all including but not limited to the rights to publish, distribute, reprints, translates, electronic and published derivatives in various arrangements or any other versions in full or abridged forms to IJET. IJET holds the copyright of Article in its own name.

Author(s) retain all rights to use author copy in his/her educational activities, own websites, institutional and/or funder's web sites by providing full citation to final version published in IJET. The full citation is provided including Authors list, title of the article, volume and issue number, and page number or using a link to the article in IJET web site. Author(s) have the right to transmit, print and share the first submitted copies with colleagues. Author(s) can use the final published article for his/her own professional positions, career or qualifications by citing to the IJET publication.

Once the copyright form is signed, any changes about the author names or order of the authors listed above are not accepted by IJET.

Authorized/Corresponding Author

Date/ Signature